THE ASSEMBLY OF PROTIST COMMUNITIES:

UNDERSTANDING DRIVERS OF HISTORICAL CONTINGENCY

AND CAUSES AND CONSEQUENCES OF BIODIVERSITY

A Dissertation
Presented to
The Academic Faculty

by

Zhichao Pu

In Partial Fulfillment
of the Requirements for the Degree
Doctor of Philosophy in the
School of Biology

Georgia Institute of Technology
May 2015

THE ASSEMBLY OF PROTIST COMMUNITIES:

UNDERSTANDING DRIVERS OF HISTORICAL CONTINGENCY

AND CAUSES AND CONSEQUENCES OF BIODIVERSITY

Approved by:

Dr. Lin Jiang, Advisor
School of Biology
Georgia Institute of Technology

Dr. Mark E. Hay
School of Biology
Georgia Institute of Technology

Dr. Joshua S. Weitz
School of Biology
Georgia Institute of Technology

Dr. Joseph P. Montoya
School of Biology
Georgia Institute of Technology

Dr. Karl Cottenie
Department of Integrative Biology
University of Guelph

Date Approved: March 06, 2015

[To the ciliates living happily in laboratory microcosms]

ACKNOWLEDGEMENTS

I want to start by thanking my advisor, Dr. Lin Jiang, who is always ready to provide suggestions for my research and encouraged me when things get stressful. His commitment to students, guidance, and patience are the most important support for me through all the past eight and half years. I also appreciate his collection of music in the lab, which adds fun to the experiments.

I wish to thank my committee members, Drs. Mark E. Hay, Joshua S. Weitz, Joseph P. Montoya, and Karl Cottenie, for their advice and support on my projects.

I appreciate the support of past and current lab members in the Jiang lab. First, I want to thank, my good friend, Dr. Jiaqi Tan, for his help in the lab work and the manuscript writing. In addition, our daily chat keeps me fluent in speaking Shanghai dialect after all these years. I thank Drs. Cyrille Violle, Wade Ryberg, and Dr. Shaopeng Li, for the insightful discussion of the interesting topics in ecology, especially the idea of traits in community assembly. I thank the undergraduate students who used to or now work in the Jiang lab for collecting protist species in local pools and sharing their knowledge from the protist experiments they conducted. I also want to thank my collaborator, Dr. Michael H. Cortez, for his expertise in mathematical models and help with programing in Matlab and Poonim Daya for her hard working in the disturbance experiment.

Finally, I want to thank the support from my family. I greatly appreciate the understanding and encouragement from my parents in these years. I thank my love, Yingying, for lighting up my days.

TABLE OF CONTENTS

LIST OF TABLES

LIST OF FIGURES

SUMMARY

Understanding mechanisms regulating the assembly of ecological communities is a major goal of community ecology. In my dissertational research, I combined experimental and theoretical approaches to investigate the influences of various ecological factors on the assembly of protist communities. Two experimental studies used freshwater heterotrophic ciliated protists as model organisms to examine how species dispersal across local communities (Chapter 1) and functional and phylogenetic diversity of the species pool (Chapter 2) influence historical contingency of the assembled communities, respectively. A third experimental study (Chapter 3) used the same model system to explore the relationship between community phylogenetic diversity and temporal stability. The theoretical study (Chapter 4) explored how phytoplankton and zooplankton coevolution drives species diversity patterns along productivity gradients.

In the study described in Chapter 1, I explored the effects of dispersal among local communities and the history of species colonization into local communities on metacommunity assembly. The differences in species colonization history led to alternative community states that substantially differed in species composition and abundances, regardless of the level of species dispersal. Fitting experimental data to Lotka-Volterra type competition models indicated that the presence of multiple community states was likely driven by the difference in the strength of species interactions associated with different histories.

In the study described in Chapter 2, I experimentally manipulated the functional and phylogenetic diversity of species pools to explore the idea that increasing ecological

similarity of species in the species pool tends to reduce the degree of historical contingency of the assembled communities. Functional diversity was quantified based on measured important protist functional traits, and phylogenetic diversity was quantified based on phylogenetic trees capturing species evolutionary relationships. Consistent with my hypothesis, the results showed that both beta diversity and the strength of inhibitive priority effects decreased as phylogenetic and functional diversity of the species pool increased. Mechanistically, I found that phylogenetic and functional diversity influenced community assembly via altering species niche, but not fitness, differences.

In the study described in Chapter 3, I explored the hypothesis that increasing community phylogenetic diversity tends to increase community temporal stability. Results from the assembled protist communities with different levels of phylogenetic diversity provided support for this hypothesis. The observed positive relationship between phylogenetic diversity and temporal stability of community biomass arose from the reduced competition among species and increased asynchronous species responses to environmental changes under higher phylogenetic diversity. The results also revealed the important influence of dominant species for community stability.

In the study described in Chapter 4, I explored plankton productivity-species diversity relationships (PDR) under the influence of phytoplankton-zooplankton coevolution using mathematical models. Specifically, combining the theory of adaptive dynamics and numerical simulations, I identified the conditions for the emergence of evolutionary divergence in phytoplankton and zooplankton and the coexistence of the evolved species with different traits (cell sizes). Numerical simulations show that coevolutionary dynamics of phytoplankton and zooplankton resulted in transient

unimodal or positive PDRs, and positive PDRs when the systems reach steady states. These findings provide an evolutionary explanation for the various PDRs observed in natural communities. The findings in my research suggest

CHAPTER 1

DISPERSAL AMONG LOCAL COMMUNITIES DOES NOT REDUCE HISTORICAL CONTINGENCIES DURING METACOMMUNITY ASSEMBLY

Abstract

Ample evidence suggests that ecological communities can exhibit historical contingencies. However, few studies have explored whether differences in assembly history can generate alternative local community states in metacommunities in which local communities are linked by dispersal. In a protist microcosm experiment, we examined the influence of species colonization history on metacommunity assembly under homogeneous environmental conditions, by manipulating both the sequence of species colonization into local communities and the rate of dispersal among local communities. Whereas the role of dispersal in structuring local communities decreased over time and became non-significant towards the end of the experiment, species colonization history significantly influenced local communities throughout the experiment. Local communities, regardless of the rate of dispersal among them, exhibited two alternative states characterized by the dominance of different species. The alternative community states, however, emerged in the absence of priority effects that were often associated with alternative community states found in other assembly studies. Rather, they were driven by variation in species interaction strength among local communities with different assembly histories. These results suggest that dispersal

among local communities may not necessarily reduce the role of species colonization history in shaping metacommunity assembly, and that differences in species colonization history need to be explicitly considered as an important factor in causing heterogeneous community states in metacommunities.

Introduction

The recent interest towards an integrative understanding of community dynamics at multiple spatial scales has given rise to the metacommunity concept (Leibold et al. 2004, Holyoak et al. 2005). Within this framework, much attention has been given to the roles of species dispersal among local communities and environmental heterogeneity in shaping metacommunity assembly. For example, the neutral metacommunity perspective suggests that local communities, in the absence of abiotic heterogeneity among them, can differ in their structure due to dispersal limitation and ecological drift (Hubbell 2000, Bell 2001). Also assuming homogenous environmental conditions, the patch-dynamics perspective posits that different local communities can arise because species trade-offs (e.g., competition-dispersal trade-off) result in species extinction followed by re-colonization in different localities at different times (i.e., asynchronous community dynamics among localities). Two metacommunity perspectives, species sorting and mass effects, emphasize the importance of environmental heterogeneity among localities. The species sorting pattern emerges when deterministic assembly processes result in variation in local community structure corresponding to different local habitat conditions (e.g., Cottenie et al. 2003, Lekberg et al. 2007), also as predicted by the classic niche theory (Chase and Leibold 2003). Species sorting gives way to mass effects when sufficiently high levels of species dispersal among localities lead to source-sink dynamics, such that

local environmental conditions and dispersal combine to influence the structure of local communities (Mouquet and Loreau 2002, 2003). The formulation of these metacommunity perspectives has stimulated a large body of empirical work characterizing natural communities by one or more metacommunity types (reviewed by Logue et al. 2011), which has resulted in a much improved understanding of local and regional processes structuring ecological communities. It is notable, however, that the current metacommunity framework does not consider the possibility that other factors, such as the history of community assembly, may also influence community properties at local and regional scales.

The idea that community assembly history can carry significant ecological consequences, which had its origin at least from the early 20th century (Gleason 1927), is now supported by a large number of theoretical and empirical studies. These studies demonstrate that communities differing in their assembly histories can differ in population dynamics (Sait et al. 2000, Jiang et al. 2011a), species composition and abundance (e.g., Drake 1991, Law and Morton 1993, Fukami and Morin 2003), and ecosystem functioning (Fukami et al. 2011, Jiang et al. 2011b). Despite these unequivocal effects of assembly history, few studies of community assembly have adopted a metacommunity perspective by considering both the history of species colonization into local communities and species dispersal among local communities. The few theoretical studies of metacommunity assembly have made inconsistent predictions. Shurin et al. (2004) used a patch occupancy model to show that alternative community states are unlikely to emerge in metacommunities that lack among-habitat abiotic heterogeneity. By contrast, other conceptual (Chase 2003) and theoretical (Fukami 2005) studies predict

that increasing the rate of dispersal among local communities tends to reduce the likelihood of alternative community states associated with different assembly histories, much as dispersal is expected to reduce β diversity among habitats characterized by heterogeneous environmental conditions (Mouquet and Loreau 2002). Likewise, the few experimental studies that have simultaneously manipulated species dispersal and initial local community composition have yielded mixed results (Cadotte et al. 2006, Matthiessen and Hillebrand 2006, Limberger and Wickham 2012). The question of whether differences in assembly history are indeed capable of generating alternative community states in empirical metacommunities thus remains largely unresolved. A definitive answer to this question will have a significant bearing on the interpretation of metacommunity patterns. For example, if assembly history works in the same direction as, or opposite direction to, environmental heterogeneity in causing structural differences among local communities within a metacommunity, then estimates of the strength of species sorting would be underestimated or overestimated if historical effects are not accounted for. Likewise, if community assembly exhibits cyclic dynamics (Law and Morton 1993, Steiner and Leibold 2004) and differences in assembly history lead to asynchronous community cycles among localities, it may create the apparent pattern of patch dynamics even if such dynamics are not present.

To answer the question whether species colonization history can influence metacommunity assembly, we conducted a laboratory protist microcosm experiment that manipulated both the order of species colonization from a common species pool into local communities and the rate of dispersal among local communities, while eliminating abiotic heterogeneity among these local communities. Laboratory microcosms contain

less ecological complexity than most natural communities and are highly amenable to experimental manipulation, allowing the examination of ecological hypotheses that may be difficult to assess in natural environments (Jessup et al. 2004; Benton et al. 2007). The short generation time of protist species allows the observation of long-term community dynamics in a relatively short time span, facilitating the evaluation of alternative community states (Connell and Sousa 1983). As such, microcosm-based research has played a particularly important role in advancing the field of community assembly (Fukami 2010). We show that the difference in assembly history can play a similar role to abiotic environmental heterogeneity in shaping local communities linked by dispersal, resulting in alternative community states within the same metacommunities.

Materials and methods

Microcosm setup

Each microcosm in our experiment consisted of a 250ml Pyrex glass bottle containing 100 ml growth medium, which was made by dissolving protozoan pellets (Carolina Biological Supply Company, Burlington, NC, USA; concentration: 0.55g pellet/L) in deionized water. To provide bacterial food for protists, we inoculated three bacterial species (*Bacillus cereus*, *Bacillus subtillis*, and *Serratia marcescens*) into the autoclave-sterilized medium. After 24 hours of bacterial incubation, we dispensed the medium into individual microcosms. Each microcosm also received two autoclaved wheat seeds that provided additional carbon. All the microcosms and stock cultures were stored in an incubator maintained at 22°C with a12/12 light-dark cycle.

Experimental organisms

Our species pool consisted of 10 free-living ciliated protist species (see Table 1.1 for the species list). All of these species are filter feeders on bacteria and other small particles. Two species, *Blepharisma americanum* and *Tetrahymena vorax*, can also produce cannibalistic forms that feed on smaller individuals of their own and other species; cannibalistic individuals of either species, however, were not abundant in our experiment. These ciliates are small to medium sized, with generation times ranging from a few hours to no more than two days. Each species was raised in separate stock cultures renewed periodically. When inoculating protists into microcosms, we always used 2-week-old stock cultures to minimize the difference in physiological conditions of species between inoculation events.

Experimental design

This experiment involved two levels of spatial-scale configuration: local community and metacommunity. Five microcosms, each receiving a different species colonization sequence (Table 1.1: S1-S5) and operating as a local community, were grouped to form a metacommunity. Species were allowed to colonize local communities via two processes. First, a species can colonize a local community from the species pool (i.e., through species introduction following the colonization sequences). Second, it may migrate into a local community from other local communities that belong to the same metacommunity (i.e., through dispersal within a metacommunity).

Table 1.1. Species list and colonization sequences used in the experiment. Species were sequentially introduced to local communities according to the colonization sequences. Species names and their abbreviations are as follows: *Blepharisma americanum* (BA), *Colpidium kleini* (CK), *Glaucoma scintillans* (GS), *Halteria grandinella* (HG), *Loxocephalus sp.* (LX), *Paramecium aurelia* (PA), *Paramecium bursaria* (PB), *Paramecium multimicronucleatum* (PM), *Spirostomum teres* (ST), and *Tetrahymena vorax* (TV).

Sequence No.	Species introduced by week				
	Week1	Week2	Week3	Week4	Week5
S1	PM, CK	TV, HG	PA, PB	ST, GS	BA, LX
S2	TV, HG	PM, CK	BA, LX	ST, GS	PA, PB
S3	ST, GS	BA, LX	PM, CK	PA, PB	TV, HG
S4	BA, LX	TV, HG	PA, PB	PM, CK	ST, GS
S5	PA, PB	ST, GS	TV, HG	BA, LX	PM, CK

We manipulated both the history of species colonization into local communities from the species pool and the level of species dispersal among local communities of a metacommunity, resulting in a two-way factorial design. For the colonization history treatments, we generated five species colonization sequences according to the following steps: first, we randomly classified the ten species into five two-species groups; second, we assigned a different group as the first colonizer for each colonization sequence; third, we randomly drew groups from the species pool to complete the rest of the colonization sequences (Table 1.1). Species were introduced sequentially into microcosms (local communities) according to the sequences in a 5-week time span (two species per week), with each local community of a metacommunity receiving a different colonization sequence. During species introduction, an inoculum of ~100 individuals of each species was dispensed into local communities. Following previous work (e.g., Cadotte and Fukami 2005, Cadotte et al. 2006), we manipulated species dispersal by weekly transferring medium among local communities after the first week of the experiment. During dispersal, a fixed volume of medium from each local community within a metacommunity was withdrawn, mixed and evenly distributed back into the local communities. Three different volumes were used to create three levels of dispersal rates: 0 ml (no dispersal), 0.5 ml (intermediate dispersal), and 5 ml (high dispersal). The no dispersal treatment served as the control in which alternative local community states, if any, would be most likely to emerge, whereas the intermediate and high dispersal treatments tested whether increasing dispersal would diminish the chance of alternative local community states through, for example, processes similar to mass effects (e.g., Chase 2003). The dispersal rate (equivalent to 0.4% of total populations weekly, or

approximately 0.04~0.2% of total populations per generation) in the intermediate dispersal treatment corresponds to migrations of thousands of individuals, allowing the comparison to other microcosm/mesocosm studies that used similar levels of dispersal rate (e.g., Forbes and Chase 2002, Cadotte et al. 2006). The dispersal rate (equivalent of 4% of total populations weekly, or approximately 0.4~2% of total populations per generation) in the high dispersal treatment approximates the high end of dispersal rates of zooplankton (of which heterotrophic protists are a part) observed in hydraulically connected natural ponds (Michels et al. 2001). Each treatment combination had three replicates, totaling 45 microcosms.

The microcosms were sampled for species abundances weekly. During the sampling, we withdrew 0.4-0.5 ml well-mixed medium from each microcosm, distributed the medium into small drops on a pre-weighted Petri dish, determined the weight of the sample using an analytic balance, and counted the number of individuals of each species in the sample under a stereoscopic microscope. Assuming that the weight of the sample approximately equals to its volume, population density (in the unit of number of individuals per milliliter) of each species was calculated from the collected data. We ran the microcosms as semi-continuous cultures by weekly replacing 10ml medium in each bottle with fresh medium, which served to replenish nutrients and remove metabolic wastes in microcosms. This weekly 10% replenishment, which has been frequently used in previous protist microcosm studies (e.g., Jiang et al. 2009, 2011a), does not appear to have significant impacts on community dynamics. The experiment continued for another 10 weeks after the five weeks of species colonization.

Statistical analyses

We conducted two main sets of analyses: one examining the effects of species colonization history and dispersal among local communities on community assembly trajectories, and the other examining their effects on final local community structure. We assessed the difference in community assembly trajectories by comparing β-diversity patterns and the rate of community turnover over time. We investigated the structural differences of local communities among the treatments using multiple multivariate techniques, including nonmetric multidimensional scaling (NMDS), permutational multivariate analysis of variance (PERMANOVA), and the Ward's minimum variance cluster analysis, in order to detect the possible presence of multiple community states. To explore possible mechanisms driving the observed multiple community states, we also quantified the strength of priority effects and the strength of interactions among the dominant species in our experiment.

In the analysis of assembly trajectories, we first performed repeated measures ANOVA (rm-ANOVA) to assess the influence of dispersal among local communities on β-diversity over time, with β-diversity measured by the average of pairwise Bray-Curtis dissimilarities among local communities in each metacommunity. We also used two-way ANOVA to discern the effects of dispersal and colonization history on the rate of community temporal turnover, calculated as the average of Bray-Curtis dissimilarities between adjacent weeks for each local community (e.g., Week 6-7, Week 7-8, and Week 8-9). Data from the species colonization period (i.e., the first five weeks) were excluded from the above analyses.

To assess the effects of assembly history and dispersal on local community structure, we calculated Bray-Curtis dissimilarities between all local communities using data collected from the last sampling day and visualized community composition in a two-dimensional space through NMDS. We then conducted PERMANOVA comparing Bray-Curtis dissimilarities between local communities of the same colonization history-dispersal treatments and between those of different treatments for each week, with 9,999 permutations (Anderson 2001, McArdle and Anderson 2001). The non-parametric PERMANOVA is conceptually analogous to MANOVA in comparing within- and between-treatment differences, but has the advantage of making no assumption about data distribution; the results from the two analyses were nevertheless similar. In addition to PERMANOVA on Bray-Curtis dissimilarities, we also used Permutational Analysis of Multivariate Dispersions (PERMDISP), with 9,999 permutations, to test whether the observed differences in dissimilarities were mainly driven by across-treatment differences or within-treatment differences (Anderson 2006, Anderson et al. 2006). Data from the species colonization period were again excluded from the analyses.

To further explore whether the treatment effects led to alternative community states, we conducted the Ward's minimum variance cluster analysis based on the log-transformed final population density data. In Ward's clustering, two clusters with the minimal within-cluster error sum of squares (ESS) are merged to generate a new cluster recursively, until the complete cluster tree is constructed. As this method splits the total sum of squares (TSS) into clusters, the proportion of variance explained by each cluster can be estimated as ESS/TSS. Since our analyses suggested the presence of two alternative community states associated with different assembly histories (see Results),

we conducted two additional tests to investigate possible driving mechanisms. First, to quantify the strength of inhibitive priority effects, which often emerges in community assembly studies (e.g., Fukami et al. 2010, Jiang et al. 2011a,Weslien et al. 2011), we regressed final population abundance (log transformed, $\log_{10}$-[density+1]) of each species against its arrival order. Negative relationships between population abundance and arrival order would indicate inhibitive priority effects. Second, assembly history may structure ecological communities by altering species interactions. Such effects could, for example, come about when early colonizing species modify the strength of interactions among later colonizing species (i.e., interaction modifications, *sensu* Wootton 1994). To assess the possibility of such interaction modifications, we measured the intrinsic growth rates and carrying capacities of the five species that persisted until the end of the experiment in a supplemental experiment that established monocultures of each species (see Appendix A), and estimated the per-capita strength of interactions between these species by fitting their population dynamics in the assembly experiment to a continuous Lotka-Volterra competition model as described below.

Our interaction strength analyses focused on five common protist species (*Blepharisma americanum, Colpidium kleini, Glaucoma scintillans, Paramecium aurelia,* and *Paramecium bursaria*). For each of the five species, we fitted its population dynamics to the following Lotka-Volterra type model:

$$\frac{dN_0}{dt} = r_0 N_0 \left(1 - \frac{N_0+\alpha_1 N_1+\alpha_2 N_2+\alpha_3 N_3+\alpha_4 N_4}{K_0}\right) - m(N_0 - \bar{N}_0)$$

(Equation 1.1)

where N_0 is population density of the focal species with intrinsic growth rate r_0 and carrying capacity K_0, m is the dispersal rate across local communities, $\bar{N}_0$ is the average population density of the focal species within a metacommunity, N_1 - N_4 are population densities of the other four competing species, and α_1 - α_4 are the per capita interaction coefficients. The r_0 and K_0 values were estimated using the monoculture data from the supplemental experiment (see Appendix A). We fitted the competition coefficients, α_1 - α_4, as the values that minimized the sum of squares of the difference between observed and predicted species abundance, by using the *ode45* differential equation solver and *fminsearch* function in Matlab (version R2012a, The MathWorks, Inc., Natick, Massachusetts, United States). When fitting the model above, we only included population dynamics from week 6 onwards when all the species had been introduced into local communities.

We performed all the statistical analyses in *R 2.15.1* (www.r-project.org), with PERMANOVA conducted using the *adonis* function and PERMDISP using the *betadisper* function implemented in the *vegan* package (Oksanen et al. 2013).

Results

Among the 10 protist species used in our experiment, four species (*Halteria grandinella*, *Loxocephalus sp.*, *Paramecium multimicronucleatum*, and *Tetrahymena vorax*) went extinct in all local communities before the end of the experiment, whereas the other species persisted in at least some local communities (Appendix A: Fig. A1). Metacommunities without dispersal among local communities attained greater β-diversity than metacommunities with dispersal among local communities (Fig. 1.1; rm-ANOVA,

dispersal: $F_{2,6} = 34.3$, $P < 0.001$). This difference, however, grew smaller over time (rm-ANOVA, dispersal × time: $F_{16,48} = 3.048$, $P = 0.002$), with dispersal having no effect on β-diversity in the last two weeks of the experiment (ANOVA, Week 14, $F_{2,6}=1.53$, $P=0.290$; Week 15, $F_{2,6} = 2.17$, $P = 0.195$). β-diversity was increasing towards the end of the experiment as the local communities with different histories shared fewer species and further diverged from one another (Fig. 1.1). Species colonization history, but not dispersal among local communities, significantly affected the rate of community temporal turnover (ANOVA, history: $F_{4,30} = 40.46$, $P < 0.001$; dispersal: $F_{2,30} = 0.16$, $P = 0.849$; history × dispersal: $F_{8,30} = 1.73$, $P = 0.132$). Tukey's HSD *post-hoc* test revealed more rapid turnover in the S1 and S4 history treatments than in the S2, S3 and S5 treatments (Table 1.2), corresponding to more species loss in the former than the latter treatments (Appendix A: Fig. A1).

PERMANOVA revealed that the effect of assembly history on local community structure persisted for the duration of the experiment, whereas the effect of dispersal diminished to being non-significant towards the end of the experiment (Fig. 1.2). Assembly history, but not dispersal, had significant effects on the Bray-Curtis dissimilarities among local communities in the last two weeks of the experiment (Fig. 1.2 and 1.3; PERMANOVA, Week 14, history: $F_{4,30} = 12.05$, $P < 0.001$, dispersal: $F_{2,30} = 2.26$, $P = 0.051$, history × dispersal: $F_{8,30} = 1.35$, $P = 0.163$; Week 15, history: $F_{4,30} = 10.18$, $P < 0.001$, dispersal: $F_{2,30} = 1.56$, $P = 0.137$, history × dispersal: $F_{8,30} = 0.11$, $P = 0.271$). PERMANOVA also revealed that communities with S1 and S4 histories, and communities with S2, S3 and S5 histories had significant between-group difference and non-significant within-group difference (Table 1.2), suggesting the possible presence of

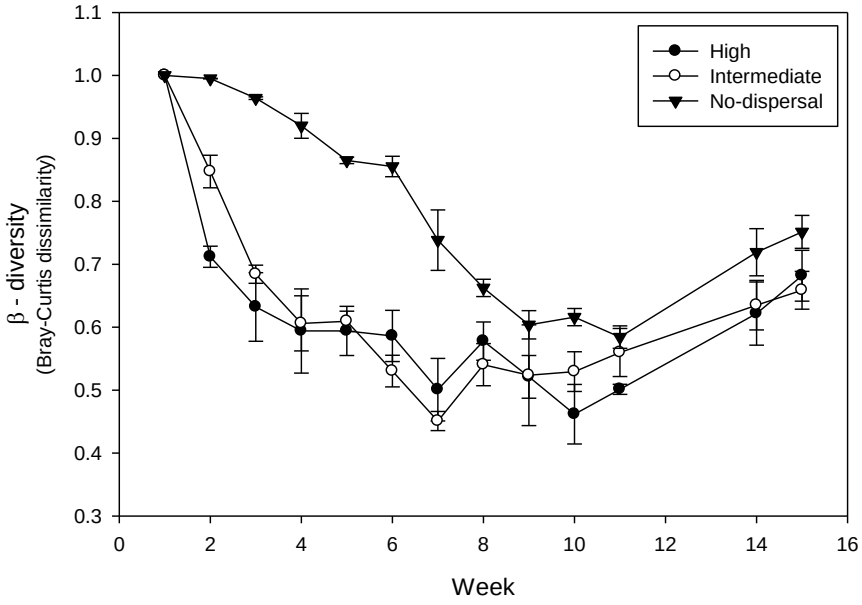

Fig. 1.1. β-diversity in metacommunities over time. For each metacommunity, we averaged Bray-Curtis dissimilarity between each pair of local communities for β-diversity. Values are plotted as means ± SE.

Table 1.2. Pairwise comparisons of temporal turnover within local communities and dissimilarities among local communities between the assembly history treatments. Tukey's HSD test was used to compare temporal turnover (Bray-Curtis dissimilarity) in local community composition (Diff = difference between two history treatments, with positive values indicating higher turnover rate in the first treatment of the comparison). Pairwise *a posteriori* comparisons in PERMANOVA and PERMDISP were based on Bray-Curtis dissimilarity among local communities. P-values in PERMANOVA were computed based on 9,999 permutations, with significance levels adjusted by Bonferroni correction. Observed P-values were reported in PERMDISP based on 9,999 permutations.

	Tukey's HSD of temporal turn-over		PERMANOVA	PERMDISP
Comparisons	Diff	P	permutation P	observed P
(S1,S2)	0.240	< **0.001**	**0.002**	0.062
(S1,S3)	0.182	< **0.001**	**0.001**	0.686
(S1,S4)	0.079	**0.009**	0.079	0.387
(S1,S5)	0.204	< **0.001**	**0.002**	**0.002**
(S2,S3)	- 0.058	0.091	0.999	0.123
(S2,S4)	- 0.161	< **0.001**	**0.002**	0.180
(S2,S5)	- 0.035	0.510	0.136	**0.042**
(S3,S4)	- 0.103	< **0.001**	**0.022**	0.676
(S3,S5)	0.023	0.840	0.564	**0.001**
(S4,S5)	0.126	< **0.001**	**0.002**	**0.001**

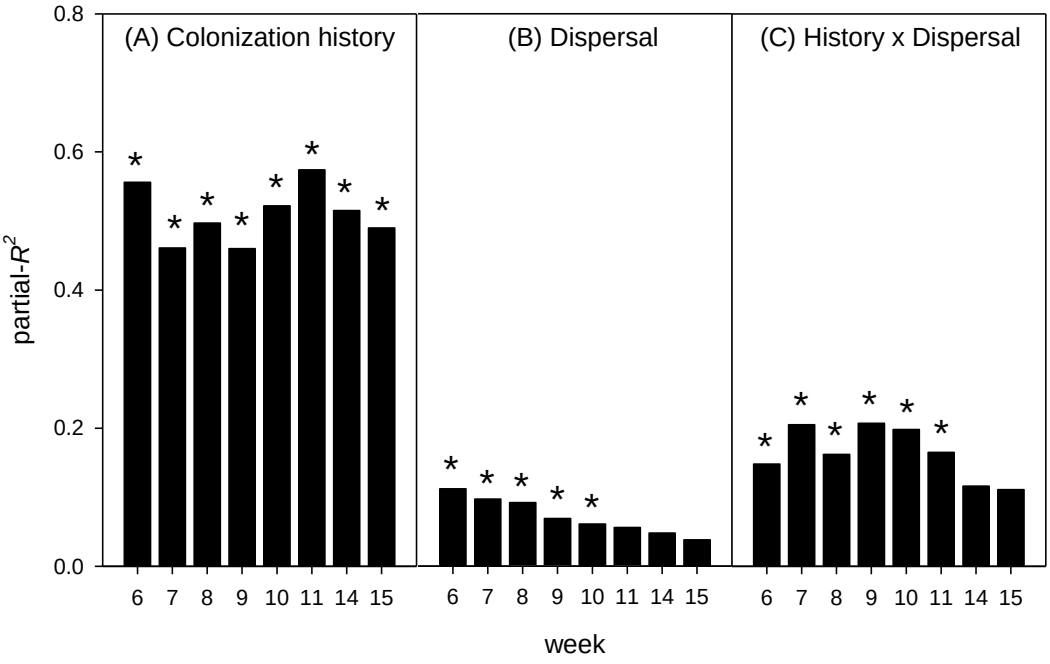

Fig. 1.2. The fraction of variance in β-diversity among local communities explained by species colonization history, dispersal among local communities, and their interaction. The explained variance (partial-R^2) was calculated by using Permutational Multivariate Analysis of Variance (PERMANOVA) based on Bray-Curtis dissimilarities. PERMANOVA with 9,999 permutations were performed separately on weekly data (week 6 – 15). The stars indicate significant treatment effects after Bonferroni correction.

two alternative community states. These results, however, could arise from across-treatment dissimilarities (i.e., the difference in community structure between history treatments) and/or within-treatment dissimilarities (i.e., similar community structure but different magnitude of dispersion of species composition among replicates of the same treatments). PERMDISP indicated that communities receiving different colonization sequences, except for S5, showed no significant differences in their dispersion of species composition (Table 1.2, Fig. 1.3). These suggested that the two community states indeed differed in their structure.

Consistent with the permutational tests, clustering also pointed to the presence of the same two alternative community states. Clustering produced two main clusters, one consisting of communities with S1 and S4 histories and the other of communities with S2, S3, and S5 histories (Fig. 1.4). These two clusters alone accounted for more than 70% of the total variance (Fig. 1.4).

Few significant negative relationships between species abundance and arrival order were found (Appendix A: Fig. A2), indicating that inhibitive priority effects were not an important driver of species abundance patterns in the observed two community states. Analyses of interaction strength revealed that interaction coefficients differed substantially among assembly history treatments. In particular, *C. kleini*, a common species in all history treatments (Appendix A: Fig. A1), exhibited significant negative per-capita effect on *P. aurelia* in communities with S2, S3, and S5 histories, but not in those with S1 and S4 histories. Moreover, the per-capita competitive effect of *P. bursaria* on other species was generally stronger in communities with S2, S3, and S5 histories than

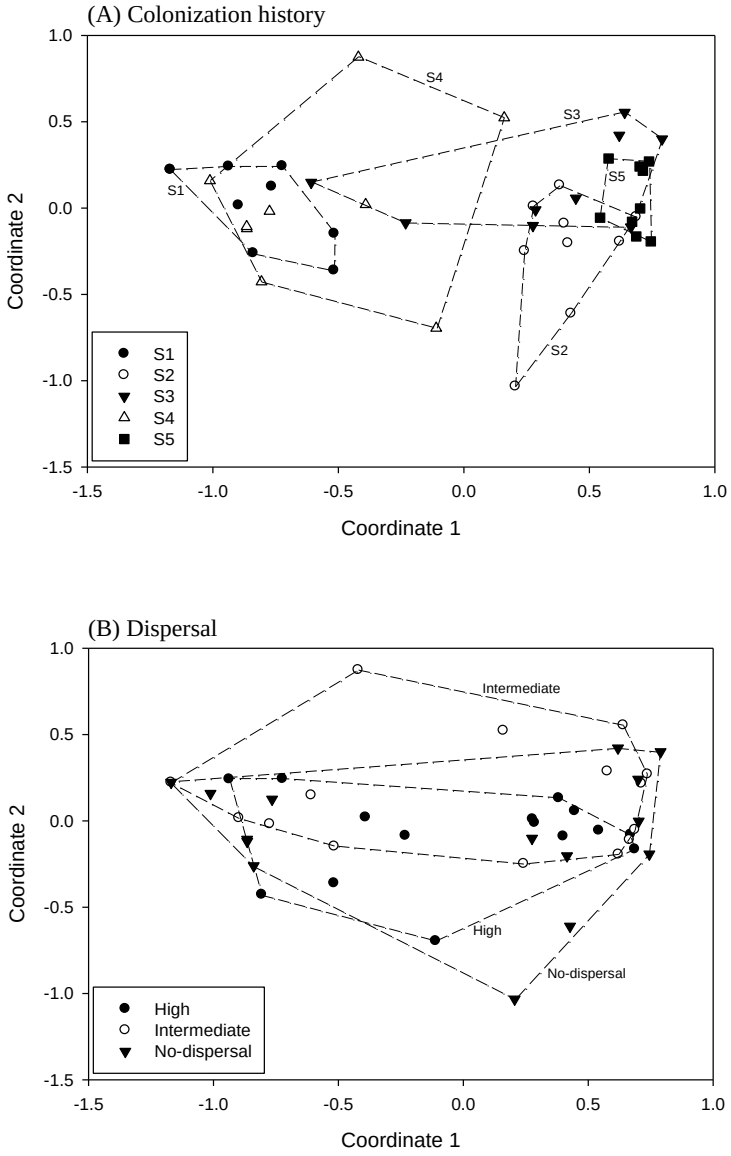

Fig. 1.3. Nonmetric multidimensional scaling (NMDS) ordination plots of local communities in a two-dimensional space. Each point corresponds to one local community. Distance between two points corresponds to the difference between the two communities as measured by Bray-Curtis dissimilarity. (A) Communities are categorized by the assembly sequences S1-S5 (as in Table 1): filled circles, open circles, filled inverted-triangles, open triangles, and filled squares indicate communities with history S1, S2, S3, S4, and S5, respectively. (B) Communities are categorized by dispersal rates among local communities: filled circles, open circles, and filled triangles represent local communities experiencing high, intermediate, and no dispersal, respectively. The dashed line indicates the minimum convex hull around each category.

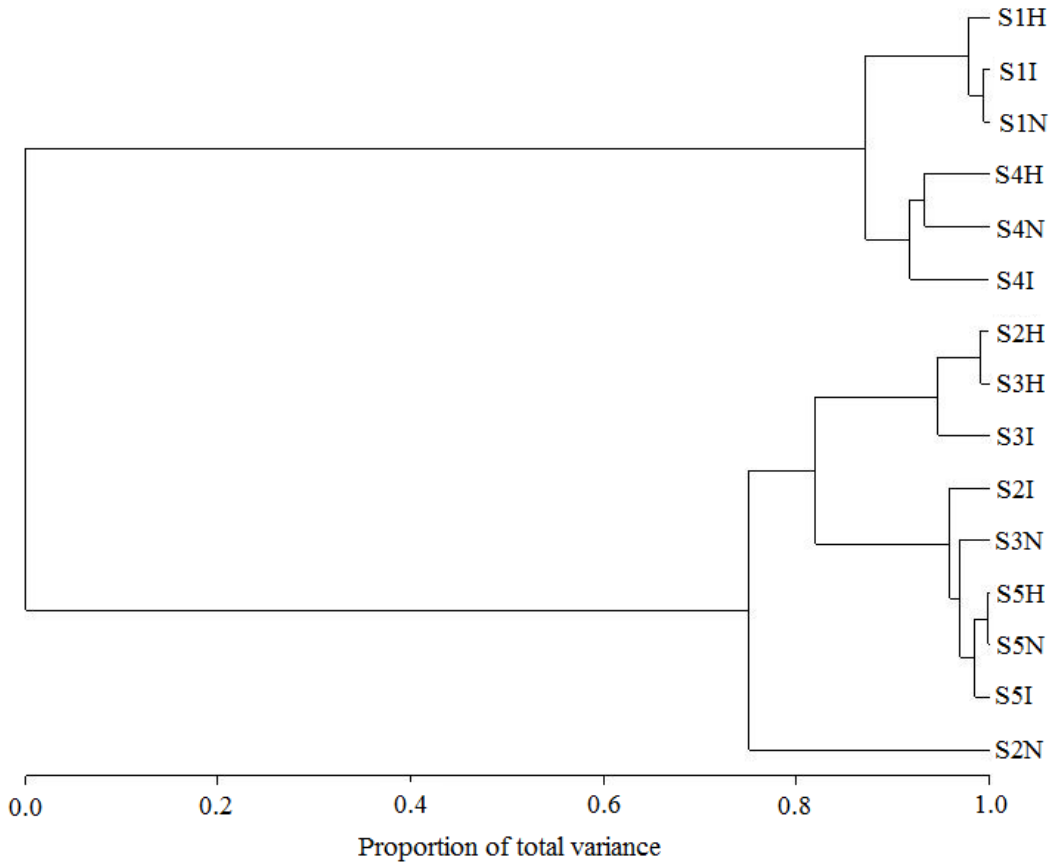

Fig. 1.4. The result of the Ward's minimum variance cluster analysis. S1 – S5 represent the five assembly history sequences (see Table 1.1 for details). The letter "N", "I", and "H" denotes the no-dispersal, intermediate dispersal, and high dispersal treatment, respectively. The x-axis indicates the proportion of variance explained by the clusters.

those with S1 and S4 histories, although it was significantly different from 0 in the S5 history treatment only (Appendix A: Fig. A3).

Discussion

Our experiment revealed different trajectories of local community assembly as the result of different species colonization sequences, which produced two alternative local community states within the same metacommunities. The alternative community states emerged despite substantial dispersal and the lack of environmental heterogeneity among local communities. This result is consistent with the predictions of Chase (2003) and Fukami (2005) on the existence of multiple community states during metacommunity assembly under homogeneous environmental conditions, but contrasts with the prediction of Shurin et al. (2004) suggesting that alternative community states are unlikely under such conditions. The model of Shurin et al. (2004), however, focused on regional competition between species that pre-empt local habitats. Similar to our experiment, both the conceptual model of Chase (2003) and the Lotka-Volterra type model of Fukami (2005) considered species coexistence at both local and regional scales. Both models also predict that increasing dispersal among local communities tends to homogenize their structure and reduce β-diversity, a result that was borne out in several experiments (e.g., Warren 1996, Forbes and Chase 2002, Kneitel and Miller 2003, Matthiessen and Hillebrand 2006, Limberger and Wickham 2012). This, however, did not occur in our experiment, where increasing dispersal neither reduced β-diversity nor diminished the presence of alternative community states. Several factors could have contributed to this discrepancy. First, our experimental duration is longer than that of most previous

experiments on the same topic (Forbes and Chase 2002, Matthiessen and Hillebrand 2006, Limberger and Wickham 2012), which allowed us to detect transient effects of dispersal that later disappeared. The observed effects of dispersal in other, shorter-term experiments may thus be interpreted as a transient pattern. Second, the difference in the type of communiteis used among studies could have played a role. For example, the use of benthic micro-algal communities in the experiments of both Matthiessen and Hillebrand (2006) and Limberger and Wickham (2012) would presumably result in pre-emptive competition for space, which may lead to strong inhibitive priority effects that were not observed in our experiment (see next paragraph). Under this circumstance, the strength of priority effects and, therefore, β-diversity is expected to decline with increasing dispersal among local communities (Chase 2003). Third, the levels of dispersal in our experiment, though comparable to natural conditions, are relatively low; greater levels of dispersal may be needed to incur mass effects with dispersal having long-lasting effects on local community structure.

Inhibitive priority effects, where earlier colonizing species tend to dominate over later colonizers, are often identified as the primary cause of alternative community states during community assembly (e.g., Chase 2003, 2010, Fukami et al. 2010, Jiang et al. 2011a, Weslien et al. 2011). This, however, is not the case in our experiment, in which the colonization order of species had idiosyncratic influence on species abundance at the end of the experiment. Early arriving species rarely dominated and some even went extinct before the end of our experiment (Appendix A: Fig. A4), despite the fact that colonization history affected the assembly trajectory and final structure of local communities. In particular, the population size of *P. aurelia* and *P. bursaria* differed

substantially between the two community states, with *P. aurelia* abundant in one community state and *P. bursaria* abundant in the other (Appendix A: Fig. A4). Note that these two species simultaneously colonized communities in our experiment (Table 1.1). The fitted interaction coefficients indicate that *P. bursaria* was, on average, a better competitor than *P. aurelia* (T_{44} = -2.124, P = 0.039 in a t-test comparing per-capita effect of *P. bursaria* and *P. aurelia* on each other), a result consistent with another microcosm experiment involving the same species pair under the same environmental conditions (Violle et al. 2011).The competitive ability (i.e., per capita competition coefficient) of *P. bursaria*, however, varied with assembly history, such that it imposed strong negative per-capita effects on other species (including *P. aurelia*) only in communities with S2, S3 and S5 histories. Furthermore, *C. kleini*, a common species across almost all history treatments, showed significant per-capita competitive effect on *P. aurelia* only in these communities (Appendix A: Fig. A3). These results suggest that the history-dependent species interactions may have played an important role in driving the difference in species abundances between the two community states. One possible explanation of these history-dependent interactions is that early colonizers may mediate the interaction among later colonizing species through higher order interactions (i.e., interaction modifications, *sensu* Wootton 1994). For example, because of the different diet preference of the bacterivorous consumers, early colonizing species may have altered bacterial communities and, consequently, the competitive interactions between the later colonizers. Testing this hypothesis directly requires data on bacterial communities in microcosms, which were not collected in our experiment. Nevertheless, we suggest that such history-dependent interaction modifications could be potentially common, and may serve as a

previously underappreciated mechanism driving alternative community states during community assembly.

The presence of different community states in our experimental metacommunities, because of different assembly histories, is akin to the existence of multiple community states caused by environmental heterogeneity as predicted by species-sorting models. First, in the species-sorting models, local environmental conditions drive community assembly through niche-based, deterministic processes, leading to either a stable endpoint community state or repeating assembly cycles (Steiner and Leibold 2004). In our experiment, although colonization sequences were randomly assigned to some extent, the results clearly indicated non-random community assembly such that communities receiving the same colonization sequences ended up with the same community states. Second, several studies have shown that high dispersal rates within metacommunities had little impacts on local communities exhibiting the species-sorting dynamics (e.g., Cottenie et al. 2003). Likewise, although there were significant effects of dispersal on local community structure during the early phase of metacommunity assembly, these effects diminished over time, with assembly history being the only significant community-structuring factor at the end of our experiment. Together, these results suggest that biotic heterogeneity associated with different colonization histories can play a similar role as abiotic environmental heterogeneity in producing different local community states within the same metacommunities. Importantly, our results also indicate that such biotic heterogeneity may not necessarily operate via priority effects.

Throughout this article, we have used *alternative community states*, rather than the more popular term *alternative stable states*, to describe communities that differ in

structure because of different assembly histories. Our choice of the term reflects the fact that assembling communities can go through long transient phases before attaining stable states (Fukami and Nakajima 2011). Inspection of community dynamics (Appendix A: Fig. A1) suggests that communities at the end of our experiment were close to, but not yet at their steady states, despite the 15-week duration that corresponds to many generations of our study organisms. The presence of such long transient states, also reported in other assembly studies (e.g., Fukami 2004; Jiang and Patel 2008), suggests that we would need more stringent criteria than one complete turnover of organisms for assessing alternative stable states, as initially proposed by Connell and Sousa (1983). Note that the increase in β-diversity towards the end of our experiment indicates that, unlike other assembly experiments that showed community convergence over time (e.g., Fukami 2004; Jiang and Patel 2008), the two alternative communities were still diverging from each other. It is thus likely that the observed alternative states would persist even after communities, which were already close to steady states, stabilize.

One issue of note is that although bacteria were essential components of our experimental communities, we did not monitor bacterial abundances because of logistic constraints. Although the lack of bacterial data did not prevent us from estimating the strength of interactions between their protist consumers, the availability of such data would help understand the mechanistic base of history-dependent interaction strength observed here. Another issue is that the sample size (0.4-0.5% of a microcosm) in our experiment was relatively small, making it difficult to detect species with extremely low abundances. To ease this problem, we considered a species extinct only when the species was continuously absent in samples and not detected at the end of the experiment.

Further, our analyses were based on abundance-based Bray-Curtis dissimilarities, which are less sensitive to species detection problems than presence/absence-based dissimilarity indices. When we assigned one individual to each absent species in all samples and re-ran our analyses, we found that our results remained unchanged, indicating their robustness to the presence/absence of rare species. Note that species abundances in each sample were still high (thousands of individuals) at the end of our experiment, and thus the use of Bray-Curtis dissimilarity index does not suffer from erratic behaviours associated with sparse samples (Clarke et al. 2006).

Our study provides unique experimental evidence that assembly history can strongly influence the structure of local communities despite dispersal among them, via mechanisms other than priority effects. This historical contingency for metacommunities has important implications for interpreting metacommunity patterns observed in nature. As noted in the introduction, the existing metacommunity perspectives do not consider variation in assembly history as a possible source of structural differences among local communities. Therefore, classifying natural communities based on the current metacommunity framework runs the risk of being unable to identify the true magnitude of environmental heterogeneity and dispersal effects, if natural communities often exhibit historical contingencies. We thus advocate the expansion of the metacommunity framework to consider species colonization history as another potentially important force, in parallel with environmental heterogeneity and dispersal, in shaping metacommunity assembly. However, we note that given that species colonization history is largely unknown for natural communities, how to distinguish the effects of these forces in nature remains a serious challenge. In our experiment, variation in species colonization history

led to different local communities within the same metacommunities, akin to environmental heterogeneity leading to different local communities as depicted by species sorting. Future experiments that independently manipulate community assembly history and environmental heterogeneity should assess their relative importance in contributing to heterogeneous local community states.

References

Anderson, M. J. 2001. A new method for non-parametric multivariate analysis of variance. Austral Ecology 26:32-46.

Anderson, M. J. 2006. Distance-based tests for homogeneity of multivariate dispersions. Biometrics 62:245-253.

Bell, G. 2001. Neutral macroecology. Science 293:2413-2418.

Cadotte, M. W., A. M. Fortner, and T. Fukami. 2006. The effects of resource enrichment, dispersal, and predation on local and metacommunity structure. Oecologia 149:150-157.

Chase, J. M. 2003. Community assembly: when should history matter? Oecologia 136:489-498.

Chase, J. M. 2010. Stochastic Community Assembly Causes Higher Biodiversity in More Productive Environments. Science 328:1388-1391.

Chase, J. M., and M. A. Leibold. 2003. Ecological niches: linking classical and contemporary approaches. University of Chicago Press, Chicago, IL.

Clarke, K. R., P. J. Somerfield, and M. G. Chapman. 2006. On resemblance measures for ecological studies, including taxonomic dissimilarities and a zero-adjusted Bray–Curtis coefficient for denuded assemblages. Journal of Experimental Marine Biology and Ecology 330:55-80.

Connell, J. H., and W. P. Sousa. 1983. On the Evidence Needed to Judge Ecological Stability or Persistence. American Naturalist 121:789-824.

Cottenie, K., E. Michels, N. Nuytten, and L. De Meester. 2003. Zooplankton metacommunity structure: Regional vs. local processes in highly interconnected ponds. Ecology 84:991-1000.

Drake, J. A. 1991. Community assembly mechanics and the structure of an experimental species ensemble. American Naturalist 137:1-26.

Forbes, A. E., and J. N. Chase. 2002. The role of habitat connectivity and landscape geometry in experimental zooplankton metacommunities. Oikos 96:433-440.

Fukami, T. 2004. Community assembly along a species pool gradient: implications for multiple-scale patterns of species diversity. Population Ecology 46:137-147.

Fukami, T. 2005. Integrating internal and external dispersal in metacommunity assembly: preliminary theoretical analyses. Ecological Research 20:623-631.

Fukami, T. 2010. Community assembly dynamics in space. Pages 45-54 in H. A. Verhoef and P. J. Morin, editors. Community Ecology: Processes, Models, and Applications. Oxford University Press, Oxford.

Fukami, T., I. A. Dickie, J. P. Wilkie, B. C. Paulus, D. Park, A. Roberts, P. K. Buchanan, and R. B. Allen. 2010. Assembly history dictates ecosystem functioning: evidence from wood decomposer communities. Ecology Letters 13:675-684.

Fukami, T., and P. J. Morin. 2003. Productivity-biodiversity relationships depend on the history of community assembly. Nature 424:423-426.

Fukami, T., and M. Nakajima. 2011. Community assembly: alternative stable states or alternative transient states? Ecology Letters 14:973-984.

Gleason, H. A. 1927. Further views on the succession-concept. Ecology 8:299-326.

Holyoak, M., M. A. Leibold, and R. Holt. 2005. Metacommunities: spatial dynamics and ecological communities. University of Chicago Press, Chicago.

Hubbell, S. P. 2001. The Unified Neutral Theory of Biodiversity and Biogeography. Priceton University Press, Princeton, NJ.

Jessup, C. M., R. Kassen, S. E. Forde, B. Kerr, A. Buckling, P. B. Rainey, and B. J. M. Bohannan. 2004. Big questions, small worlds: microbial model systems in ecology. Trends in Ecology & Evolution 19:189-197.

Jiang, L., L. Brady, and J. Tan. 2011. Species diversity, invasion, and alternative community states in sequentially assembled communities. The American Naturalist 178:411-418.

Jiang, L., H. Joshi, S. K. Flakes, and Y. Jung. 2011. Alternative community compositional and dynamical states: the dual consequences of assembly history. Journal of Animal Ecology 80:577-585.

Jiang, L., H. Joshi, and S. N. Patel. 2009. Predation alters relationships between biodiversity and temporal stability. The American Naturalist 173:389-399.

Jiang, L., and S. N. Patel. 2008. Community assembly in the presence of disturbance: A microcosm experiment. Ecology 89:1931-1940.

Kneitel, J. M., and T. E. Miller. 2003. Dispersal rates affect species composition in metacommunities of Sarracenia purpurea inquilines. American Naturalist 162:165-171.

Law, R., and R. D. Morton. 1993. Alternative Permanent States of Ecological Communities. Ecology 74:1347-1361.

Leibold, M. A., M. Holyoak, N. Mouquet, P. Amarasekare, J. M. Chase, M. F. Hoopes, R. D. Holt, J. B. Shurin, R. Law, D. Tilman, M. Loreau, and A. Gonzalez. 2004. The metacommunity concept: a framework for multi-scale community ecology. Ecology Letters 7:601-613.

Lekberg, Y., R. T. Koide, J. R. Rohr, L. Aldrich-Wolfe, and J. B. Morton. 2007. Role of niche restrictions and dispersal in the composition of arbuscular mycorrhizal fungal communities. Journal of Ecology 95:95-105.

Limberger, R., and S. A. Wickham. 2012. Transitory versus Persistent Effects of Connectivity in Environmentally Homogeneous Metacommunities. Plos One 7:e44555.

Logue, J. B., N. Mouquet, H. Peter, H. Hillebrand, and M. W. Grp. 2011. Empirical approaches to metacommunities: a review and comparison with theory. Trends in Ecology & Evolution 26:482-491.

Matthiessen, B., and H. Hillebrand. 2006. Dispersal frequency affects local biomass production by controlling local diversity. Ecology Letters 9:652-662.

McArdle, B. H., and M. J. Anderson. 2001. Fitting multivariate models to community data: A comment on distance-based redundancy analysis. Ecology 82:290-297.

Michels, E., K. Cottenie, L. Neys, and L. De Meester. 2001. Zooplankton on the move: first results on the quantification of dispersal of zooplankton in a set of interconnected ponds. Hydrobiologia 442:117-126.

Mouquet, N., and M. Loreau. 2002. Coexistence in metacommunities: The regional similarity hypothesis. American Naturalist 159:420-426.

Mouquet, N., P. Munguia, J. M. Kneitel, and T. E. Miller. 2003. Community assembly time and the relationship between local and regional species richness. Oikos 103:618-626.

Oksanen, J., F. G. Blanchet, R. Kindt, P. Legendre, P. R. Minchin, R. B. O'Hara, G. L. Simpson, P. Solymos, M. H. H. Stevens, and H. Wagner. 2013. vegan: Community Ecology Package. R package version 2.0-10.

Sait, S. M., W. C. Liu, D. J. Thompson, H. C. J. Godfray, and M. Begon. 2000. Invasion sequence affects predator-prey dynamics in a multi-species interaction. Nature 405:448-450.

Shorrocks, B., and M. Bingley. 1994. Priority effects and species coexistence - experiments with fungal-breeding Drosophila. Journal of Animal Ecology 63:799-806.

Shurin, J. B., P. Amarasekare, J. M. Chase, R. D. Holt, M. F. Hoopes, and M. A. Leibold. 2004. Alternative stable states and regional community structure. Journal of Theoretical Biology 227:359-368.

Steiner, C. F., and M. A. Leibold. 2004. Cyclic assembly trajectories and scale-dependent productivity-diversity relationships. Ecology 85:107-113.

Violle, C., D. R. Nemergut, Z. C. Pu, and L. Jiang. 2011. Phylogenetic limiting similarity and competitive exclusion. Ecology Letters 14:782-787.

Warren, P. H. 1996. The effects of between-habitat dispersal rate on protist communities and metacommunities in microcosms at two spatial scales. Oecologia 105:132-140.

Weslien, J., L. B. Djupstrom, M. Schroeder, and O. Widenfalk. 2011. Long-term priority effects among insects and fungi colonizing decaying wood. Journal of Animal Ecology 80:1155-1162.

Wootton, J. T. 1994. The nature and consequences of indirect effects in ecological communities. Annual Review of Ecology and Systematics:443-466.

CHAPTER 2

REDUCED HISTORICAL CONTINGENCY IN COMMUNITIES WITH HIGHER FUNCTIONAL AND PHYLOGENETIC DIVERSITY

Abstract

Considerations of species traits and phylogeny are thought to improve our understanding of community assembly, but direct experimental tests of this idea are rare. We performed a laboratory microcosm experiment involving bacterivorous protists to examine how species' ecological differences in the species pool, characterized by functional and phylogenetic distances, influences community assembly. Our results showed that β-diversity among communities with different assembly histories decreased with both functional and phylogenetic diversity, whereas α-diversity of the assembled communities increased with both functional and phylogenetic diversity. Mechanistically, species niche differences increased with functional and phylogenetic diversity, facilitating coexistence and reducing the strength of priority effects. Species fitness differences, which explained little variation in α- and β-diversity, were less important. The utility of the combined use of functional and phylogenetic diversity in identifying important functional traits is also discussed. These results advocate the use of functional and phylogenetic knowledge for better understanding the mechanisms underlying community assembly.

Introduction

One major goal of community ecology is to understand the mechanisms driving the assembly of ecological communities where individual species colonize and subsequently interact with each other. Two general classes of processes, niche-based deterministic processes (Chase and Leibold 2003) and random events-based stochastic processes (Bell 2001, Hubbell 2001), are known to operate in ecological communities. Recently, the debate on their relative importance for community assembly has been linked to modern species coexistence theory that differentiates the role of species niche and relative fitness differences (Chesson 2000, Adler et al. 2007, Mayfield and Levine 2010, HilleRisLambers et al. 2012). According to this theory, large niche and/or fitness differences among species would promote the importance of deterministic processes, whereas small niche and fitness differences would promote the importance of stochastic processes (Adler et al. 2007, HilleRisLambers et al. 2012). Under this framework, species' ecological differences become the key factor influencing the outcome of community assembly.

The ecological differences among species are often quantified using two approaches: the functional approach based on species functional traits (McGill et al. 2006, Violle et al. 2007), and the phylogenetic approach based on their evolutionary relationships (Webb et al. 2002, Cavender-Bares et al. 2009). The functional approach assumes that the differences in species functional traits, not their identity, translate into niche and fitness differences among species and thus would be linked to species' performance in community assembly (McGill et al. 2006, HilleRisLambers et al. 2012). While recognizing the utility of the functional approach, the phylogenetic approach

further assumes that species evolutionary history constrains changes in their functional traits and thus phylogenetic relationships between species would be an effective proxy of the overall differences in their traits (Webb et al. 2002). Although each approach has its own advantages and weaknesses (Cadotte et al. 2013), studying ecological communities with the functional and/or phylogenetic perspective has proven to be useful in helping understand mechanisms regulating community assembly (Best et al. 2012, Spasojevic and Suding 2012, Gerhold et al. 2013, Herben and Goldberg 2014). Notably, ecologists have recently just begun examining the basic assumptions of these approaches and that functional and phylogenetic relationships among species can adequately capture their niche and fitness differences (Best et al. 2012, Narwani et al. 2013, Godoy et al. 2014).

One important aspect of community assembly is the history of species colonization. It has long been hypothesized that variation in community assembly history may result in differences in species composition and abundance in the assembling communities (Gleason 1927, Egler 1954, Diamond 1975), an idea that has received supports from numerous theoretical and experimental investigations of community assembly (Drake 1991, Law and Morton 1993, Jiang and Patel 2008). The historical contingency of community structure observed in these studies thus highlights the importance of stochasticity associated with community assembly. However, an appreciable number of other studies have shown that variation in assembly history may not necessarily alter the structure of the assembled communities (Sommer 1991, Law and Morton 1996, Fukami 2004), pointing to the importance of deterministic processes. These different outcomes of community assembly have prompted investigations of various mechanisms influencing the historical contingency of ecological communities

(Chase 2003). Here we focus on examining the idea that ecological similarity of species in the regional species pool, captured by functional/phylogenetic diversity, may strongly influence the degree of community historical contingency.

In situations where regional species pools are characterized by low functional and phylogenetic diversity, earlier colonizing species, which share similar niche and fitness with later colonizing species, should have strong negative effects on the latter in the form of priority effects. The variation in the structure of local communities associated with priority effects would demonstrate the stochastic aspect of community assembly. On the other hand, in situations where species pools are characterized by high functional/phylogenetic diversity, large differences in species functional traits may be expressed as stabilizing niche differences and/or fitness differences. When stabilizing niche differences overcome relative fitness differences, large niche differences associated with high functional/phylogenetic diversity should promote the coexistence of various colonizing species. By contrast, when relative fitness differences overwhelm stabilizing niche differences, high functional/phylogenetic diversity of the species pool should favor the exclusion of competitively inferior species. In either case, high functional/phylogenetic diversity would be expected to promote deterministic community assembly, with assembly outcomes insensitive to changes in assembly history. Nevertheless, despite the general appeal of the above hypotheses and their importance for understanding community assembly, they have yet undergone rigorous experimental testing. Notably, the few studies that have conducted preliminary examinations of these hypotheses have not attempted to quantify species niche and fitness differences (Tan et al. 2012, Vannette and Fukami 2014). As a result, the mechanistic linkage between

functional/phylogenetic diversity of the species pool and deterministic/stochastic community assembly remain unsubstantiated.

In this chapter, we report on a laboratory experiment that examined the relevance of functional and phylogenetic diversity of the species pool for community assembly, using bacterivorous ciliated protist communities as our model systems. This model system allows direct measures of niche and fitness differences of species involved in community assembly, based on their influence on the composition and abundance of bacterial prey communities. This differs from the majority of existing empirical work that has tested the modern coexistence theory, which has generally quantified species niche/fitness differences through fitting data from competition experiments to mathematical models (e.g., Levine and HilleRisLambers 2009, Adler et al. 2010). The short generation times of protists also allowed us to study multi-generational community assembly in a relatively short period (Benton et al. 2007). We found that increasing functional and phylogenetic diversity of the species pool increase the determinism of community assembly, mainly through its positive effect on species niche differences.

Materials and Methods

Experimental organisms and microcosms

We assembled protist communities from 15 freshwater ciliated protist species (including *Blepharisma americanum, Colpidium kleini, Colpidium striatum, Colpoda sp., Glaucoma scintillans, Halteria grandinella, Loxocephalus sp., Paramecium aurelia, Paramecium bursaria, Paramecium caudatum, Paramecium multimicronucleatum, Paramecium tetraurelia, Spirostomum teres, Stylonychia notophora,* and *Tetrahymena*

pyriformis; Appendix B: Fig. B1). Among these species, *B. americanum*, *C. striatum*, and *T. pyriformis* were bought from Carolina Biological Supply (Burlington, NC, USA), whereas the other species were isolated from local ponds in Atlanta (GA, USA). Each protist species had been separately maintained in stock cultures on a mixture of bacteria, including *Bacillus cereus*, *Bacillus subtilis*, *Serratia marcescens*, and a number of unidentified bacterial species. All protist species can sustain their populations by feeding on bacteria; *B. americanum* is also known to produce cannibalistic forms that prey on smaller individuals of the same and other protist species. The cannibalistic forms, however, were rarely observed in our experiment.

Our microcosms were 250mL sterile glass bottles filled with 100mL bacterized nutrient medium, which was made by dissolving 0.5g Protozoan Pellets (Carolina Biological Supply, Burlington, NC, USA) per liter of deionized water. Three days before inoculating protist species to microcosms, we autoclaved the medium and inoculated it with a mixture of bacteria, obtained by mixing 1mL medium from the stock culture of each protist species and filtering the mixed medium through a syringe filter (pore size: 1.0μm) to remove all protists. After three-day incubation, we dispensed 100mL of the bacterized medium and added two autoclaved wheat seeds into each bottle to initiate the microcosms. We set up the first batch of stock cultures 15 days before the experiment and established new stock cultures every five days, using the same protocols as in the experiment. When introducing protist species to microcosms in the experiment, we only used the 15-day old stock cultures to minimize the potential physiological difference among individuals introduced on different dates. All the microcosms were incubated under 22^{o}C with a 12/12 light-dark cycle during the experiment.

Protist functional traits

To assess the functional differences between the 15 protist species, we measured six traits, including three morphological traits (cell volume, mouth size, and filter-feeding mode), one ethological trait (swimming speed), and two demographic traits (intrinsic growth rate and carrying capacity) (Table 2.1), which are most likely to influence species fitness (Violle et al. 2007). Values of traits, except for filter-feeding mode that is binary and obtained from Fenchel (1987), were measured as continuous variable in a separate experiment, which had the same microcosm setup as the main experiment but included only protist monocultures (see Appendix B for more details). Trait values were then standardized to have a mean of zero and a standard deviation of one. The Euclidean distance calculated based on the standardized six-trait matrix was used as the functional distance between species.

Phylogeny construction

We used small subunit ribosomal RNA (SSU rRNA) gene sequences for the construction of the phylogeny of the 15 ciliated protist species. The highly conserved SSU rRNA gene is known to well represent the evolutionary relationships among ciliates (e.g., Baroin-Tourancheau et al. 1992, Van de Peer et al. 1996). We constructed a maximum likehood tree and transformed the phylogeny into an ultrametric tree by using the nonparametric rate smoothing method (see Appendix B2 for more details). The phylogenetic distance between species was calculated by summing branch lengths of the intervening braches between them on the phylogeny (Faith 1992). A phylogenetic tree with the Bayesian method were also constructed and produced qualitatively similar results.

Table 2.1. A list of the traits used to calculate trait differences between the protist species and the phylogenetic signals of individual traits.

Type	Level of measure	Trait	Why is the trait important in our experiment?
Morphological	Individual	Cell volume	Optimal particle size for filter-feeding and clearance rate are proportional to cell size (Fenchel 1986).
		Mouth size	Mouth size differences correlate with the frequency of competitive exclusion (Violle *et al.* 2011).
		Filtration mode*	Water velocity and particle retention differ between different filtration mode (Fenchel 1987).
Demographic	Population	Intrinsic growth rate	Intrinsic growth rate indicates the rate a species can occupy a habitat as an early colonizer (Haddad *et al.* 2008).
		Carrying capacity	Carrying capacity indicates the maximum population size early colonizers can reach (Haddad *et al.* 2008).
Ethological	Individual	Swimming speed	Swimming speed may represent the ability of resource exploration in the water column and the rate of species dispersal.

* The filtration mechanism trait is a binary variable (oligohymenophorans / polyhymenophorans) determined from Fenchel (1987).

Assembly experiment

To eliminate the possible effect of species richness, which is potentially confounded with functional diversity, we manipulated the initial functional diversity of the protist communities in our experiment while fixing initial species richness at five. We calculated mean pairwise functional distance (MFD), the dendrogram-based FD (FD, Petchey and Gaston 2002; Fig. B1), the functional dispersion (FDis, Laliberté and Legendre 2010) for all possible five-species pools. Measures of functional diversity were highly correlated, and we only report our results based on MFD. We included three levels of functional diversity (low, medium, and high) in our experiment, and selected two combinations of five species (Table 2.2) at each functional diversity level according to their MFD. As species functional and phylogenetic distances were significantly correlated (Mantel's test, $r = 0.460$, $P < 0.001$), the established species pools also differed in their phylogenetic diversity. Notably, depending on whether the functional or the phylogenetic distances translate into key traits among species' traits, the correlation between species functional and phylogenetic distances may vary considerably (e.g., Best et al. 2013). Disentangling the influence of functional and phylogenetic distances on community structure, however, is beyond the scope of this paper.

To assemble communities from each species pool, we introduced species into microcosms following five different colonization sequences. The five sequences within each species pool differed in the identity of the first colonizing species, and had the remaining of species colonization order randomly determined. Each of the functional diversity-assembly history treatment combinations was replicated three times, resulting in a total of 90 microcosms. Following the colonization sequences, we inoculated ~100

Table 2.2. Species pool of the communities at low, medium, and high functional diversity treatments.

Species compositions	MFD
C. striatum, G. scintillans, Loxocephalus sp., P. aurelia, P. multimicronucleatum	2.282
B. americanum, C. kleini, P. aurelia, P. multimicronucleatum, S. notophora	2.880
C. kleini, H. grandinella, P. aurelia,S. notophora, T. pyriformis	3.039
Colpoda sp., H. grandinella, Loxocephalus sp.,P. caudatum, P. tetraurelia	3.089
Colpoda sp., C. striatum, H. grandinella, P. bursaria, S. teres	3.237
G. scintillans, P. bursaria, P. caudatum,S. notophora, S. teres	3.391

individuals of each species into the microcosms with a five-day interval. Starting from Day 5, we monitored population abundances in each microcosm every five days by taking a small sample (0.3~0.4 mL) from each microcosm, weighing and dispensing the sample on a petri-dish, and counting the numbers of individuals of each protist species in the sample under a dissecting microscope. After all species were introduced (Day 25), we added ~100 individuals of each species with population density lower than 10 individuals/mL (total population size < 1,000 individuals) to each microcosm after each counting event to minimize the risk of species extinction due to demographic stochasticity. Every five days from Day 12, we replenished each microcosm by replacing 5mL of medium with the same amount of fresh nutrient medium. The experiment lasted 60 days.

Measurement of species niche and relative fitness differences

We measured protist species' niche and relative fitness differences in a separate experiment by quantifying the composition and abundance of bacteria in their monocultures. Bacteria is the only food sources of protists in experimental microcosms. We considered the bacterial composition as a measure of niches for protists, and bacterial abundance as a measure of relative fitness for protists. The experiment contained 15 monocultures, one for each protist species and was replicated three times for a total of 45 microcosms. We sampled each microcosm for bacterial composition and abundance 15 days after protist species inoculation. The samples were serially diluted and plated on agar plates. After incubating the plates at room temperature for 7 days, we counted the number of colony forming units (CFUs) for each operational taxonomic group identified

based on bacterial colony morphology for each microcosm. For each protist species, we calculated total bacterial density in its monoculture as its R* (Tilman 1982), with lower R* indicative of greater competitive ability and differences in R* representing differences in their competitive ability (differences in relative fitness). Fox (2002) showed that despite the presence of multiple bacterial species, protist species with lower R* tended to be better competitors under the same environmental conditions as ours, as predicted by the R* rule (Tilman 1982). Fox (2002) also showed that R*s measured using plate counts were comparable to those measured using direct counts in the same study system. The relative fitness difference between each species pair was thus calculated as the absolute value of the difference in R* between species. The abundance of each bacterial species was then standardized to have a mean of zero and a standard deviation of one. The niche difference between each species pair was calculated as the Euclidean distance in a multi-dimensional space (the number of dimensions equals the number of bacterial species observed), based on the standardized bacterial abundance matrix.

Data analysis

To detect the phylogenetic signal of each functional trait, we performed the Blomberg's *K* tests (Blomberg et al. 2003) with 9,999 permutations. A value of $K > 1$ indicates greater phylogenetic signal than the null expectation that the trait is under Brownian motion evolution across the phylogeny; a value of $K < 1$ indicates less phylogenetic signal than the null expectation. To assess the relationship between species functional distance based on all six traits and phylogenetic distance, we conducted a Mantel's test with 9,999 permutations between the two distance matrices. We also used

Mantel's tests with 9,999 permutations to examine how species niche differences and fitness differences were related to functional and phylogenetic distance.

For each species pool, we calculated its functional diversity as mean pairwise functional distance (MFD) and its phylogenetic diversity as mean pairwise phylogenetic distance (MPD), following Webb et al. (2002). Despite the weekly inoculation of rare species during our experiment, some of these species (e.g., *Colpoda sp.* and *P. multimicronucleatum*) were constantly absent in our samples. These species were considered effectively extinct and not included in the calculation of realized α diversity, quantified as the number of species present in each microcosm at the end of the experiment.

If community assembly is historically contingent, local communities sharing the same species pool but assembled with different histories would differ in their species composition and abundance, resulting in high β-diversity between communities sharing the same species pool. In our experiment, this β-diversity between communities was calculated as the modified Gower's dissimilarities (Anderson et al. 2006),

$$\beta_{MG} = \sum_{k=1}^{p} w_k |x'_{1k} - x'_{2k}| \,/\, \sum_{k=1}^{p} w_k \qquad \text{(Equation 2.1)}$$

where p is the total number of species, $w_k = 0$ for joint absence and $w_k = 1$ otherwise, x'_{1k} and x'_{2k} are the transformed species abundances in the two communities being compared, $x'_k = \log_2 x + 1$ if the abundance $x > 0$ and $x'_k = 0$ otherwise (results remained qualitatively unchanged when using the log10 transformation). This dissimilarity index accounts for both changes in species composition and abundance, the

weight of which can be adjusted by changing the base of the logarithm transformation. This modified Gower's dissimilarity does not suffer from the lack of the ability to discriminate among highly similar communities (Cao et al. 1997) or erratic behavior in communities with sparse data (Clarke et al. 2006), as was found with the Bray-Curtis dissimilarity (Anderson et al. 2006). Finally, we directly estimated the strength of priority effects on a species within a given species pool, quantified as the slope of the linear regression of the abundance (log-transformed) of the species against its colonization order into the communities sharing the same species pool. Whereas slope values close to zero correspond to little priority effect, negative slopes values would indicate that populations were inhibited by earlier colonizing species, suggesting inhibitory priority effects. The overall priority effects of a species pool was calculated as the average of the strength of priority effects of each member species in that species pool.

To assess how functional/phylogenetic diversity of the species pool influenced species coexistence, we regressed the observed α diversity in local communities against MFD/MPD of the corresponding species pool. We then regressed α diversity against species niche and fitness differences, averaged across all species belonging to the same species pool, to discern how the two types of species differences contributed to coexistence. Similarly, we used simple regressions to assess the relationships between MDF/MPD of the species pool and β diversity across local communities sharing the same species pool, and the relationships between species niche/fitness differences and β diversity. Finally, we related the strength of the priority effect on a species to MDF/MPD and species niche/fitness differences of the species pool using a linear mixed model, by considering all species together and treating species identity as the random factor.

All statistical analyses were conducted in R 3.0.2 (http://www.R-project.com). The Blomberg's *K* test and phylogenetic diversity calculations were performed in the *picante* package (Kembel et al. 2010), and functional dispersion calculations were performed in the *FD* package (Laliberté and Legendre 2010).

Results

The Blomberg's *K* test indicated that the three morphological traits (cell volume, mouth size, and filtration mode), but not the two demographic traits (intrinsic growth rate and carrying capacity) or the ethological trait (swimming speed), exhibited significant phylogenetic signal (Appendix B: Fig. B1, Table B1). When all traits were considered together, species functional differences were positively related to their phylogenetic differences (Mantel's test, $r = 0.460$, $P < 0.001$). Species niche differences were positively related to both functional and phylogenetic distances (Mantel's test, functional distance, $r = 0.363$, $P = 0.009$; phylogenetic distance, $r = 0.374$, $P = 0.017$). Species relative fitness differences, however, were positively related to phylogenetic distances only (Mantel's test, functional distance, $r = 0.032$, $P = 0.383$; phylogenetic distance, $r = 0.216$, $P = 0.048$).

Increasing MFD and MPD of the species pools resulted in an increase of α diversity of the assembled communities (MFD, $R^2 = 0.193$ $P < 0.001$, Fig. 2.1a; MPD, $R^2 = 0.172$, $P < 0.001$; Fig. 2.1b). Considering species niche and fitness differences, we found that α diversity of the assembled communities increased with niche difference ($R^2 = 0.394$, $P < 0.001$, Fig. 2.2a), but not relative fitness difference ($R^2 = 0$, $P = 0.583$; Fig. 2.2b), of the species pool.

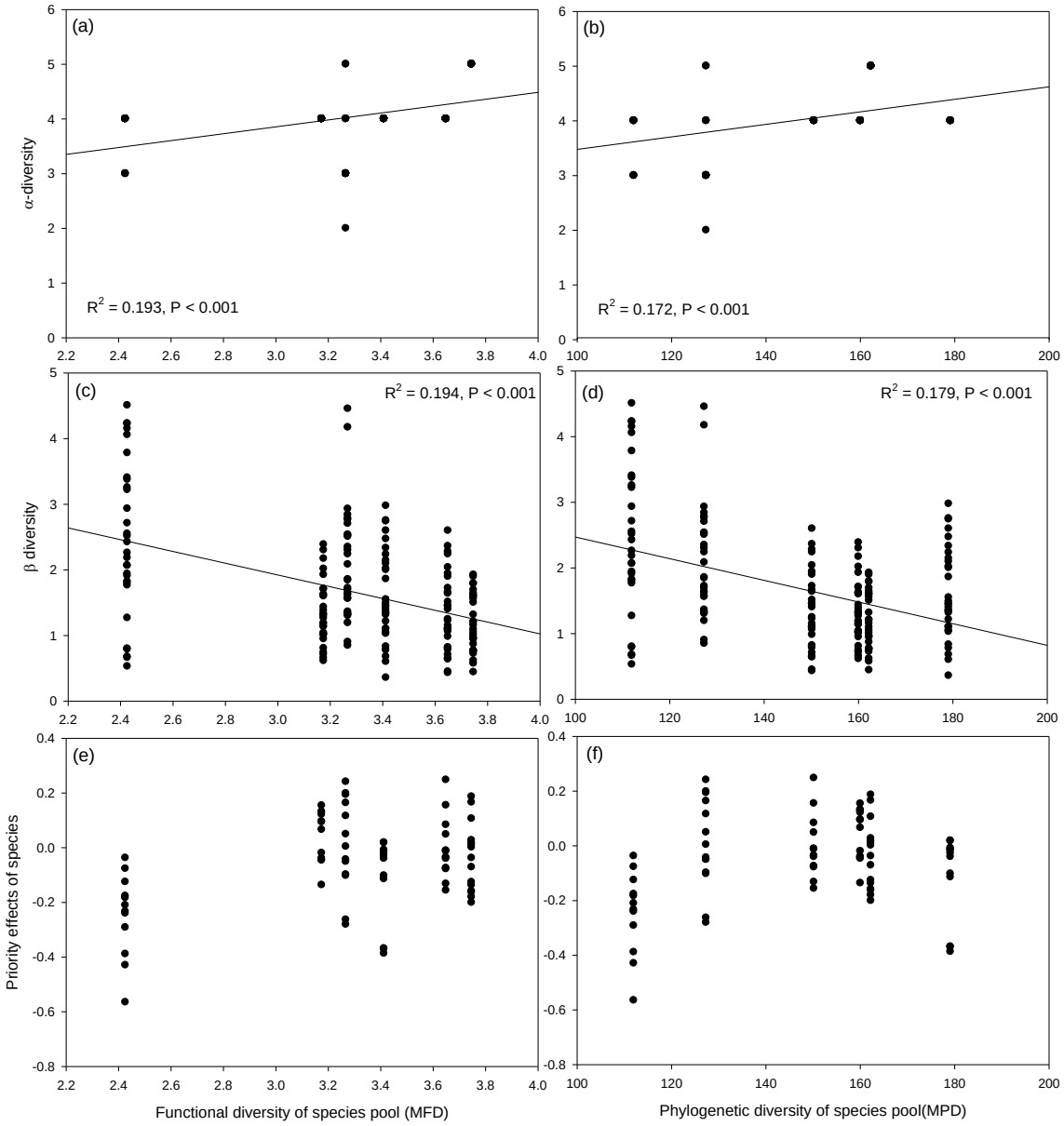

Fig. 2.1. The relationships between initial functional diversity of species pools (MFD) and initial phylogenetic diversity of species pools (MPD) and (a, b) α diversity, (c, d) β diversity, and (e, f) the strength of priority effects of species. (a, b) Each point represents α diversity in a community. (c, d) Each point represents the average modified Gower's dissimilarity between a pair of communities characterized by the same species pool. (e, f) Each point represents the strength of priority effects of a species, based on the estimated slope of linear regressions between species colonization order and species abundance, in a species pool (see Methods for details). The solid lines in plot (a-c) represent the fitted lines in linear regressions.

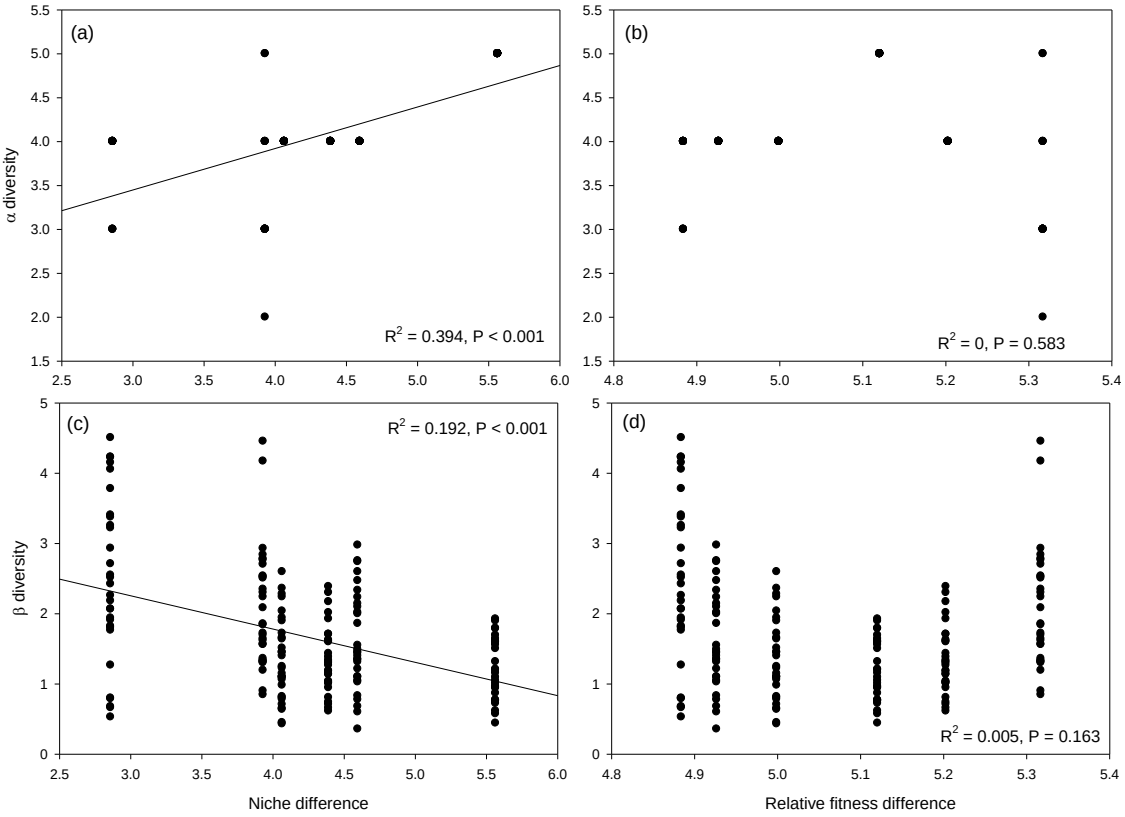

Fig. 2.2. The relationships between α diversity and the strength of priority effects of species, and niche difference and relative fitness difference. (a, b) Each point represents α diversity of a community. (c, d) Each point represents the strength of priority effects of a species. See Methods for the details of estimating priority effects. The solid lines represent the fitted lines in linear regressions.

β diversity among communities sharing the same species pools but subjected to different assembly histories significantly decreased as functional and phylogenetic diversity of the species pools increased (MFD, $R^2 = 0.194$, $P < 0.001$, Fig. 2.1c; MPD, $R^2 = 0.179$, $P < 0.001$, Fig. 2.1d). β diversity also showed a significant negative relationship with species niche difference in the species pool ($R^2 = 0.192$, $P < 0.001$; Appendix B, Fig. B2a), but showed little response to changes in species fitness difference in the species pool ($R^2 = 0.005$, $P = 0.163$; Appendix B, Fig. B2b).

The value of priority effects was positively related to MFD and MPD (linear mixed model, MFD, $t_{63} = 6.131$, $P < 0.001$, Fig. 2.1e; MPD, $t_{63} = 4.883$, $P < 0.001$, Fig. 2.1f), indicating stronger inhibitory priority effects (i.e., more negative values) in communities with lower MFD/MPD. Both increasing niche difference (linear mixed model, $t_{63} = 4.666$, $P < 0.001$) and relative fitness difference (linear mixed model, $t_{63} = 3.371$, $P = 0.001$) resulted in decreased inhibitive priority effects. As expected, β diversity was greater in communities with stronger inhibitive priority effects ($R^2 = 0.137$, $P < 0.001$; Appendix B, Fig. B2c), indicating the latter as an important contributor to the former.

Discussion

Our results showed that increasing functional and phylogenetic diversity of a regional species pool reduced β-diversity among the assembled communities subjected to different colonization histories. A significant proportion of the variation in β-diversity was driven by priority effects, which were more negative (i.e., stronger inhibition of earlier species on later species) in communities with lower functional and phylogenetic diversity. These findings provide strong support for our hypothesis that that increased

functional and phylogenetic diversity of the species pool tends to reduce the likelihood of historical contingency in community assembly. Moreover, by explicitly considering species coexistence mechanisms, our study produces the unique finding that functional and phylogenetic diversity influenced community assembly mainly through altering species niche differences. To our knowledge, our study is the first to link species functional traits, niche and fitness differences, and diversity within and between communities together to gain a more mechanistic understanding of community assembly.

Using contemporary species coexistence theory (Chesson 2000) as a framework, we hypothesized that the negative relationship between functional/phylogenetic diversity and β-diversity could arise from varied species' ecological differences along the functional/phylogenetic diversity gradient, characterized by species niche and relative fitness differences. Our results showed that both species functional and phylogenetic distance translated into their niche differences, and phylogenetic distances also translated into relative fitness differences. We further showed that species niche differences, but not fitness differences, strongly influenced β-diversity. These results, combined with the finding that niche differences, not relative fitness differences, were also a significant predictor of α-diversity, suggest the predominant role of species niche differences in structuring the assembled communities. Presumably, communities with the species pools of lower functional/phylogenetic diversity experienced strong competitive interactions due to lower niche differences among them, resulting in lower α-diversity and stronger historical contingency (both contributing to high β-diversity). On the other hand, greater niche differences among species in the species pools characterized by higher functional and phylogenetic diversity resulted in weakened competition, favoring species

coexistence and reducing the strength of inhibitive priority effects (both contributing to low β-diversity).

Our results on α-diversity support Darwin's phylogenetic limiting similarity hypothesis, which states that closely related species compete strongly by virtue of their similar niches (Darwin 1859). Previous empirical tests of this hypothesis, however, have produced mixed results (positive findings: Jiang et al. 2010, Violle et al. 2011, Peay et al. 2012, Tan et al. 2012; negative findings: Cahill et al. 2008, Best et al. 2012, Narwani et al. 2013, Godoy and Levine 2014, Godoy et al. 2014). One explanation for this discrepancy is that competitive outcomes are driven by not only species niche differences but also by their relative fitness differences (Chesson 2000), such that the phylogenetic limiting similarity hypothesis, which only considers niche differences, may not necessarily hold if relative fitness differences are important (Mayfield and Levine 2010). A related explanation is that even if species niche differences are important, we still may not observe a clear relatedness-competition pattern if these differences are not phylogenetically conserved (Mayfield and Levine 2010). Several recent studies have considered both niche and fitness differences in testing the phylogenetic limiting similarity hypothesis. For example, Nawarni et al. (2013) reported that the evolutionary relationships among freshwater green algae did not predict species niche or fitness differences, and consequently, held little predictive power for competitive outcomes within the taxonomic group. Godoy et al. (2014) reported that fitness differences, not niche differences, were phylogenetically conserved among the annual plant species they studied in California. Nevertheless, a non-significant effect of relatedness on competitive outcomes still resulted because of more distantly related species exhibiting larger

variations in their fitness differences. Using bacterivorous ciliated protists, we demonstrate that although both niche and relative fitness differences increased with phylogenetic distances, niche differences were the main driver of species coexistence. We suggest that this scenario may also apply to the study of Violle et al. (2011), who reported patterns consistent with Darwin's hypothesis emerging among 10 competing ciliate bacterivores but did not look into coexistence mechanisms. The overwhelming importance of niche difference in our study reflects the ability of ciliate bacterivores to differentiate among different bacterial prey resources (Fencel 1987). Overall, the extremely small number of existing studies that linked species niche and fitness differences to relatedness and their conflicting findings precludes any general conclusions, emphasizing the need for more empirical studies on this topic.

Inhibitive priority effects, where species that colonize a habitat early have negative effects on later colonizing species, constitute an important mechanism contributing to the historical contingency of community assembly (Chase 2003). Consistent with our hypothesis, our results showed that early colonizers more strongly inhibited the population size of later colonizers when the species pools were phylogenetically and functionally less diverse (Fig. 2.1). This result is also consistent with another hypothesis of Darwin (1859) stating that native communities containing species closely related to invaders are better at resisting biological invasions (i.e., Darwin's naturalization hypothesis). While empirical tests of Darwin's naturalization hypothesis have been largely observational in nature (but see Jiang et al. 2010, Castro et al. 2014) and have yielded mixed findings (Diez et al. 2009; Schaefer et al. 2011; Park and Potter 2013; reviewed by Thuiller et al. 2010), the few experimental studies that

quantified the strength of priority effects in relation to phylogenetic/functional diversity has produced similar results to ours (Peay et al. 2012, Tan et al. 2012, Vannette and Fukami 2014). Nevertheless, previous experimental studies have followed the logic of Darwin and attributed their results to increased niche similarity between more closely related species only. Building on these studies, our experiment explicitly evaluated the relative importance of niche and fitness differences for priority effects. Unlike α-diversity and β-diversity, which were affected by niche differences only, we found that both niche and fitness differences contributed to the variation in priority effects. This result thus points to the role of species competitive ability, in addition to niche characteristics, for regulating their abundance in competition. Therefore, changing functional and phylogenetic diversity of the species pool in our experiment altered priority effects through changing both niche and fitness differences. Note, however, that niche differences still accounted for more variation in priority effects than fitness differences, and that when we considered both differences together in a single regression model, the effect of niche differences was no longer significant (niche difference, $t_{62} = 3.909$, $P < 0.001$; fitness difference, $t_{62} = 0.790$, $P = 0.432$). This important role of niche differences for priority effects is consistent with its predominant effects on α- and β-diversity.

Phylogenetic knowledge has been increasingly used as a source of information complementary to the knowledge of species trait in identifying mechanisms regulating the structure of natural communities (Pavoine and Bonsall 2011). Here we suggest that considering the effect of both functional and phylogenetic diversity on community assembly experiments could also bring considerable benefits, particularly in identifying functionally important traits (Table 2.3). Functional diversity in our experiment were

Table 2.3. The use of both functional diversity (FD) and phylogenetic diversity (PD) can help pinpoint key functional traits.

	PD	
FD	Significant/strong effect	Non-significant/weak effect
Significant/strong effect	Key functional traits are phylogenetically conserved and have been measured	Key functional traits are not phylogenetically conserved and have been measured
Non-significant/weak effect	Key functional traits are phylogenetically conserved and have not been measured	Key functional traits are not phylogenetically conserved and have not been measured

based on six functional traits, with each trait reflecting some aspect of species ecological difference (Table 2.1). Functional and phylogenetic diversity showed similar predictive power for α-diversity, β-diversity, and priority effects, suggesting a pattern consistent with our prediction when functional diversity and phylogenetic diversity translated into the variation of key functional traits and that key functional traits are phylogenetically conserved (Table 2.3). However, the fact that species fitness differences were related to species phylogenetic distances, but not functional distances, suggests that important traits controlling species fitness remain unidentified. Therefore, while the traits we measured did not capture the full spectrum of ecological differences among species, they nevertheless captured key niche differences important for driving community assembly. As another example, Best et al. (2013) found that feeding trait diversity, not phylogenetic diversity, explained the structure of experimentally assembled marine amphipod herbivore communities. According to Table 2.3, this finding suggests that important feeding traits are not phylogenetically conserved and need to be measured instead of assumed from phylogeny, a result confirmed by Best et al. (2013).

In a highly provocative paper, Chase (2003) asked the question when history matters for community assembly. To address this question, we experimentally manipulated species ecological differences, characterized by functional and phylogenetic diversity of the species pool, and demonstrated their importance for modulating the degree of historical contingency of community assembly. In doing so, we found that not all ecological differences mattered: niche differences, rather than fitness differences, played a predominant role in driving community assembly in our experiment. Our findings help identify two important areas for future research. First, our results showed

that the functional traits we measured were relevant for species niches, but not fitness. Nevertheless, little empirical knowledge exists on how different species traits relate to niche and relative fitness differences (but see Kraft et al. 2015). There is therefore an urgent need for futures studies to identify and distinguish important functional traits linked to the two types of ecological differences. Second, whereas ecological theory suggests that species niche and fitness differences combine to influence community assembly (Chesson 2000, Mayfield and Levine 2011, HilleRisLambers et al. 2012), our results demonstrated the overriding importance of niche differences. The existence of few empirical studies on this topic (Levine and HilleRisLambers 2009, Narwani et al. 2013, Godoy et al. 2014) means that more studies are needed before we can draw any general conclusions on the relative importance of niche and fitness differences for community assembly.

References

Adler, P. B., J. HilleRisLambers, and J. M. Levine. 2007. A niche for neutrality. Ecology Letters 10:95-104.

Anderson, M. J., K. E. Ellingsen, and B. H. McArdle. 2006. Multivariate dispersion as a measure of beta diversity. Ecology Letters 9:683-693.

Baroin-Tourancheau, A., P. Delgado, R. Perasso, and A. Adoutte. 1992. A broad molecular phylogeny of ciliates: identification of major evolutionary trends and radiations within the phylum. Proceedings of the National Academy of Sciences 89:9764-9768.

Bell, G. 2001. Neutral macroecology. Science 293:2413-2418.

Benton, T. G., M. Solan, J. M. J. Travis, and S. M. Sait. 2007. Microcosm experiments can inform global ecological problems. Trends in Ecology & Evolution 22:516-521.

Best, R. J., N. C. Caulk, and J. J. Stachowicz. 2013. Trait vs. phylogenetic diversity as predictors of competition and community composition in herbivorous marine amphipods. Ecology Letters 16:72-80.

Blomberg, S. P., T. Garland, and A. R. Ives. 2003. Testing for phylogenetic signal in comparative data: Behavioral traits are more labile. Evolution 57:717-745.

Darwin, C. 1859. On the origin of species. John Murray, London.

Cadotte, M., C. H. Albert, and S. C. Walker. 2013. The ecology of differences: assessing community assembly with trait and evolutionary distances. Ecology Letters 16:1234-1244.

Cahill, J. F., S. W. Kembel, E. G. Lamb, and P. A. Keddy. 2008. Does phylogenetic relatedness influence the strength of competition among vascular plants? Perspectives in Plant Ecology, Evolution and Systematics 10:41-50.

Cao, Y., W. P. Williams, and A. W. Bark. 1997. Similarity measure bias in river benthic Aufwuchs community analysis. Water Environment Research 69:95-106.

Castro, S. A., V. M. Escobedo, J. Aranda, and G. O. Carvallo. 2014. Evaluating Darwin's Naturalization Hypothesis in Experimental Plant Assemblages: Phylogenetic Relationships Do Not Determine Colonization Success. Plos One 9.

Cavender-Bares, J., K. H. Kozak, P. V. A. Fine, and S. W. Kembel. 2009. The merging of community ecology and phylogenetic biology. Ecology Letters 12:693-715.

Chase, J. M. 2003. Community assembly: when should history matter? Oecologia 136:489-498.

Chase, J. M., and M. A. Leibold. 2003. Ecological niches: linking classical and contemporary approaches. University of Chicago Press, Chicago, IL.

Chesson, P. 2000. Mechanisms of maintenance of species diversity. Annual Review of Ecology and Systematics:343-366.

Clarke, K. R., P. J. Somerfield, and M. G. Chapman. 2006. On resemblance measures for ecological studies, including taxonomic dissimilarities and a zero-adjusted Bray–

Curtis coefficient for denuded assemblages. Journal of Experimental Marine Biology and Ecology 330:55-80.

Diamond, J. M. 1975. Assembly of Species Communities. Pages 342-444 in M. L. Cody and J. M. Diamond, editors. in Ecology and Evolution of Communities. Harvard.

Diez, J. M., P. A. Williams, R. P. Randall, J. J. Sullivan, P. E. Hulme, and R. P. Duncan. 2009. Learning from failures: testing broad taxonomic hypotheses about plant naturalization. Ecology Letters 12:1174-1183.

Drake, J. A. 1991. Community assembly mechanics and the structure of an experimental species ensemble. American Naturalist 137:1-26.

Egler, F. E. 1954. Vegetation science concepts I. Initial floristic composition, a factor in old-field vegetation development with 2 figs. Vegetatio 4:412-417.

Faith, D. P. 1992. Conservation evaluation and phylogenetic diversity. Biological Conservation 61:1-10.

Fenchel, T. 1987. Ecology of Protozoa. Science Tech, Madison, WI.

Fox, J. W. 2002. Testing a simple rule for dominance in resource competition. American Naturalist 159:305-319.

Fukami, T. 2004. Assembly history interacts with ecosystem size to influence species diversity. Ecology 85:3234-3242.

Gerhold, P., J. N. Price, K. Pussa, R. Kalamees, K. Aher, A. Kaasik, and M. Partel. 2013. Functional and phylogenetic community assembly linked to changes in species diversity in a long-term resource manipulation experiment. Journal of Vegetation Science 24:843-852.

Gleason, H. A. 1927. Further views on the succession-concept. Ecology 8:299-326.

Godoy, O., N. J. Kraft, and J. M. Levine. 2014. Phylogenetic relatedness and the determinants of competitive outcomes. Ecology Letters.

Godoy, O., and J. M. Levine. 2014. Phenology effects on invasion success: insights from coupling field experiments to coexistence theory. Ecology 95:726-736.

Haddad, N. M., M. Holyoak, T. M. Mata, K. F. Davies, B. A. Melbourne, and K. Preston. 2008. Species' traits predict the effects of disturbance and productivity on diversity. Ecology Letters 11:348-356.

Herben, T., and D. E. Goldberg. 2014. Community assembly by limiting similarity vs. competitive hierarchies: testing the consequences of dispersion of individual traits. Journal of Ecology 102:156-166.

HilleRisLambers, J., P. Adler, W. Harpole, J. Levine, and M. Mayfield. 2012. Rethinking community assembly through the lens of coexistence theory. Annual Review of Ecology, Evolution, and Systematics 43:227-248.

Hubbell, S. P. 2001. The Unified Neutral Theory of Biodiversity and Biogeography. Priceton University Press, Princeton, NJ.

Jiang, L., and S. N. Patel. 2008. Community assembly in the presence of disturbance: A microcosm experiment. Ecology 89:1931-1940.

Jiang, L., J. Q. Tan, and Z. C. Pu. 2010. An Experimental Test of Darwin's Naturalization Hypothesis. American Naturalist 175:415-423.

Kembel, S. W., P. D. Cowan, M. R. Helmus, W. K. Cornwell, H. Morlon, D. D. Ackerly, S. P. Blomberg, and C. O. Webb. 2010. Picante: R tools for integrating phylogenies and ecology. Bioinformatics 26:1463-1464.

Kraft, N. J., O. Godoy, and J. M. Levine. 2015. Plant functional traits and the multidimensional nature of species coexistence. Proceedings of the National Academy of Sciences 112:797-802.

Laliberté, E., and P. Legendre. 2010. A distance-based framework for measuring functional diversity from multiple traits. Ecology 91:299-305.

Law, R., and R. D. Morton. 1993. Alternative Permanent States of Ecological Communities. Ecology 74:1347-1361.

Law, R., and R. D. Morton. 1996. Permanence and the assembly of ecological communities. Ecology 77:762-775.

Levine, J. M., and J. HilleRisLambers. 2009. The importance of niches for the maintenance of species diversity. Nature 461:254-257.

Mayfield, M. M., and J. M. Levine. 2010. Opposing effects of competitive exclusion on the phylogenetic structure of communities. Ecology Letters 13:1085-1093.

McGill, B. J., B. J. Enquist, E. Weiher, and M. Westoby. 2006. Rebuilding community ecology from functional traits. Trends in Ecology & Evolution 21:178-185.

Narwani, A., M. A. Alexandrou, T. H. Oakley, I. T. Carroll, and B. J. Cardinale. 2013. Experimental evidence that evolutionary relatedness does not affect the ecological mechanisms of coexistence in freshwater green algae. Ecology Letters 16:1373-1381.

Park, D. S., and D. Potter. 2013. A test of Darwin's naturalization hypothesis in the thistle tribe shows that close relatives make bad neighbors. Proceedings of the National Academy of Sciences of the United States of America 110:17915-17920.

Pavoine, S., and M. B. Bonsall. 2011. Measuring biodiversity to explain community assembly: a unified approach. Biological Reviews 86:792-812.

Peay, K. G., M. Belisle, and T. Fukami. 2012. Phylogenetic relatedness predicts priority effects in nectar yeast communities. Proceedings of the Royal Society B-Biological Sciences 279:749-758.

Petchey, O. L., and K. J. Gaston. 2002. Functional diversity (FD), species richness and community composition. Ecology Letters 5:402-411.

Schaefer, H., O. J. Hardy, L. Silva, T. G. Barraclough, and V. Savolainen. 2011. Testing Darwin's naturalization hypothesis in the Azores. Ecology Letters 14:389-396.

Sommer, U. 1991. Convergent Succession Of Phytoplankton In Microcosms With Different Inoculum Species Composition. Oecologia 87:171-179.

Spasojevic, M. J., and K. N. Suding. 2012. Inferring community assembly mechanisms from functional diversity patterns: the importance of multiple assembly processes. Journal of Ecology 100:652-661.

Tan, J. Q., Z. C. Pu, W. A. Ryberg, and L. Jiang. 2012. Species phylogenetic relatedness, priority effects, and ecosystem functioning. Ecology 93:1164-1172.

Thuiller, W., L. Gallien, I. Boulangeat, F. de Bello, T. Munkemuller, C. Roquet, and S. Lavergne. 2010. Resolving Darwin's naturalization conundrum: a quest for evidence. Diversity and Distributions 16:461-475.

Tilman, D. 1982. Resource competition and community structure. Princeton University Press, Princeton, N.J.

Van de Peer, Y., G. Van der Auwera, and R. De Wachter. 1996. The evolution of stramenopiles and alveolates as derived by “substitution rate calibration» of small ribosomal subunit RNA. Journal of Molecular Evolution 42:201-210.

Vannette, R. L., and T. Fukami. 2014. Historical contingency in species interactions: towards niche-based predictions. Ecology Letters 17:115-124.

Violle, C., M. L. Navas, D. Vile, E. Kazakou, C. Fortunel, I. Hummel, and E. Garnier. 2007. Let the concept of trait be functional! Oikos 116:882-892.

Violle, C., D. R. Nemergut, Z. C. Pu, and L. Jiang. 2011. Phylogenetic limiting similarity and competitive exclusion. Ecology Letters 14:782-787.

Webb, C. O., D. D. Ackerly, M. A. McPeek, and M. J. Donoghue. 2002. Phylogenies and community ecology. Annual Review of Ecology and Systematics 33:475-505.

CHAPTER 3

PHYLOGENETIC DIVERSITY STABILIZES COMMUNITY BIOMASS

Abstract

The relationship between biodiversity and ecological stability is a long-standing issue in ecology. Current diversity-stability studies, which have largely focused on species diversity, often report an increase in the stability of aggregate community properties with increasing species diversity. Few studies have examined the linkage between phylogenetic diversity, another important dimension of biodiversity, and stability. By taking species evolutionary history into account, phylogenetic diversity may better capture the diversity of traits and niches of species in a community than species diversity and better relate to temporal stability. In this study, we investigated whether phylogenetic diversity could affect temporal stability of community biomass independent of species diversity.

We performed an experiment in laboratory microcosms with a pool of 12 bacterivorous ciliated protist species. To eliminate the possibility of species diversity effects confounding with phylogenetic diversity effects, we assembled communities that had the same number of species but varied in the level of phylogenetic diversity. Weekly disturbance, in the form of short-term temperature shock, was imposed on each microcosm and species abundances were monitored over time. We examined the relationship between temporal stability of community biomass and phylogenetic

diversity, and evaluated the role of several stabilizing mechanisms for explaining the influence of phylogenetic diversity on temporal stability.

Our results showed that increasing phylogenetic diversity promoted temporal stability of community biomass. Both total community biomass and summed variances showed a U-shaped relationship with phylogenetic diversity, driven by the presence of large, competitively superior species that attained large biomass and high temporal variation in their biomass in both low and high phylogenetic diversity communities. Communities without these species showed patterns consistent with the reduced strength of competition and increasingly asynchronous species responses to environmental changes under higher phylogenetic diversity, two mechanisms that can drive positive diversity-stability relationships. These results support the utility of species phylogenetic knowledge for predicting ecosystem functions and their stability.

Introduction

The question of how biodiversity affects ecosystem functioning has received much recent attention from ecologists (Cardinale et al. 2012, Hooper et al. 2012, Naeem et al. 2012), due to the increasing concern on the global biodiversity loss and its potential consequences for the sustainability of natural and managed ecosystems that support humanity. The temporal stability of ecosystem functions is a fundamental property of ecological communities, and understanding its regulatory mechanisms is important for effective conservation and management of ecosystems in the face of environmental changes (Srivastava and Vellend 2005). Considerable research in the past two decades has examined the linkage between species diversity, arguably the most studied

component of biodiversity, and temporal stability, one of the most studied concepts of ecological stability (e.g., Tilman et al. 2006, Jiang et al. 2009). This research, which ties with the classic work on the relationship between ecological complexity and stability (MacArthur 1955, May 1973, McCann 2000), has shown that increasing species diversity tends to increase the temporal stability of aggregate community biomass (reviewed by Jiang and Pu 2009, Campbell et al. 2011). Theory has identified two main mechanisms that can lead to positive diversity-stability relationships. First, differential species responses to environmental changes allow species in a community to produce asynchronous population dynamics in the event of environmental fluctuations, resulting in more stable aggregate biomass in more diverse communities (Ives and Hughes 2002, Loreau and de Mazancourt 2008, 2013). This insurance hypothesis (*sensu* Yachi and Loreau 1999), which has received some direct experimental support (e.g., Leary and Petchey 2009), emphasizes the role of niche differences among species for promoting community stability. Second, reduction in the strength of interspecific competition has recently been identified as a potentially important mechanism for stabilizing ecological communities (Loreau and de Mazancourt 2013). Reduced interspecific competition facilitates species coexistence and increases community biomass (i.e., overyielding, Tilman 1999), which acts to mitigate the influences of demographic stochasticity (Loreau and de Mazancourt 2013). Note that this mechanism of reduced competition also arises from differences in species niches, specifically those related to resource use. A number of studies have reported overyielding associated with positive relationships between species diversity and community biomass stability (summarized in Jiang and Pu 2009), yet none of these studies have investigated how changing species diversity alters the strength of

competition or more directly, the degree of niche differences among species. It is important to note, however, that the number of species in a community is a relatively crude proxy of the diversity of species traits and niches in the community (Diaz and Cabido 2001, McGill et al. 2006), making it difficult to manipulate the importance of stabilizing mechanisms by changing species diversity.

Aspects of species niches are often conserved over evolutionary timescales such that more closely related species tend to share more similar niches (Wiens and Graham 2005, Wiens et al. 2010), a phenomenon termed phylogenetic niche conservatism. Under phylogenetic niche conservatism, phylogenetic diversity, which accounts for species evolutionary relationships, may represent an effective approach to characterizing the niche differences among species in a community without actually quantifying individual species niches. Thus, higher phylogenetic diversity could potentially allow communities to occupy more niches and utilize more resources, translating into greater levels of ecosystem functioning. Consistent with this idea, several studies have shown that increasing community phylogenetic diversity resulted in increased ecosystem functions such as biomass production (Cadotte et al. 2008, 2009, Flynn et al. 2011, Tan et al. 2012) and decomposition (Tan et al. 2012). Here we suggest that increasing phylogenetic diversity may increase temporal stability of aggregate community properties by promoting stabilizing mechanisms. First, under niche conservatism, species in communities with higher phylogenetic diversity would exhibit more diverse responses to environmental fluctuations, promoting the degree of asynchrony in their population dynamics. Second, as originally hypothesized by Darwin (1859), greater differences in species niches in communities with higher phylogenetic diversity may act to reduce the

intensity of competition; this may, in turn, result in overyielding that buffers communities against demographic stochasticity (Loreau and de Mazancourt 2013). Using bacterivorous protists as model organisms, Violle et al. (2011) provided strong experimental evidence for the linkage between competition strength and phylogenetic diversity as predicted by Darwin (1859). Finally, increasing phylogenetic diversity may also increase the temporal stability of aggregate community biomass by increasing the likelihood that more diverse communities contain clades characterized with relatively stable dynamics (the phylogenetic sampling effect; Cadotte et al. 2012). This phylogenetic sampling effect is based on the assumption that population stability is phylogenetically conserved, such that species in different clades of a phylogenetic tree potentially differ in their stability.

We examined the effect of phylogenetic diversity on the temporal stability of community biomass with a protist microcosm experiment in which we monitored the dynamics of bacterivorous protist communities that differed in phylogenetic diversity. To eliminate the possibility that effects of species diversity may confound with those of phylogenetic diversity, we fixed the initial number of species in each microcosm at a constant level (three species); the majority of microcosms retained their initial species composition without losing species during the experiment. Protist competition for bacterial resources is well depicted by Lotka-Volterra models (e.g., Gause 1934, Vandermeer 1969), making them an excellent model system for testing predictions from the same type of models that were often used to investigate diversity and stability relationships (e.g., Ives and Hughes 2002, Loreau and de Mazancourt 2013). Data on community dynamics over multiple generations of study organisms are essential for

temporal stability analyses, which were facilitated by the short generation times of our experimental protists (ranging from a few hours to days).

Methods

Experimental organisms

The protist communities in our experiment were assembled from a pool of 12 bacterivorous ciliated protist species (Fig. 3.1). These species were chosen because they maintain robust populations in stock cultures and because their 18S rRNA gene sequences, which can be used for phylogeny construction, are available online. Because of its highly conserved sequences and ubiquity in eukaryotic organisms, the 18S rRNA gene has been frequently used to determine evolutionary relationships within and between different eukaryotic taxa, including ciliates (e.g., Baroin-Tourancheau *et al.* 1992, Van de Peer *et al.* 1996). Prior to the experiment, each species had been cultured on a mixture of bacteria, including *Bacillus cereus*, *Bacillus subtilis*, *Serratia marcescens*, and a number of unidentified species. The same multi-species bacterial assemblage, which allowed the coexistence of multiple protist species (e.g., Jiang et al. 2011), was also used in our experiment. The stock culture of each protist species was separately raised in an aqueous medium containing 0.55 g/L protozoan pellet (Carolina Biological Supply Company, Burlington, NC, USA) per liter of deionized water.

Phylogeny reconstruction

The phylogeny of the 12 protist species was constructed based on their 18S rRNA gene sequences. The aligned 18S rRNA sequences of these species plus an

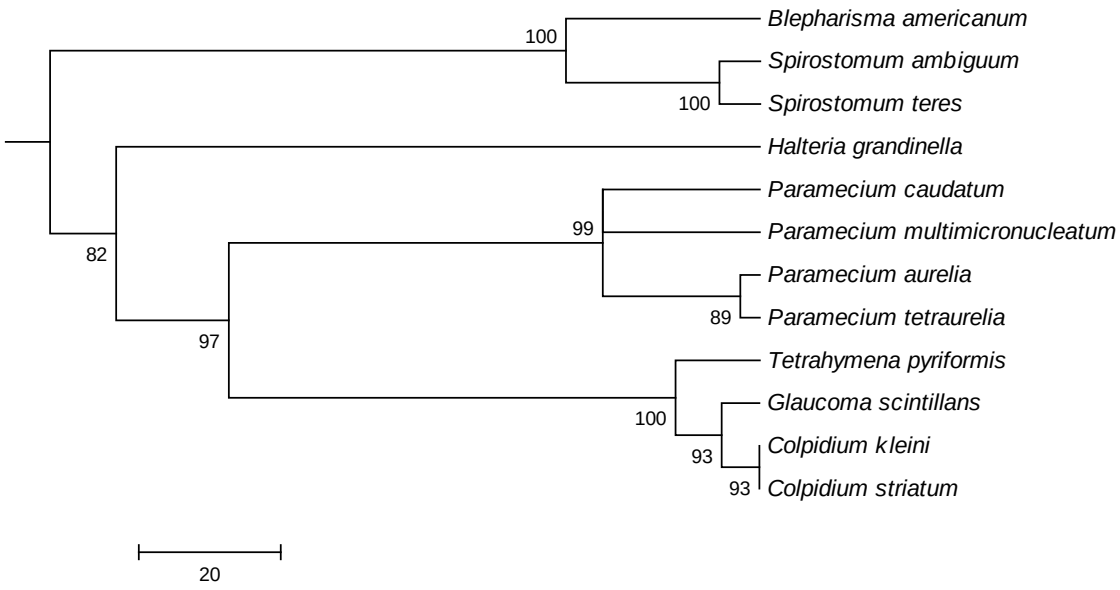

Fig. 3.1. The phylogenetic tree of the 12 bacterivorous protozoan species used in the experiment. The phylogeny was reconstructed using the maximum likelihood method based on the 18S rRNA sequences of each species (see main text for details). Values on the nodes indicate scores of the approximate likelihood ratio test as statistical nodal support (Guindon et al., 2010).

outgroup species, *Sarcocystis lacerate*, were obtained from the SILVA rRNA database (Pruesse *et al.*, 2007), and checked manually and in Gblocks (Castresana, 2000) to remove poorly aligned or highly divergent regions. Model testing with jModelTest 2 (Darriba *et al.*, 2012) suggested the HKY model with gamma-distributed (HKY+G, gamma = 0.181) rate variation among sites as the best substitution model. We constructed a maximum likelihood (ML) phylogenetic tree in PhyML with a BIONJ starting tree, and transformed the ML tree into an ultrametric tree that accommodates evolution rate heterogeneity across lineages using r8s with the nonparametric rate smoothing method (Sanderson, 2003). Results of a phylogenetic tree produced by the Bayesian method are qualitatively similar.

Experimental design and setup

Based on the ultrametric phylogenetic tree, we assembled protist communities that each contained three species but differed in the level of phylogenetic diversity (three levels: low, medium, and high; Table 3.1). We calculated phylogenetic diversity of a community as the sum of lengths of the intervening branches of its member species on the phylogenetic tree, following Faith (1992). Because each of the constructed communities contains three species, our measure of phylogenetic diversity is mathematically equivalent to another measure of phylogenetic diversity—mean pairwise phylogenetic distance (MPD, Webb et al. 2002). Results based on several other phylogenetic diversity metrics, such as mean nearest taxon distance (MNTD, Webb et al. 2002) and E_{ED} (Cadotte et al. 2010), were also qualitatively similar. Nested within each level of phylogenetic diversity were three communities that differed in species

Table 3.1. Species composition of the communities in the low, medium, and high phylogenetic diversity treatments. The phylogenetic diversity (PD) for each community was calculated as the sum of all branch lengths connecting its member species on the phylogenetic tree in Fig. 3.1, following Faith (1992).

Phylogenetic diversity level	Species composition	PD
Low	*B. americanum, S. ambiguum, S. teres*	60.39
	C. striatum, G. scintillans, P. aurelia	154.90
	C. kleini, P. caudatum, T. pyriformis	161.41
Medium	*H. grandinella, P. multimicronucleatum, P. Tetraurelia*	203.43
	C. kleini, G. scintillans, S. teres	205.34
	P. multimicronucleatum, S. ambiguum, S. teres	205.73
High	*H. grandinella, S. ambiguum, T. pyriformis*	290.66
	B. americanum, C. kleini, P. caudatum	274.78
	C. striatum, P. aurelia, S. teres	274.78

composition. Additional criteria for choosing these communities include the minimization of the number of shared species between communities and differences in species morphology that allow species in a community to be differentiated under a stereoscopic microscope. Each species composition treatment was replicated three times.

Our experimental microcosms consisted of 250 ml glass bottles each filled with 100 ml aqueous medium, made by dissolving 0.55g protozoan pellet per liter of water (the same medium used in the stock cultures). This medium was autoclaved and inoculated with bacteria before protists were introduced into the microcosms. To provide a homogeneous bacterial diet for protist species in all communities, we species and passing the mixed culture through a 1.0 μm pore size filter to remove protist individuals. The bacterized medium was incubated for three days under room temperature (~22 °C), before introducing ~100 individuals of each protist species into its belonging microcosms.

After protist introduction, we incubated the microcosms in an incubator without light at 22ºC for two weeks before subjecting them to a short-term temperature shock. The temperature shock represented a disturbance event that perturbs ecological communities away from their steady states, facilitating the investigation of temporal stability. We perturbed the communities by placing the microcosms in a 32ºC incubator for two hours on a weekly base. The abundance of each protist species was monitored three times a week (one day before disturbance, immediately after disturbance, and five days after disturbance). To estimate protist abundances, we took a small sample (~0.3 ml) from each microcosm, and counted the number of individuals by species under a stereoscopic microscope. Samples containing large protist populations were diluted

before counting. For the duration of the experiment, we replenished each microcosm every week by disposing 10 ml of its content and adding back 10 ml fresh medium. Between week 3 and 5, we added ~200 individuals of each species that were not detected in its microcosms weekly. Between week 6 and 7, we added ~200 individuals of each protist species weekly to each of its belonging microcosms, regardless of whether it went extinct or not. This simulates species dispersal that buffers species against extinction in natural communities. The experiment lasted for a total of 52 days.

We also set up a short-term monoculture experiment to gauge the response of individual protist species to the same perturbation experienced by the three-species communities. In this experiment, we first allowed protist populations to grow for two weeks before subjecting them to the two-hour 32ºC temperature shock. Protist abundance data were collected three times, one day before disturbance, immediately after disturbance, and 5 days after disturbance.

Statistical analysis

Effective species extinction occurred only in communities containing *Paramecium multimicronucleatum, Spirostomum ambiguum,* or *Spirostomum teres*, where *P. multimicronucleatum* was consistently missing (i.e., below the detection limit) despite repeated re-inoculation. We excluded data on these communities from statistical analyses; analyses including communities that lost species produced qualitatively similar results. Our analyses focused on data collected from the last two weeks of the experiment, when communities experienced weekly disturbance and the reintroduction of all their member species.

For each population, we obtained its biomass (biovolume) by multiplying its population density with the average individual biovolume of the species (available from our laboratory database). Population temporal stability was calculated as the inverse of coefficient of variation of population biomass over time. Aggregate biomass of a community was obtained by summing population biomass across its member species. For each community, we calculated its temporal stability as the inverse of coefficient of variation of aggregate biomass over time. Temporal stability from different phylogenetic diversity treatments was compared using ANOVA and Tukey's HSD *post-hoc* test. Regressions were also used to delineate the relationship between temporal stability and phylogenetic diversity of communities.

To explore possible mechanisms driving the observed diversity-stability relationships, we calculated summed variances, summed covariances, and total biomass for each microcosm and examined their relationships to phylogenetic diversity. To assess the effect of phylogenetic diversity on the degree of synchrony in population fluctuations, we calculated the community-wide synchrony statistic φ, following Loreau and de Mazancourt (2008). This measure ranges from 0 to 1, corresponding to complete asynchrony and synchrony, respectively. Its relationship with phylogenetic diversity was examined using regressions. The temporal variance of biomass of a species generally scales positively with its mean biomass (Taylor 1961), and the slope of this relationship has been shown to influence the effects of species diversity on biomass stability (the portfolio effect, Tilman 1999). Although the portfolio effect did not operate in our communities that contained the same number of species, biomass variance-mean scaling relationships could still potentially affect their stability. For instance, increasing

phylogenetic diversity may increase biomass temporal stability if it leads to large increases in mean species biomass but small increases in variance. We thus calculated the temporal mean and variance of biomass for each species in each microcosm and obtained the scaling coefficients by running regression on the logarithms of the two variables across all species. We also calculated Simpson's evenness index (Smith and Wilson 1996) for each microcosms using protist abundance data, and tested for relationships between evenness and phylogenetic diversity using regressions. Increasing phylogenetic diversity could increase evenness if it leads to the reduction of competition between species and, therefore, reduced species dominance. To test for the phylogenetic sampling effect, we calculated population stability of each species from the monoculture experiment and used Blomberg's *K* (Blomberg *et al.*, 2003) to assess whether this stability is phylogenetically conserved. Blomberg's *K* compares the observed variation of trait values (population stability in our study) across the phylogenetic tree to trait variation under Brownian motion evolution (Blomberg et al., 2003). A value of $K > 1$ indicates greater phylogenetic signal than expected, whereas $K < 1$ indicates lesser phylogenetic signal than expected. We tested the significance of the *K* statistic through a permutation test with 999 permutations, by shuffling the tips across the phylogenetic tree in each permutation. Finally, we ran repeated-measures ANOVA on data from the monoculture experiment to compare the response of individual species to temperature shock, with species abundances as the response variable and species identity as the predictor variable. All statistical analyses were conducted in *R* 2.15.1 (http://ww.R-project.org), with the *K* statistic calculated using the *picante* package (Kembel *et al.*, 2010).

Results

Communities with different levels of phylogenetic diversity differed in their temporal stability (Fig. 3.2). When classified into the three phylogenetic diversity groups, communities with higher phylogenetic diversity tended to exhibit greater temporal stability ($F_{2, 21} = 3.733$, $P = 0.041$), with significant differences detected between the low and high phylogenetic diversity groups (Fig. 3.2a). When examined along the continuous phylogenetic diversity gradient, these communities exhibited a marginally significant positive relationship between phylogenetic diversity and temporal stability (Fig. 3.2b; $R^2 = 0.105$, $P = 0.067$). The diversity-stability pattern, however, differed between communities with and without *Spirostomum* (either *S. ambiguum* or *S. teres*), species with the largest body size. Whereas temporal stability increased with phylogenetic diversity in communities lacking *Spirostomum* (Fig. 3.2b; $R^2 = 0.489$, $P = 0.007$), it remained roughly constant along the phylogenetic gradient in communities containing *Spirostomum* (Fig. 3.2b; $R^2 = 0$, $P = 0.509$).

Both summed variances and total protist community biomass showed a U-shaped pattern along the phylogenetic gradient (Fig. 3.3a, c; Quadratic regression: summed variances, $R^2 = 0.499$, $P < 0.001$; community biomass, $R^2 = 0.781$, $P < 0.001$). This peculiar pattern was largely driven by the large biomass and variance in communities containing *Spirostomum* at both low and high ends of the phylogenetic gradient. The coefficients of the biomass mean-variance scaling relationship for communities with and without *Spirostomum* were 1.507 and 1.658, respectively (Fig. 3.4), which did not differ from each other (ANCOVA: $F_{1,63} = 1.534$, $P = 0.220$); the large-bodied *Spirostomum* attained the largest population biomass and exhibited the largest variances in their biomass.

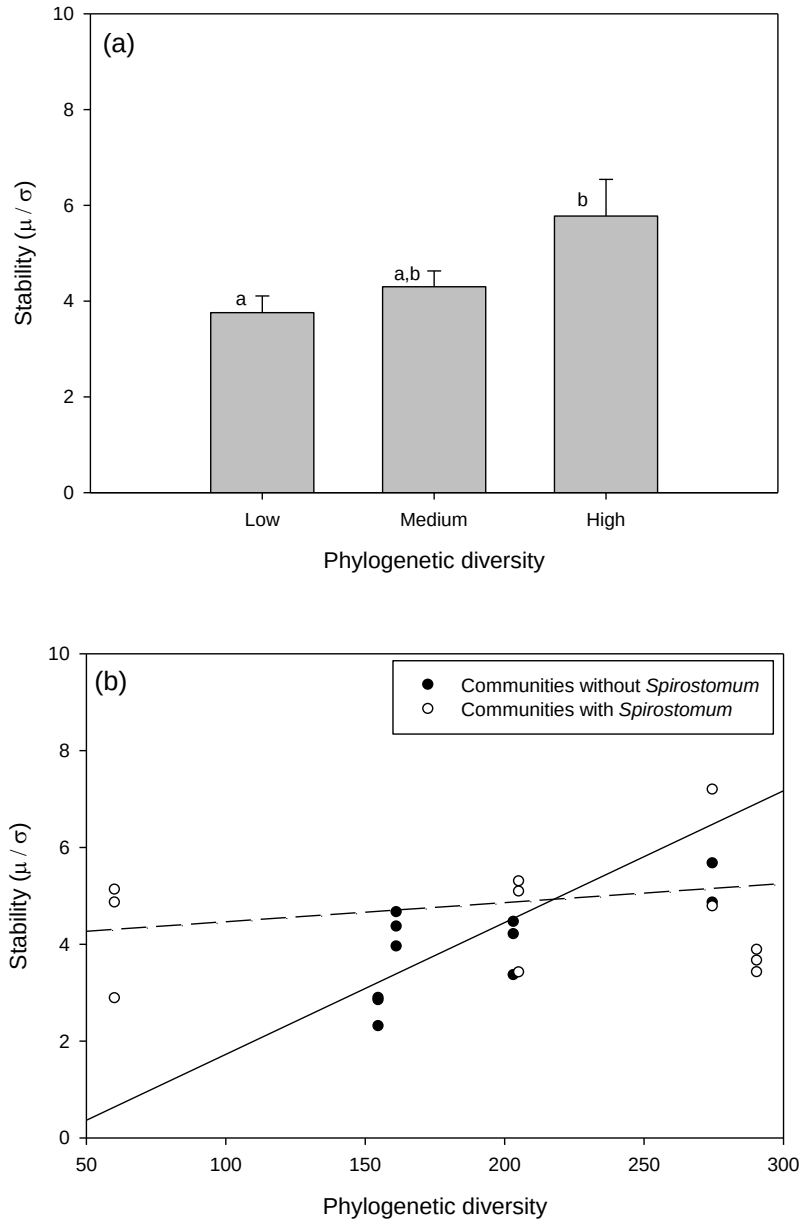

Fig. 3.2. Temporal stability of aggregate biomass in communities with different phylogenetic diversity. Temporal stability was calculated as the ratio of temporal mean and standard deviation of community aggregate biomass. (a) Average temporal stability in the three phylogenetic diversity groups (Low, Medium, and High). Groups sharing the same letter do not differ in stability in a *post-hoc* Tukey's HSD test at the level of P = 0.05. (b) Temporal stability along the continuous phylogenetic diversity gradient. The filled and open dots correspond to communities without and with *Spirostomum*, respectively. The statistically significant linear regression line (R^2 = 0.489, P = 0.007) for communities without *Spirostomum* is shown as a solid line.

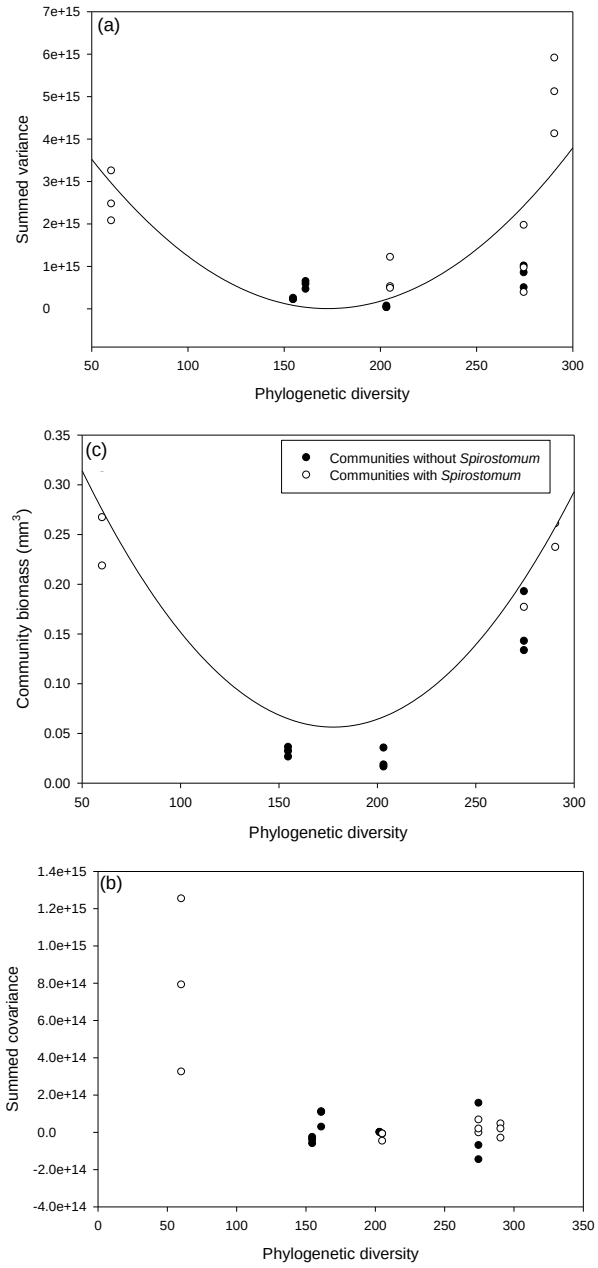

Fig. 3.3. Summed variances (a), summed covariances (b), and aggregate community biomass (c) along the phylogenetic diversity gradient. Filled and open dots correspond to communities without and with *Spirostomum*, respectively. The solid lines in panels (a) and (c) are the fitted quadratic regressions curves (summed variances, $R^2 = 0.499$, $P < 0.001$; community biomass, $R^2 = 0.781$, $P < 0.001$). The quadratic regression accounted for significantly more variation than a simple linear regression in depicting the relationship between summed variances and phylogenetic diversity (ANOVA:$F_{1,21} = 23.37$, $P < 0.001$) (a), and in depicting the relationship between community biomass and phylogenetic diversity (ANOVA:$F_{1,21} = 83.01$, $P < 0.001$) (c).

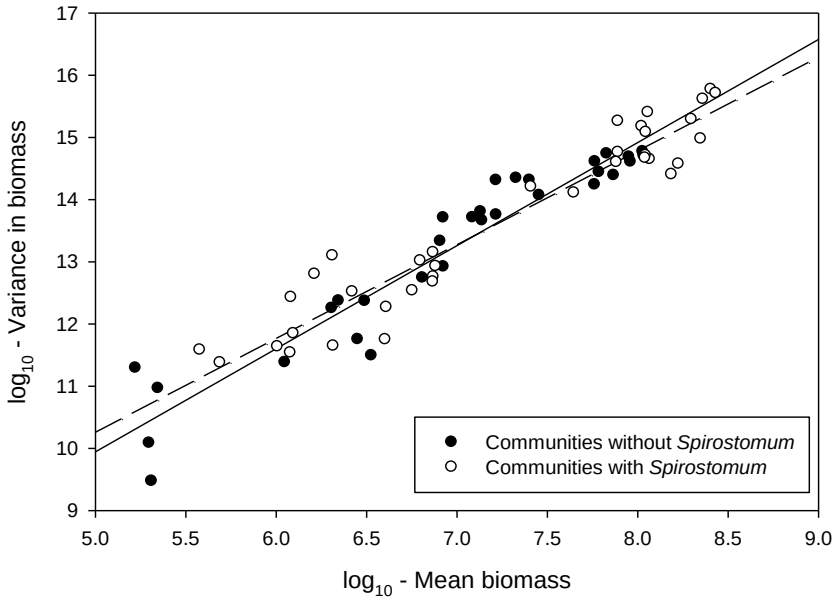

Fig. 3.4. The mean-variance scaling relationship in communities with (open dots) and without (filled dots) *Spirostomum*. The dashed and solid lines are the regression lines for communities with and without *Spirostomum*, respectively.

Summed covariances attained the highest values at the lowest phylogenetic diversity level, but remained at relatively low values at other diversity levels (Fig. 3.3b). When only communities without *Spirostomum* were considered, increasing phylogenetic diversity did not affect summed variances or covariances, but resulted in increased community biomass (Fig. 3.3c; ANOVA, $F_{2,9} = 9.625$, $P = 0.006$). Species synchrony patterns also differed between communities with and without *Spirostomum* (Fig. 3.5a). Synchrony showed a non-significant trend of decrease with phylogenetic diversity in communities where *Spirostomum* was absent ($R^2 = 0.067$, $P = 0.210$), but showed a significant positive relationship with phylogenetic diversity in communities where *Spirostomum* was present ($R^2 = 0.508$, $P = 0.006$). The opposite pattern existed for species evenness (Fig. 3.5b), which exhibited a positive relationship with phylogenetic diversity in communities without *Spirostomum* ($R^2 = 0.470$, $P = 0.008$), and a negative relationship with phylogenetic diversity in communities with *Spirostomum* ($R^2 = 0.916$, $P < 0.001$).

Population stability did not exhibit a significant phylogenetic signal across the 12 protist species, according to Blomberg's *K* test ($K = 0.006$, $P = 0.502$). The 12 species, however, differed in their responses to temperature shock (Fig. 3.6), as revealed by the significant species × time term in the repeated-measures ANOVA ($F_{22, 48} = 1.932$, $P = 0.028$).

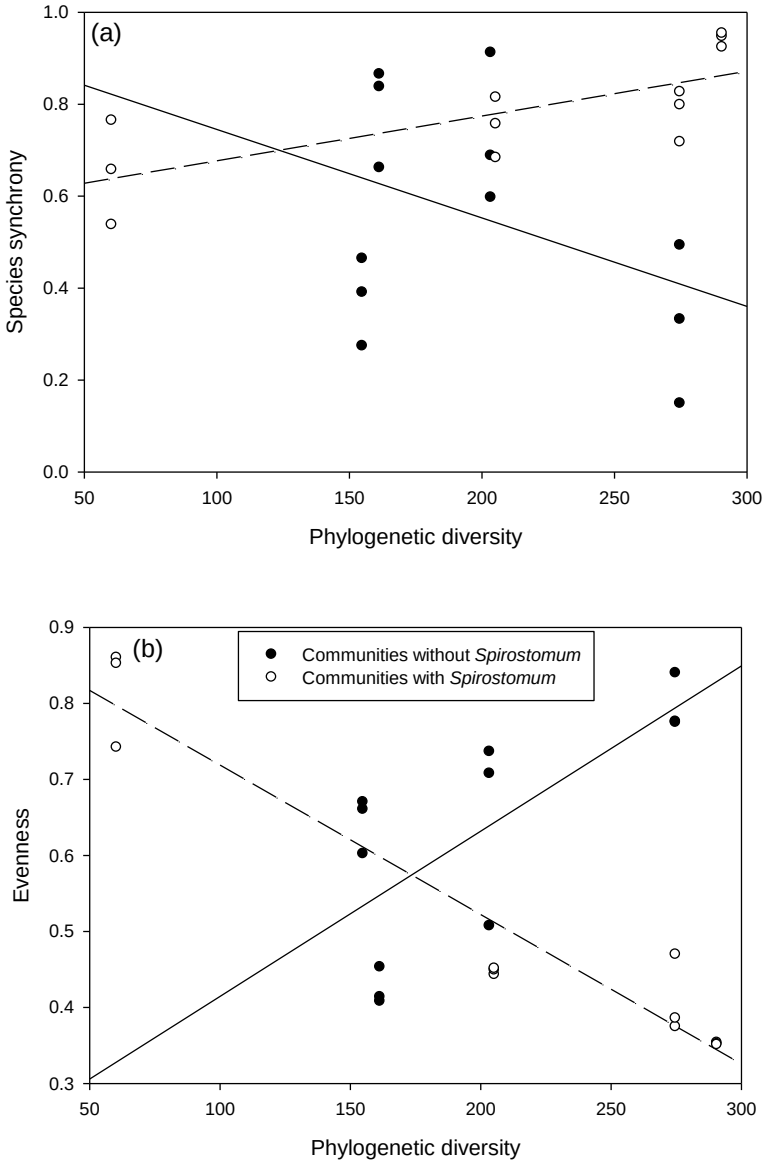

Fig. 3.5. Species synchrony (a) and evenness (b) along the phylogenetic diversity gradient. Species synchrony was measured by the ratio of the temporal variance of community biomass to the square of the sum of temporal standard deviation of species biomass (Loreau and de Mazancourt 2008). Species evenness is calculated as$(1/D)/SR$, where D is the Simpson's dominance index and SR is species richness. Communities with *Spirostomum* (open dots) exhibited a positive relationship between species synchrony and phylogenetic diversity (a) and a negative relationship between species evenness and phylogenetic diversity (b), while the communities without *Spirostomum* (filled dots) show opposite patterns. Solid and dashed regression lines are for communities without and with *Spirostomum*, respectively.

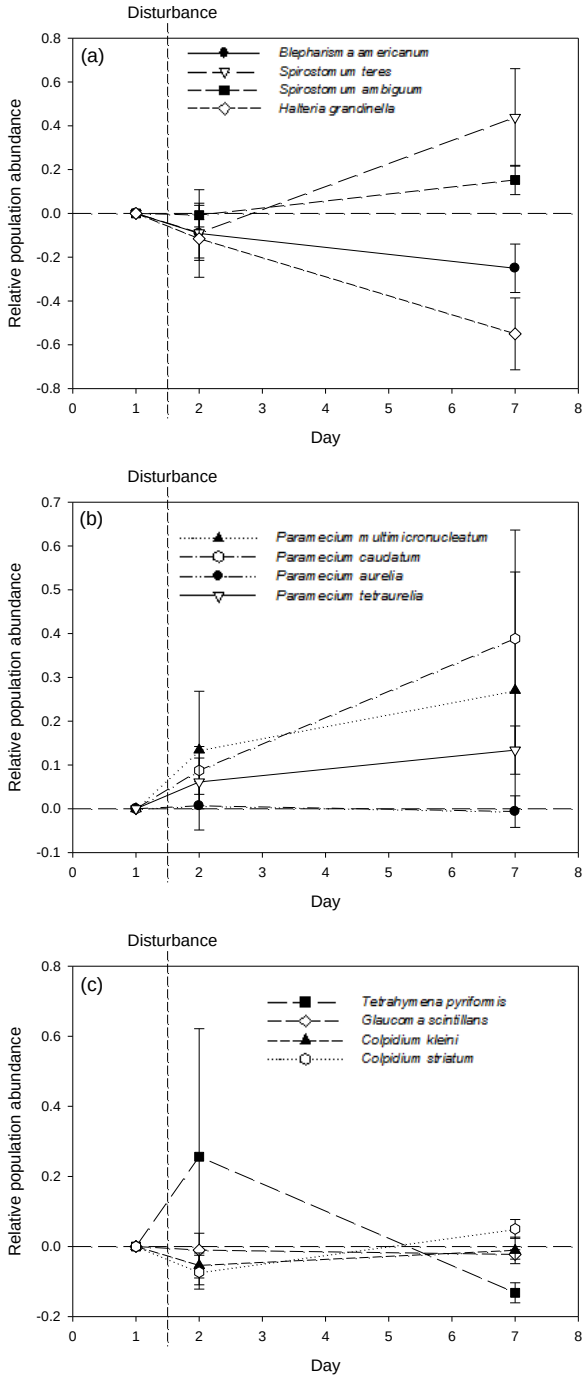

Fig. 3.6. Species responses to disturbance in the monoculture experiment (data are split in three panels for clarity). The monocultures were sampled one day before disturbance (day 1), immediately after disturbance (day 2), and five days after disturbance (day 7). Relative population abundance was quantified as the logarithm of the ratio of the after-disturbance (day 2 or 7) population abundance to pre-disturbance (day 1) population abundance.

Discussion

Our study is among the first to experimentally explore the relationship between phylogenetic diversity and community temporal stability. In a pioneer work, Cadotte et al. (2012) examined how plant phylogenetic diversity affected the temporal stability of aboveground biomass of grassland ecosystems in one of the longest running experiments on biodiversity and ecosystem functioning (since 1994). While our experimental duration is short in absolute terms, it encompassed multiple generations of fast-growing protists as experimental organisms, reducing the possibility of our results being transient patterns. Unlike Cadotte et al. (2012) who manipulated phylogenetic diversity by changing species diversity and composition, our experiment established a phylogenetic diversity gradient via changing species composition within a single level of species diversity, eliminating potential confounding effects of species and phylogenetic diversity. Both our study and that of Cadotte et al. (2012), however, reported that phylogenetic diversity stabilizes community biomass. Phylogenetic diversity has also been reported to have positive effects on the magnitude of ecosystem functions. For example, Cadotte et al. (2008, 2009) and Flynn et al. (2011) showed that grassland communities with higher phylogenetic diversity tended to be more productive. Tan et al. (2012) showed that increasing phylogenetic diversity enhanced the ability of bacterial communities to produce biomass and break down organic matter. Maherali and Klironomos (2007) reported that arbuscular mycorrhizal fungal communities with higher phylogenetic diversity supported the coexistence of more fungal species, resulting in increased biomass of associated plants. Taken together, these results support the utility of phylogenetic diversity as an important dimension of biodiversity in predicting the magnitude and

stability of ecosystem functions. These results also indicate that across various taxonomic groups, phylogenetic diversity is often a reasonable surrogate of the diversity of functional traits relevant for ecological functioning, providing indirect evidence that at least some of the functionally important traits are phylogenetically conserved (see Tan et al. 2012 for an explicit example).

Similar to what Cadotte et al. (2012) found in their experiment, we found that population stability did not show a significant phylogenetic signal. One explanation for this result is that population stability of a species is a higher-level property that is determined by lower-level properties such as resistance to disturbance and resilience after disturbance, which are in turn influenced by a host of species traits that may not necessarily be phylogenetically conserved. Another possibility is that although the 2-hour temperature shock elicited different species responses (Fig. 3.6), it may have been too short or too weak to drive sufficiently large population changes that can be detected by our test statistic. Regardless, this result suggests that the phylogenetic sampling effect, where phylogenetically more diverse communities can be more stable because of the increased probabilities of including and being dominated by stable clades, failed to operate in our experiment. Note that in theory, the opposite of the phylogenetic sampling effect may also operate if communities tend to be dominated by species that are dynamically unstable, possibly resulting in negative diversity-stability relationships (analogous to the negative selection effect that can cause negative relationships between species diversity and ecosystem functions; *sensu* Jiang et al. 2008). Current empirical evidence, however, indicates that dominant species are often dynamically more stable than subordinate species (Bai et al. 2004, Leps 2004, Polley et al. 2007, Grman et al.

2010, Roscher et al. 2011), suggesting that patterns (if any) consistent with the phylogenetic sampling effect may be more likely observed in ecological communities.

Based on the assumption that species that are more distantly related tend to be ecologically less similar (i.e., phylogenetic niche conservatism), Darwin (1859) hypothesized that the strength of competition should be weaker in communities characterized by higher phylogenetic diversity. Several recent experiments support this hypothesis (Burns and Strauss 2011, Violle et al. 2011). In particular, Violle et al. (2011) demonstrated weaker competition between less related bacterivorous protist species, several of which were also used in the current experiment. The reduction in competition strength may contribute to community stability by lowering population variances and increasing community biomass production, which serves to reduce the strength of demographic stochasticity (Loreau and de Mazancourt 2013). Cadotte et al. (2012) found evidence for lower summed variances associated with reduced competition in their higher phylogenetic diversity communities. This, however, is not the case in our experiment, where large variances in *Spirostomum* communities at low and high phylogenetic diversity levels led to a U-shaped relationship between phylogenetic diversity and summed variances, and no significant diversity-summed variances relationships were detected in *Spirostomum*-less communities (Fig. 3.3a). By contrast, the increased biomass production under higher phylogenetic diversity was indeed observed in these *Spirostomum*-less communities. Furthermore, the increasing evenness with phylogenetic diversity in these communities (Fig. 3.5b) is consistent with a reduction in competition strength. These results thus support the mechanism that increasing phylogenetic diversity promotes community temporal stability by reducing the strength of competition. It is not

exactly clear what caused the peculiar results in communities containing *Spirostomum*, which is known to be a better competitor compared with smaller bacterivorous protists (Cadotte et al. 2006, Violle et al. 2010). In fact, our data indicated that *Spirostomum* contributed more predominantly to community biomass as phylogenetic diversity increased (Fig. 3.5b), a result at odds with the prediction of higher phylogenetic diversity weakening competitive interactions. One possibility is that *Spirostomum*'s large body and mouth size (Violle et al. 2010) allowed them to capture a broad range of bacterial resources, which would diminish niche differentiation between itself and other species and make it a better competitor regardless of the phylogenetic diversity of the community. Unfortunately, we did not collect bacterial data in our experiment to allow us to test this hypothesis.

Theory has identified asynchrony in species responses to environmental changes as a major stabilizing mechanism driving positive diversity-stability relationships (Ives and Hughes 2002, Loreau and de Mazancourt 2008, 2013). Consistent with this prediction, several studies have reported asynchronous population fluctuations associated with positive relationships between species diversity and biomass stability (e.g., Isbell et al. 2009, Grman et al. 2010, Roscher et al. 2011); few of these studies, however, have directly quantified differences in species response to environmental fluctuations (but see Leary and Petchey 2009) and linked asynchrony in species response with asynchrony in population dynamics. Here we show that our experimental protists showed different responses to temperature shock (Fig. 3.6) and our experimental communities consisting of these species exhibited different degree of asynchrony (Fig. 3.5a). Interestingly, based on the synchrony statistic recommended by Loreau and de Mazancourt (2008),

population dynamics in communities without *Spirostomum* became less synchronous with increasing phylogenetic diversity (Fig. 3.5). This result appears to contradict the theoretic prediction that weaker competition, which applies to our experimental communities with higher phylogenetic diversity, should make populations more synchronous (Loreau and de Mazancourt 2008, 2013). This discrepancy, however, may be at least partly explained by the fact that the values of the frequently used synchrony statistic (Loreau and de Mazancourt 2008) can be strongly influenced by species relative abundances. In particular, highly uneven communities generally yield large synchrony values, even if there is little synchrony among the interacting populations. Indeed, across all our experimental communities evenness accounted for 47.4% of the variation in the synchrony statistic values ($P = 0.001$). Note that other similar synchrony statistics, such as the variance ratio (Vasseur and Gaedke 2007), also suffer from similar problems. Summed covariances have also been frequently used as a proxy of population synchrony; however, mathematical constraints limit its ability to differentiate communities with different degrees of population synchrony (Brown et al. 2004, Loreau and de Mazancourt 2008). There is thus an urgent need for the development of robust, unbiased synchrony/asynchrony statistics.

In conclusion, our experiment demonstrated the stabilizing effect of phylogenetic diversity on community biomass and identified reduced competition and species asynchronous responses to environmental fluctuations as possible driving mechanisms. A more definitive conclusion on these mechanisms would require knowing that the niches of our study species were phylogenetically conserved, which would need to be assessed by future experiments that directly quantify niches of these species (i.e., their bacterial

usage patterns). Notably, the violation of phylogenetic niche conservatism, an assumption made by many phylogenetic community ecology studies including ours, would potentially diminish the predictive power of phylogenetic diversity for ecosystem functions (Srivastava et al. 2012). Indeed, in our experiment different phylogenetic diversity-stability patterns and mechanisms were observed in a subset of communities that contained large species whose superior competitive ability seemed to be unrelated to their phylogeny, providing an example of the lack of niche conservatism complicating a general understanding of relationships between phylogenetic diversity and community temporal stability. These results emphasize the need for more empirical studies to explore how phylogenetic diversity, as an important component of diversity that accounts for species evolutionary relationships, influences ecosystem functions and their stability, and how the strength of their effects varies with the degree of phylogenetic niche conservatism. Our results also call for the development of new statistics that provide unbiased measures of population synchrony.

References

Baroin-Tourancheau, A., P. Delgado, R. Perasso, and A. Adoutte. 1992. A broad molecular phylogeny of ciliates: identification of major evolutionary trends and radiations within the phylum. Proceedings of the National Academy of Sciences 89:9764-9768.

Blomberg, S. P., T. Garland, and A. R. Ives. 2003. Testing for phylogenetic signal in comparative data: Behavioral traits are more labile. Evolution 57:717-745.

Brown, J., E. Bedrick, S. Ernest, J. Cartron, and J. Kelly. 2004. Constraints on negative relationships: mathematical causes and ecological consequences. Pages 298-308 in M. Taper and S. Lele, editors. The nature of scientific evidence: Statistical, philosophical, and empirical considerations. University of Chicago Press, Chicago.

Burns, J. H., and S. Y. Strauss. 2011. More closely related species are more ecologically similar in an experimental test. Proceedings of the National Academy of Sciences 108:5302-5307.

Darwin, C. 1859. On the origin of species. John Murray, London.

Cadotte, M. W., B. J. Cardinale, and T. H. Oakley. 2008. Evolutionary history and the effect of biodiversity on plant productivity. Proceedings of the National Academy of Sciences 105:17012-17017.

Cadotte, M. W., J. Cavender-Bares, D. Tilman, and T. H. Oakley. 2009. Using Phylogenetic, Functional and Trait Diversity to Understand Patterns of Plant Community Productivity. Plos One 4.

Cadotte, M. W., R. Dinnage, and D. Tilman. 2012. Phylogenetic diversity promotes ecosystem stability. Ecology 93:S223-S233.

Cadotte, M. W., T. Jonathan Davies, J. Regetz, S. W. Kembel, E. Cleland, and T. H. Oakley. 2010. Phylogenetic diversity metrics for ecological communities: integrating species richness, abundance and evolutionary history. Ecology Letters 13:96-105.

Cadotte, M. W., D. V. Mai, S. Jantz, M. D. Collins, M. Keele, and J. A. Drake. 2006. On Testing the Competition-Colonization Trade-Off in a Multispecies Assemblage. The American Naturalist 168:704-709.

Campbell, V., G. Murphy, and T. N. Romanuk. 2011. Experimental design and the outcome and interpretation of diversity–stability relations. Oikos 120:399-408.

Cardinale, B. J., J. E. Duffy, A. Gonzalez, D. U. Hooper, C. Perrings, P. Venail, A. Narwani, G. M. Mace, D. Tilman, and D. A. Wardle. 2012. Biodiversity loss and its impact on humanity. Nature 486:59-67.

Castresana, J. 2000. Selection of conserved blocks from multiple alignments for their use in phylogenetic analysis. Molecular Biology and Evolution 17:540-552.

Darriba, D., G. L. Taboada, R. Doallo, and D. Posada. 2012. jModelTest 2: more models, new heuristics and parallel computing. Nature Methods 9:772-772.

Díaz, S., and M. Cabido. 2001. Vive la difference: plant functional diversity matters to ecosystem processes. Trends in Ecology & Evolution 16:646-655.

Faith, D. P. 1992. Conservation evaluation and phylogenetic diversity. Biological Conservation 61:1-10.

Flynn, D. F., N. Mirotchnick, M. Jain, M. I. Palmer, and S. Naeem. 2011. Functional and phylogenetic diversity as predictors of biodiversity-ecosystem-function relationships. Ecology 92:1573-1581.

Gause, G. F. 1934. The struggle of Existence. Williams & Wilkins, Baltimore.

Grman, E., J. A. Lau, D. R. Schoolmaster, and K. L. Gross. 2010. Mechanisms contributing to stability in ecosystem function depend on the environmental context. Ecology Letters 13:1400-1410.

Guindon, S., J. F. Dufayard, V. Lefort, M. Anisimova, W. Hordijk, and O. Gascuel. 2010. New Algorithms and Methods to Estimate Maximum-Likelihood Phylogenies: Assessing the Performance of PhyML 3.0. Systematic Biology 59:307-321.

Hooper, D. U., E. C. Adair, B. J. Cardinale, J. E. Byrnes, B. A. Hungate, K. L. Matulich, A. Gonzalez, J. E. Duffy, L. Gamfeldt, and M. I. O'Connor. 2012. A global synthesis reveals biodiversity loss as a major driver of ecosystem change. Nature 486:105-108.

Isbell, F. I., H. W. Polley, and B. J. Wilsey. 2009. Biodiversity, productivity and the temporal stability of productivity: patterns and processes. Ecology Letters 12:443-451.

Ives, A. R., and J. B. Hughes. 2002. General relationships between species diversity and stability in competitive systems. The American Naturalist 159:388-395.

Jiang, L., L. Brady, and J. Tan. 2011. Species diversity, invasion, and alternative community states in sequentially assembled communities. The American Naturalist 178:411-418.

Jiang, L., H. Joshi, and S. N. Patel. 2009. Predation Alters Relationships between Biodiversity and Temporal Stability. American Naturalist 173:389-399.

Jiang, L., Z. Pu, and D. R. Nemergut. 2008. On the importance of the negative selection effect for the relationship between biodiversity and ecosystem functioning. Oikos 117:488-493.

Jiang, L., and Z. C. Pu. 2009. Different Effects of Species Diversity on Temporal Stability in Single-Trophic and Multitrophic Communities. American Naturalist 174:651-659.

Kembel, S. W., P. D. Cowan, M. R. Helmus, W. K. Cornwell, H. Morlon, D. D. Ackerly, S. P. Blomberg, and C. O. Webb. 2010. Picante: R tools for integrating phylogenies and ecology. Bioinformatics 26:1463-1464.

Leary, D. J., and O. L. Petchey. 2009. Testing a biological mechanism of the insurance hypothesis in experimental aquatic communities. Journal of Animal Ecology 78:1143-1151.

Lepš, J. 2004. Variability in population and community biomass in a grassland community affected by environmental productivity and diversity. Oikos 107:64-71.

Loreau, M., and C. de Mazancourt. 2008. Species synchrony and its drivers: neutral and nonneutral community dynamics in fluctuating environments. The American Naturalist 172:E48-E66.

Loreau, M., and C. de Mazancourt. 2013. Biodiversity and ecosystem stability: a synthesis of underlying mechanisms. Ecology Letters 16:106-115.

MacArthur, R. 1955. Fluctuations of animal populations and a measure of community stability. Ecology 36:533-536.

Maherali, H., and J. N. Klironomos. 2007. Influence of phylogeny on fungal community assembly and ecosystem functioning. Science 316:1746-1748.

May, R. M. 1973. Stability and complexity in model ecosystems. Princeton University Press.

McCann, K. S. 2000. The diversity–stability debate. Nature 405:228-233.

McGill, B. J., B. J. Enquist, E. Weiher, and M. Westoby. 2006. Rebuilding community ecology from functional traits. Trends in Ecology & Evolution 21:178-185.

Naeem, S., J. E. Duffy, and E. Zavaleta. 2012. The functions of biological diversity in an age of extinction. Science 336:1401-1406.

Proulx, R., C. Wirth, W. Voigt, A. Weigelt, C. Roscher, S. Attinger, J. Baade, R. L. Barnard, N. Buchmann, and F. Buscot. 2010. Diversity promotes temporal stability across levels of ecosystem organization in experimental grasslands. Plos One 5:e13382.

Pruesse, E., C. Quast, K. Knittel, B. M. Fuchs, W. G. Ludwig, J. Peplies, and F. O. Glockner. 2007. SILVA: a comprehensive online resource for quality checked and aligned ribosomal RNA sequence data compatible with ARB. Nucleic Acids Research 35:7188-7196.

Roscher, C., A. Weigelt, R. Proulx, E. Marquard, J. Schumacher, W. W. Weisser, and B. Schmid. 2011. Identifying population-and community-level mechanisms of diversity–stability relationships in experimental grasslands. Journal of Ecology 99:1460-1469.

Sanderson, M. J. 1997. A nonparametric approach to estimating divergence times in the absence of rate constancy. Molecular Biology and Evolution 14:1218-1231.

Sanderson, M. J. 2003. r8s: inferring absolute rates of molecular evolution and divergence times in the absence of a molecular clock. Bioinformatics 19:301-302.

Smith, B., and J. B. Wilson. 1996. A consumer's guide to evenness indices. Oikos:70-82.

Srivastava, D. S., M. W. Cadotte, A. A. M. MacDonald, R. G. Marushia, and N. Mirotchnick. 2012. Phylogenetic diversity and the functioning of ecosystems. Ecology Letters 15:637-648.

Srivastava, D. S., and M. Vellend. 2005. Biodiversity-ecosystem function research: is it relevant to conservation? Annual Review of Ecology, Evolution, and Systematics:267-294.

Tan, J. Q., Z. C. Pu, W. A. Ryberg, and L. Jiang. 2012. Species phylogenetic relatedness, priority effects, and ecosystem functioning. Ecology 93:1164-1172.

Taylor, L. 1961. Aggregation, variance and the mean. Nature 189:732-735.

Tilman, D. 1999. The ecological consequences of changes in biodiversity: A search for general principles. Ecology 80:1455-1474.

Tilman, D., P. B. Reich, and J. M. Knops. 2006. Biodiversity and ecosystem stability in a decade-long grassland experiment. Nature 441:629-632.

Van de Peer, Y., G. Van der Auwera, and R. De Wachter. 1996. The evolution of stramenopiles and alveolates as derived by "substitution rate calibration» of small ribosomal subunit RNA. Journal of Molecular Evolution 42:201-210.

Vandermeer, J. H. 1969. The competitive structure of communities: an experimental approach with protozoa. Ecology:362-371.

Vasseur, D. A., and U. Gaedke. 2007. Spectral analysis unmasks synchronous and compensatory dynamics in plankton communities. Ecology 88:2058-2071.

Violle, C., D. R. Nemergut, Z. C. Pu, and L. Jiang. 2011. Phylogenetic limiting similarity and competitive exclusion. Ecology Letters 14:782-787.

Violle, C., Z. Pu, and L. Jiang. 2010. Experimental demonstration of the importance of competition under disturbance. Proceedings of the National Academy of Sciences 107:12925-12929.

Wayne Polley, H., B. J. Wilsey, and J. D. Derner. 2007. Dominant species constrain effects of species diversity on temporal variability in biomass production of tallgrass prairie. Oikos 116:2044-2052.

Webb, C. O., D. D. Ackerly, M. A. McPeek, and M. J. Donoghue. 2002. Phylogenies and community ecology. Annual Review of Ecology and Systematics 33:475-505.

Wiens, J. J., D. D. Ackerly, A. P. Allen, B. L. Anacker, L. B. Buckley, H. V. Cornell, E. I. Damschen, T. Jonathan Davies, J. A. Grytnes, and S. P. Harrison. 2010. Niche conservatism as an emerging principle in ecology and conservation biology. Ecology Letters 13:1310-1324.

Wiens, J. J., and C. H. Graham. 2005. Niche conservatism: integrating evolution, ecology, and conservation biology. Annual Review of Ecology, Evolution, and Systematics:519-539.

Yachi, S., and M. Loreau. 1999. Biodiversity and ecosystem productivity in a fluctuating environment: the insurance hypothesis. Proceedings of the National Academy of Sciences 96:1463-1468.

CHAPTER 4

PREDATOR-PREY COEVOLUTION DRIVES PRODUCTIVITY-DIVERSITY RELATIONSHIPS IN PLANKTONIC SYSTEMS

Abstract

The relationship between environmental productivity and species diversity often varies among empirical studies, and despite much research, simple explanations for this phenomenon remain elusive. We investigated diversity patterns of phytoplankton and zooplankton undergoing evolution along a productivity gradient, using a simple nutrient-phytoplankton-zooplankton model that incorporates size-dependent metabolic rates summarized from empirical studies. Disruptive selection leads to evolutionary branching of phytoplankton and zooplankton. Both the time to evolutionary branching and the number of diversification events in phytoplankton and zooplankton tend to increase with productivity, producing a transient unimodal or positive productivity-diversity relationship but a positive steady-state productivity-diversity relationship for both groups at the steady state. Our findings suggest that coevolution between phytoplankton and zooplankton could drive the two common forms (unimodal and positive) of productivity-diversity relationships in nature.

Introduction

A fundamental question in community ecology is how the number of species in a habitat relates to environmental productivity. This seemingly simple question has

inspired numerous empirical investigations that have documented various forms of productivity-diversity relationships (PDRs) (e.g., Waide et al. 1999, Mittelbach et al. 2001, Gillman and Wright 2006, Gurevitch and Mengersen 2010, Hillebrand and Cardinale 2010). Positive and unimodal PDRs, in general, are the two most commonly observed patterns (Mittelbach et al. 2001, Gillman and Wright 2006) and have attracted the most attention. Consistent with these general patterns, extensive evidence in freshwater and marine planktonic systems often finds unimodal or positive PDRs on the regional scale (Dodson et al. 2000, Irigoien et al. 2004, Ptacnik et al. 2008, Korhonen et al. 2011, Stomp et al. 2011), although the response of species diversity to productivity can vary on the local scale (Dodson et al. 2000, Korhonen et al. 2011). To date, many factors are suggested to affect species diversity along the productivity gradient, including predation (Leibold 1996), light condition (Huisman et al. 2004), resource ratio (Cardinale et al. 2009a), and ecosystem size (Stomp et al. 2011). However, a comprehensive understanding towards the mechanistic basis of the various PDRs is still lacking.

A host of hypotheses has been proposed to explain the observed PDRs (e.g., Wright 1983, Rosenzweig and Abramsky 1993, Tilman and Pacala 1993, Leibold 1998, Partel et al. 2010), mostly focusing on processes operating on ecological timescales (typically involving competition). While these hypotheses have helped us gain considerable insight into some of the ecological mechanisms regulating species diversity along productivity gradients, they did not consider the possibility that evolutionary processes may also contribute to PDRs observed in various communities, which some ecologists have begun to explore (e.g., Hochberg and van Baalen 1998, Jansen and Mulder 1999, Partel et al. 2007). For example, Partel et al. (2007), based on the rationale

that habitat evolutionary history may affect PDRs through its influence on the size of the species pool, suggested that the paucity and short evolutionary history of productive habitats are responsible for the unimodal PDRs commonly found for temperate plant communities. Nevertheless, studies relating evolution to PDRs are scarce, and the question of how evolutionary time and environmental productivity combine to influence species diversity (Partel et al. 2007, Zobel and Partel 2008), in particular, remains largely unanswered.

To address the above question, we examined the influence of evolutionary processes on PDRs in phytoplankton-zooplankton communities. We explored how phytoplankton-zooplankton coevolution drives different species diversity along a productivity gradient by using a simple nutrient-phytoplankton-zooplankton (NPZ) model. Taking advantage of the extensive work on metabolic rates and functional responses in planktonic organisms, we incorporated body size-dependent population growth and trophic interactions into the evolutionary NPZ model. Body size was the focal trait in our model that dictated the fitness of phytoplankton and zooplankton populations. Using the theory of adaptive dynamics (Dieckmann and Law 1996, Geritz et al. 1998, Doebeli and Dieckmann 2000), we investigated plankton evolutionary dynamics through the analysis of evolutionary singular strategies. We also conducted numerical simulations to explore patterns of evolved species diversity along the productivity gradient.

NPZ Model and Methods

Ecological component of the NPZ model

To study the PDRs of phytoplankton and zooplankton during their coevolution, we developed a simple NPZ model based on the one used by Jiang et al. (2005) that

explored the adaptive evolution of body size in zooplankton and phytoplankton. Similar to traditional NPZ models, the ecological component of our model describes the dynamics of three variables: nutrient concentration (N), phytoplankton density (P), and zooplankton density (Z). As a first approach to studying the effects of evolutionary processes on PDRs, we do not consider how other abiotic factors (e.g. temperature) influence phytoplankton growth. We characterized phytoplankton populations by two key parameters, population densities (P) and cell size (x). Similarly, Z and y represent zooplankton population density and body size, respectively. The model is:

$$\frac{dN}{dt} = I - dN - \mu(x)g(N)PQ(x) + \gamma B(P,Z) \qquad \text{(Equation 4.1a)}$$

$$\frac{dP}{dt} = P\left[\mu(x)g(N) - m - s(x) - C(x,y)Z\right] \qquad \text{(Equation 4.1b)}$$

$$\frac{dZ}{dt} = Z\left[\phi\frac{Q(x)}{q(y)}C(x,y)P - \delta\right] \qquad \text{(Equation 4.1c)}$$

All model parameters and functions are defined in Table 4.1. The amount of nutrient N is determined by the nutrient supply rate I (i.e., the measure of environmental productivity), a constant rate d of nutrient loss (due to outflow) proportional to N, and nutrient recycling $\gamma B(P,Z)$. The phytoplankton population is determined by four processes: a size-dependent nutrient uptake rate $\mu(x)g(N)$; mortality due to sinking $s(x)$ (following the Stoke's Law) and a constant mortality rate m; and size-dependent zooplankton capture rate $C(x,y)$. The dynamics of zooplankton population is determined by: the rate of consumption and assimilation of phytoplankton biomass, which depends on a size-dependent capture rate $C(x,y)$;

Table 4.1. The definitions and units of parameters and functions in the model (Equations 4.1a-c). See Appendix C.2 for the estimates of value range from empirical studies.

Parameter/Function	Definition	Unit
N	nutrient concentration	μmol/L
P	phytoplankton density	10^8cells/L
Z	zooplankton density	10^6indv./L
x	phytoplankton cell size (Estimated Spherical Diameters, ESD)	μm
y	zooplankton cell size (ESD)	μm
I	nutrient inflow rate	μmol /L/day
d	nutrient outflow rate	1/day
$\mu(x) = x/(c_1x^2 + c_2x + c_3)$	maximum phytoplankton growth rate	1/day
(c_1, c_2, c_3)	coefficients of $\mu(x)$	(1/μm ^{2},1/μm,unitless)
$g(N) = N/(N + K)$	Nutrient limitation for phytoplankton growth	unitless
K	half saturation constant	μmol /L
$Q(x) = \beta x^{b_1}$	phytoplankton nutrient quota	μmol/10^8 cells
β	phytoplankton nutrient quota coefficient	μmol nutrient/cell/μm $^{-b_1}$
b_1	phytoplankton nutrient quota exponent	unitless
γ	fraction of recycled detritus	unitless
m	phytoplankton mortality rate	1/day
$s(x) = \alpha x^2$	phytoplankton sinking rate	1/day
α	sinking rate coefficient	1/day/μm ^{2}
$C(x, y) = C_m \exp[-\frac{1}{\lambda}(x - \theta y)^2]$	zooplankton clearance rate	L/10^6 indv./day
C_m	maximum clearance rate	L/day
λ	clearance rate coefficient	μm ^{2}
θ	clearance rate coefficient	unitless
ϕ	conversion rate	indv./cells
$q(y) = \rho y^{b_2}$	zooplankton nutrient quota	μmol/10^6 indv.
ρ	zooplankton nutrient quota coefficient	μmol nutrient/indv./μm $^{-b_2}$
b_2	zooplankton nutrient quota exponent	unitless
δ	zooplankton mortality rate	1/day

the size-dependent nutrient quota of the phytoplankton $Q(x)$; the size-dependent nutrient quota of the zooplankton $q(y)$; and the size-independent assimilation efficiency of the zooplankton ϕ. The rate of nutrient recycling is $\gamma B(P,Z) = \gamma[mQ(x)P + \delta q(y)Z + (1-\phi)Q(x)C(x,y)PZ]$ where γ is the proportion of recycled detritus and nutrients loss during phytoplankton consumption.

We used the nutrient supply I to indicate environmental productivity for two reasons. First, the primary productivity usually estimated by chlorophyll *a* or phytoplankton biomass is not a direct measure of resource supply but itself an ecosystem function of phytoplankton, which usually correlates with environmental resource supply (Cardinale et al. 2009b). Thus, the relationship between primary productivity and phytoplankton diversity in our model would be a diversity-productivity relationship rather than a causal productivity-diversity relationship. Second, the primary productivity in our model is subject to change during the phytoplankton-zooplankton coevolution even if the resource supply remains constant. Manipulating primary productivity can implicitly affect coevolution dynamics in the model. Instead, the abiotic nutrient supply I would be unequivocal indicator of resource supply (i.e., environmental productivity).

The function $\mu(x)$ describes how the maximum phytoplankton growth rate depends on phytoplankton cell size. Empirical observations suggest that the scaling relationship between phytoplankton growth rate and cell size is not monotonic. Nielsen (2006) suggested that growth rates of unicellular green algae and cyanobacteria decrease with cell sizes, following a power function with the exponent ranging from -1/3 to -1/4. At smaller cell size, however, picoplankton show a positive or unimodal scaling relationship (Raven 1994, Bec et al. 2008). By using different phyla of marine

phytoplankton, Maranon et al. (2013) showed unimodal size scaling relationships of phytoplankton growth. Therefore, phytoplankton growth rate is likely unimodal function of cell size along a wide range of cell sizes. In addition, mechanistic models involving size-dependent catalytic limitation and resouce uptake kinetics often find a unimodal relationship between growth rates and cell size (Verdy et al. 2009, Wirtz 2011). Here we define the scaling relationship between phytoplankton growth rate and cell size by

$$\mu(x) = \frac{x}{c_1 x^2 + c_2 x + c_3} \qquad \text{(Equation 4.2)}$$

where the unimodal shape of the function is enforced by the conditions

$$\begin{cases} \mu'(x) > 0; \mu''(x) < 0 & \text{small } x \\ \mu'(x) < 0; \mu''(x) > 0 & \text{large } x \end{cases} \qquad \text{(Inequality 4.3)}$$

Empirical evidence suggests that zooplankton consumption rates are maximized when zooplankton feed on particles with an optimal predator-prey size ratio although the size ratio may vary across species (e.g., Hansen et al. 1994). Thus, we formulated $C(x, y)$ as:

$$C(x, y) = C_m \exp[-\tfrac{1}{\lambda}(x - \theta y)^2] \qquad \text{(Equation 4.4)}$$

where the maximum consumption rate C_m occurs when zooplankton encounter phytoplankton at the optimal predator-prey ratio θ. The consumption rate would decrease

from $C_m$with a rate λ when the phytoplankton size x deviates from the optimal prey size θy.

Let (N^*, P^*, Z^*) denote the ecological coexistence equilibrium of the residents. The equilibrium values in the model (Equations 4.1a-c) can be estimated as:

$$P^* = \frac{\delta q(y)}{\phi Q(x) C(x,y)} \quad \text{(Equation 4.5a)}$$

$$Z^* = \frac{\mu(x) g(N^*)}{C(x,y)} - \frac{m + s(x)}{C(x,y)} \quad \text{(Equation 4.5b)}$$

$$N^* = I - \mu(x) g(N^*) P^* Q(x) + \gamma B(P^*, Z^*) \quad \text{(Equation 4.5c)}$$

Evolutionary component of the NPZ model

We use the theory of adaptive dynamics theory (Dieckmann and Law 1996, Geritz et al. 1998, Doebeli and Dieckmann 2000) to model the evolution in the NPZ model system. In this study, we focus on eco-evolutionary dynamics of phytoplankton size (*x*) and zooplankton size (*y*). Following the adaptive dynamics theory, we assume that ecological processes are much faster than the evolutionary processes; the phenotypes (size) of mutant offspring are close to the phenotype of the parents (i.e., the size of mutant phytoplankton x_1 and mutant zooplankton y_1 should be close to the resident size *x* and *y* are close to the sizes of resident phytoplankton and zooplankton species (x and y). We denote the fitness of a mutant phytoplankton (x_1) at the coexistence equilibrium (N^*, P^*, Z^*) of the residents (x and y) by $F(x_1, x, y)$ and the fitness of a mutant zooplankton (y_1) at the coexistence equilibrium of the residents by $G(y_1, x, y)$. Following Dieckmann and Law (1996), the evolutionary dynamics of phytoplankton and zooplankton cell sizes can be estimated as:

$$\frac{dx}{dt} = M_1 P^* \frac{\partial}{\partial x_1} F(x_1, x, y)|_{x_1=x} \qquad \text{(Equation 4.6a)}$$

$$\frac{dy}{dt} = M_2 Z^* \frac{\partial}{\partial y_1} G(y_1, x, y)|_{y_1=y} \qquad \text{(Equation 4.6b)}$$

where M_1 and M_2 are the respective mutation rates of the phytoplankton and the zooplankton. The functions $F(x_1, x, y)$ and $G(y_1, x, y)$ can be written as:

$$F(x_1, x, y) = \mu(x_1) g(N^*) - s(x_1) - m - C(x_1, y) Z^* \qquad \text{(Equation 4.7a)}$$

$$G(y_1, x, y) = \phi P^* Q(x) \frac{C(x, y_1)}{q(y_1)} - \delta(y_1) \qquad \text{(Equation 4.7b)}$$

Analytical Analysis

In this study, we are interested in the conditions that lead to diversification in phytoplankton with size x and zooplankton with size y. According to Equations 4.6 and 4.7, x and y become evolutionary singular points when:

$$0 = \frac{\partial}{\partial x_1} F(x_1, x, y)|_{x_1=x} \qquad \text{(Equation 4.8a)}$$

$$0 = \frac{\partial}{\partial y_1} G(y_1, x, y)|_{y_1=y} \qquad \text{(Equation 4.8b)}$$

Due to the complexity of the NPZ model, we perform analytical analysis on the special case where there is no nutrient recycling ($\gamma = 0$) (Appendix C.1) to make predictions of species diversification. First, we explore the stability of the ecological

coexistence equilibrium (Equations 4.5) in Appendix C.1.1. We then study the conditions for evolutionary diversification at the evolutionary singular points (Equations 4.8) in two cases, the evolution of phytoplankton in the absence of zooplankton (Appendix C.1.2) and the coevolution between phytoplankton and zooplankton (Appendix C.1.3). Notably, after diversification occurs in the model system, coevolution could lead to further adaptive radiation in new coalition of singular points.

The increasing polymorphisms made it difficult to obtain analytical solutions of our model (e.g., McGill and Brown 2007). To validate the predictions from the analytical analysis in more general cases, we examined further adaptive radiation of phytoplankton and zooplankton with positive γ in a set of numerical simulations.

Numerical Simulations

Our numerical simulations were done in the following way. The size spaces for the phytoplankton and zooplankton populations were discretized into bins of width 0.1 μm and 0.2 μm, respectively. Each simulation began with a single monomorphic population for each trophic level. The size bin of the initial monomorphic phytoplankton is determined by the ESS (Evolutionary Stable Strategy) -stable phytoplankton size in the absence of zooplankton (Appendix C.1.2) and the size bin of the initial monomorphic zooplankton is the associated optimal consumer size (x/θ). In the simulation, we generated the ecological dynamics of the model (Equations 4.1a-c) for a fixed time length (50 days) using *ode45* in Matlab. At the end of the time period, the number of mutant offspring that arose in each population were computed and then distributed into the adjacent size bins. The simulation was then restarted and the sequence was repeated until

the total length of time for the simulation reached 20,000 days. In our simulations, different combinations of *per capita* mutation rates of phytoplankton and zooplankton (M_1 and M_2 in Equation 4.5), ranging from 10^{-6} to 10^{-8} respectively, generated qualitatively similar results. Thus, we only report the results with mutation rates 10^{-6} for both trophic levels in this paper.

To assess PDRs in the simulated ecological and evolutionary processes, we ran simulations with seven different productivity levels (I = 20, 50, 100, 150, 200, 300, and 400 μmol nutrient/L/day). As discussed in more detail in Appendix C.1.3, evolutionary branching of both phytoplankton and zooplankton is likely when $\mu(x)$satisfies Inequality 4.3. To demonstrate the evolutionary divergence with different shapes of $\mu(x)$, we ran simulations for six different forms of $\mu(x)$ (see $\mu_1 - \mu_6$ in Fig. 4.1). The functions $\mu_1 - \mu_4$ were generated by randomly selecting parameters values that yield functions that fall within the range of observed scaling relationship of phytoplankton growth rates and cell size (see Appendix C.2 for details). Note that the observed scaling relationship of phytoplankton constrained the shape of the functions $\mu_1 - \mu_4$ to be unimodal. We also ran simulations with a monotonically increasing function (μ_5) and a monotonically decreasing function (μ_6) (Fig. 4.1). Each combination of the seven productivity levels and six forms of $\mu(x)$ received 10 replicated runs, totaling 420 separate runs.

To generate PDRs at different evolution time, we collected the following data from each simulation. We recorded the log-transformed abundances of phytoplankton and zooplankton in each size bin, every 500 days in the simulation, to generate size and abundance distributions for phytoplankton and zooplankton at 40 evolution time points. At each time point, a species was defined as a phenotypic cluster with similar cell sizes of

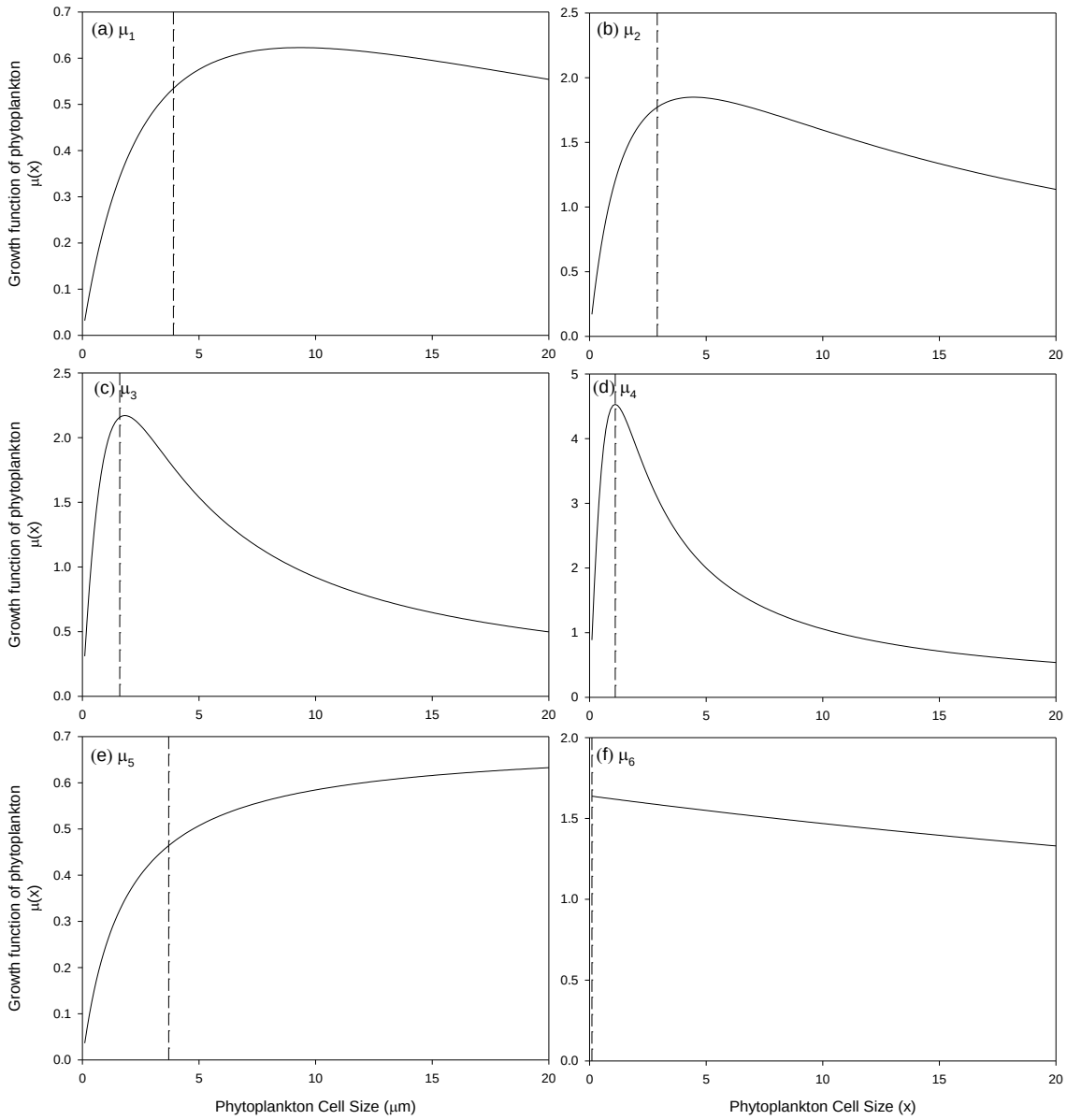

Fig. 4.1. Six parameter sets ($\mu_1 - \mu_6$) for the growth rate of phytoplankton $\mu(x)$ as a function of phytoplankton cell size x. The parameter values of $c_1 - c_3$ are randomly generated for $\mu_1 - \mu_4$ within the approximated range of phytoplankton size-dependent growth rates (Appendix C.2). The parameter values are: (a) μ_1: $c_1 = 0.04, c_2 = 0.95, c_3 = 3.06$; (b) μ_2: $c_1 = 0.03, c_2 = 0.29, c_3 = 0.56$; (c) μ_3: $c_1 = 0.09, c_2 = 0.12, c_3 = 0.31$; (d) μ_4: $c_1 = 0.09, c_2 = 0.02, c_3 = 0.11$; (e) μ_5: $c_1 = 0, c_2 = 1.45, c_3 = 2.61$ and (f) μ_1: $c_1 = 0.01, c_2 = 0.61, c_3 = 0$. Dash line in each plot denotes the evolutionary stable cell size of phytoplankton when zooplankton is absent.

phytoplankton or zooplankton. The number of such phenotypic clusters (species diversity) was estimated by using the Expectation–Maximization algorithm implemented from the *Mixtools* package (Benaglia et al. 2009) in *R* 3.0.3 (http://www.r-project.org). For a given number of phenotypic clusters (*n*), the Expectation–Maximization algorithm searches for *n* sets of parameters for normal distributions that best describe the populations with *n* phenotypic clusters. The fitness of different numbers of phenotypic clusters estimated by the Expectation–Maximization algorithm was then compared by using the function *boot.comp* in the *mixtools* package. Species richness was assessed as the amount of multiple normal-distributed phenotypic clusters best fitted for the simulated size and abundance distributions. To assess the shape of PDRs with different forms of $\mu(x)$, we performed Mitchell-Olds tests for the simulated species richness along the productivity gradient at each time step by using the *vegan* package (Oksanen et al. 2013) in R. We used quadratic regressions to test the relationship between environmental productivity and species richness when the Mitchell-Old tests suggested a significant quadratic hump (or pit) of species richness located within the range of the simulated environmental productivity. Otherwise, simple linear regressions were used.

Results

Here we present the analytical results of the conditions for evolutionary diversification on a special case with no nutrient recycling ($\gamma = 0$) in the model system (Equations 4.1). All analytic analysis and results are in detail in Appendix C.1. In the absence of zooplankton, phytoplankton would not diversify regardless of the level of environmental productivity (Appendix C.1.2). In the presence of zooplankton, co-

evolutionary divergence in phytoplankton and zooplankton can be driven by diversification in the phytoplankton (which then causes diversification in the zooplankton) or diversification in the zooplankton (which then causes diversification in the phytoplankton) (Appendix C.1.3). Phytoplankton-driven divergence is likely to occur when the zooplankton have a nearly optimal size for consuming phytoplankton ($x = \theta y$); the phytoplankton sinking rate $s(x)$ is nearly linear at the evolutionary singular point x; and selection initially favors large or small phytoplankton cell sizes (Appendix C.1.3). Zooplankton-driven divergence is likely to occur when the zooplankton consumption rate $C(x, y)$ is nearly linear at the evolutionary singular point y and the nutrient quota $q(y)$ is nearly linear at y (Appendix C.1.3). The first condition for zooplankton-driven divergence (linear consumption rate) is not likely to arise since it implies a suboptimal match between the zooplankton and phytoplankton cell sizes where zooplankton are too larger or too smaller than its optimal size ($\theta y = x$). Thus, our results suggest that in our system coevolutionary diversification is more likely to be driven by diversification in the phytoplankton.

Our numerical simulation showed no diversification when $\mu(x)$ is monotonic decreasing (μ_6). Thus, we only present the simulation results for the five different functions of $\mu(x)$ ($\mu_1 - \mu_5$) in this paper (see Fig. C1 as an example of evolutionary dynamics). With long evolution time, only positive PDRs are observed in both phytoplankton (Fig. 4.2, Table C1) and zooplankton (Fig. 4.3, Table C1). At some intermediate evolution time points, unimodal PDRs are present in the simulations (Fig. 4.2 and 4.3, Table C1). For example, the PDRs with μ_3 showed a unimodal pattern in the

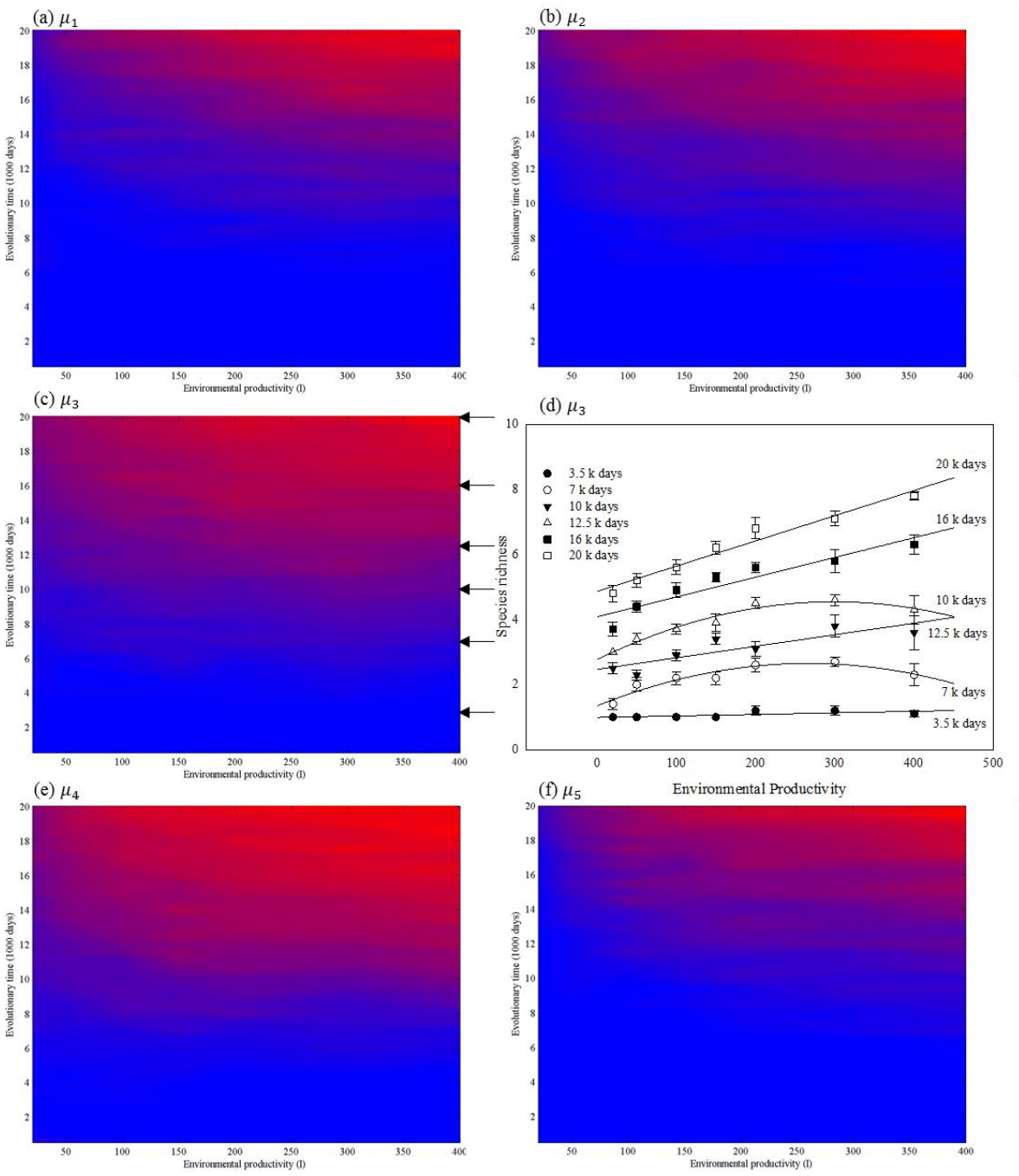

Fig. 4.2. The contours of phytoplankton species richness along the environmental productivity at different evolutionary time in the simulations. Species richness was estimated by using the Expectation–Maximization algorithm (see the Numerical Simulations section for more details). Contours in Panels a, b, c, e, and f show simulation results using five different forms of phytoplankton growth rate ($\mu_1 - \mu_5$), and are colored based on the average species richness in the simulations with the red color representing highest species richness and the blue color representing lowest species richness. (Fig. 4.2 legend continued on next page).

Fig. 4.2. Phytoplankton did not diverge with μ_6 in the simulations and is not plotted here. The parameter values used are following the approximation range in Appendix C.2: $\alpha = 0.001, \beta = 5.44 \times 10^{-9}, \rho = 1.36 \times 10^{-9}, \gamma = 0.1, \theta = 0.5, \lambda = 0.2, C_m = 10^{-5}, m = 0.071, \delta = 0.05, K = 2, \varphi = 0.1, d = 0.01, M_x = M_y = 10^{-6}$. The parameter values of $c_1 - c_3$ for the growth rate function of phytoplankton $\mu(x)$ are as in Fig. 4.1. Panel d explains how PDRs are demonstrated in the contour (Panel c). The PDRs in Panel d represent the species richness along the environmental productivity gradient at six different evolution time points in Panel c (as denoted by the arrows). Solid lines in Panel d represent the fitted lines in linear regressions or quadratic regressions based on the Mitchell-Olds tests (see the Numerical Simulations section for more details).

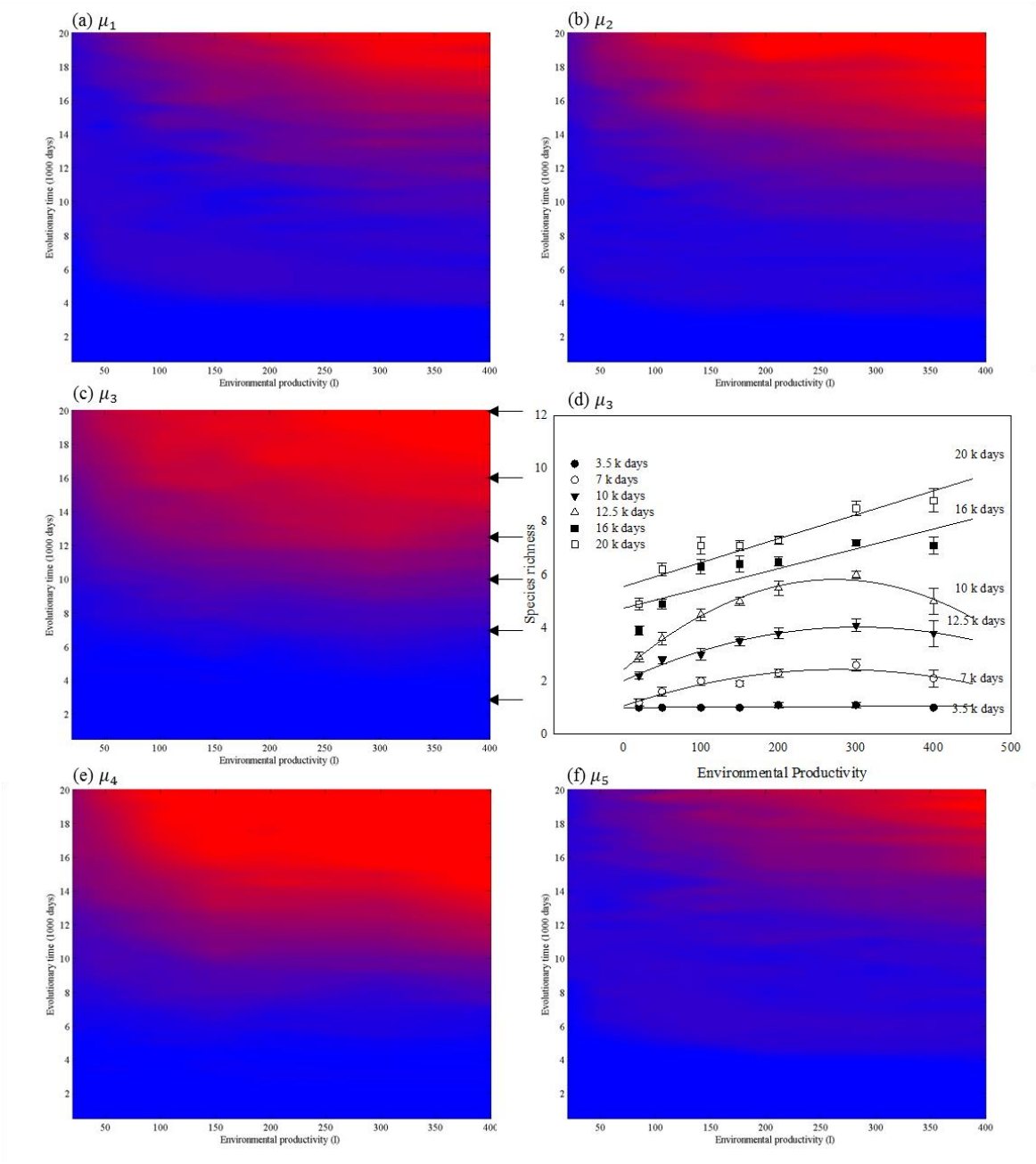

Fig. 4.3. The contours of zooplankton species richness along the environmental productivity at different evolutionary time in the simulations. Species richness was estimated by using the Expectation–Maximization algorithm and is represented by the blue color (lower richness) to red color (higher richness). Contours in Panels a, b, c, e, and f show simulation results using five different forms of phytoplankton growth rate ($\mu_1 - \mu_5$), and are colored following the same way as explained in Fig. 4.2. The PDRs in Panel d represent PDRs at six different evolution time points from Panel c (as denoted by the arrows). Solid lines in Panel d represent the fitted lines in linear regressions or quadratic regressions.

intermediate evolution time points and became positive at the end of simulation (Fig. 4.2d and 4.3d). We observed similar PDRs in the numerical simulation with monotonic decreasing $\mu(x)$ (μ_5) (Fig. 4.2f and 4.3f, Table C1).

Discussion

In our model, the coevolution of phytoplankton and zooplankton results in varied forms of transient PDRs (unimodal and positive) and positive steady-state PDRs given sufficient long periods of evolution time. The observed evolutionary dynamics were driven by two factors: resource competition among phytoplankton and predator-prey interactions between phytoplankton and zooplankton. In the absence of zooplankton, competition in phytoplankton followed the R* rule (Tilman 1982), resulting in a single population with the most competitive trait (Appendix C.1.2). The predator-prey interactions, on the other hand, may alter the fitness landscape of both trophic levels and lead to diversification in the coevolutionary dynamics. Our analytical results showed that this coevolutionary diversification is more likely driven by the diversification of phytoplankton (Appendix C.1.3). The evolutionary branching in phytoplankton, in turn, may cause diversification in zooplankton. Similar to the findings in other studies on the evolution of food webs (Loeuille and Loreau 2005, Ito and Ikegami 2006), the simultaneous top-down and bottom-up controls in the coevolutionary dynamics can further lead to recursive diversification in phytoplankton and zooplankton in our model system (e.g., Fig. C1). It is this recursive diversification that produces similar PDRs for phytoplankton and zooplankton (Fig. 4.2 and 4.3).

We attribute unimodal transient PDRs in our model to the slow tempo of evolution at high levels of productivity. Although more species may coexist at higher productivities (hence the positive PDRs), it takes longer for phytoplankton and zooplankton to attain evolutionary singular points at higher productivities (e.g., Fig. C1). Further, once diversification occurs, large resident populations supported at high productivities mean that it would take longer for rare mutants to gain a foothold and be recognized as a new species in the evolving community. The combination of the decreasing tempo of evolution and the increasing steady-state PDRs thus combine to produce various patterns of transient PDRs. Given different length of evolution time, our model predicts a nonsignificant PDR in a newly evolved community, an increasing saturating PDR in a fully evolved community, and transient unimodal PDRs in between (Fig. 4.2 and 4.3, Table C1). Consistent with our predictions, paleoecological evidence suggests that increase of marine phytoplankton (and zooplankton) diversity in the Cambrian and the Ordovician is likely due to the increased nutrient availability (e.g., Servais et al. 2008, 2010). In addition, the diversification of oceanic phytoplankton in the Cambrian and the Ordovician was coupled with the diversification of zooplankton (Tappan and Loeblich 1973, Moczydlowska 2002, Servais et al. 2008, but see Vecoli and Le Herisse 2004), indicating the important role of predator-prey coevolution as emphasized in our model.

The prediction of the evolving PDRs in our model can also help explain contemporary PDRs on different spatial scale. In a numerical sense, the relative fitness of a rare mutant in an evolving community is equivalent to the likelihood for an immigrant species to establish during community assembly. Thus, our results can translate into

predicting contemporary PDRs. PDRs mediated by predator-prey interactions can vary at the early stage of community assembly and unimodal to asymptotic positive at the late stage of community assembly. At the local scale, PDRs can vary considerably because of the different history of community assembly across local communities. Consistent with this prediction, similar patterns were shown in lake phytoplankton communities (Dodson et al. 2000, Korhonen et al. 2011). At the regional scale, larger spatial scale is more likely to involve productive habitats with longer history of community assembly, resulting in positive saturating (or unimodal) regional PDRs as frequently observed in lake or ocean plankton communities (e.g., Dodson et al. 2000, Irigoien et al. 2004, Korhonen et al. 2011, Stomp et al. 2011).

Our model also makes predictions on the evolutionary emergence of plankton body sizes. The average size of plankton in the steady-state PDRs increases with productivity (Fig. C2), which is consistent with empirical patterns of marine phytoplankton (Irigoien et al. 2004). Considering the reduced evolutionary rate with increasing productivity, large cell sizes at high productivity levels are expected to evolve much later. This prediction agrees with the fact that phytoplankton and zooplankton with larger body size recovered much more slowly after the end-Cretaceous mass extinction (Finkel 2007). In our model, the steady-state distribution of evolved plankton body sizes is characterized by regularly spaced coexisting sizes (e.g., Fig. C1). This discontinuous size distribution is most likely driven by predator-prey coevolution, consistent with the pattern found in a recent NPZ model, which also considers size-dependent trophic interactions (Banas 2011). Notably, our prediction does not completely contradict with the smooth size distribution commonly expected in the planktonic system. Large spatial

scale would consist of various evolving communities with different evolutionary history and steady-state size distribution as expected in our model. The size variation across these communities can combine to result in a continuous size distribution on large spatial scale. On the other hand, plankton communities indeed showed discontinuous cell size distributions in freshwater lakes (Havlicek and Carpenter 2001) and in marine ecosystems (Vergnon et al. 2009).

Despite the many consistencies between our predictions and empirical evidence, the model that we used to explore predator-prey coevolution is rather simple. For example, we assumed simple resource competition in phytoplankton with one limiting resource that leads to monomorphic phytoplankton population in the absence of zooplankton; it is possible that adding trade-offs in competition (e.g., Jansen and Mulder 1999) may influence the shape of PDRs. Nevertheless, the unequivocal demonstration of such tradeoffs remains elusive. In addition, we assumed constant mortality rate for phytoplankton and zooplankton in the model. However, our analytical results (Appendix C.1.3) suggest that our results will hold if the assumptions on these parameters are relaxed. Another issue of note is that we used a specific function $\mu(x)$ to describe to scaling relationship between phytoplankton growth rate and cell size and tested the PDRs with different shapes of $\mu(x)$ with parameter values falling within the range of observed pattern of the scaling relationship (Appendix C.2). A more mechanistic model for phytoplankton growth (e.g., Verdy et al. 2009) would generate similar size scaling relationship of phytoplankton growth under particular conditions (see details in Appendix C.3). Thus, we expect that our conclusion is unlikely to change if mode mechanistic models are used to describe phytoplankton growth.

Our results demonstrate that differences in evolutionary time can lead to different PDRs for coevolving phytoplankton and zooplankton. While our model was developed with the planktonic system in mind, we believe that our results may also apply to other systems, given that a variety of ecological interactions can lead to evolutionary branching (Doebeli and Dieckmann 2000) and that the general mechanisms driving PDRs in our model (e.g., slow tempo of evolution at high productivities) may similarly operate in other models. If confirmed, differences in evolutionary time may provide a simple explanation for the coexistence of the two most common PDRs observed in a variety of ecological communities.

References

Abrams, P. A., H. Matsuda, and Y. Harada. 1993. Evolutionary Unstable Fitness Maxima and Stable Fitness Minima of Continuous Traits. Evolutionary Ecology 7:465-487.

Banas, N. S. 2011. Adding complex trophic interactions to a size-spectral plankton model: Emergent diversity patterns and limits on predictability. Ecological Modelling 222:2663-2675.

Bec, B., Y. Collos, A. Vaquer, D. Mouillot, and P. Souchu. 2008. Growth rate peaks at intermediate cell size in marine photosynthetic picoeukaryotes. Limnology and Oceanography 53:863-867.

Benaglia, T., D. Chauveau, D. R. Hunter, and D. S. Young. 2009. mixtools: An R package for analyzing finite mixture models. Journal of Statistical Software 32:1-29.

Brown, J. H., J. F. Gillooly, A. P. Allen, V. M. Savage, and G. B. West. 2004. Toward a metabolic theory of ecology. Ecology 85:1771-1789.

Brown, J. S., and T. L. Vincent. 1992. Organization of Predator-Prey Communities as an Evolutionary Game. Evolution 46:1269-1283.

Cardinale, B. J., D. M. Bennett, C. E. Nelson, and K. Gross. 2009. Does productivity drive diversity or vice versa? A test of the multivariate productivity-diversity hypothesis in streams. Ecology 90:1227-1241.

Cardinale, B. J., H. Hillebrand, W. S. Harpole, K. Gross, and R. Ptacnik. 2009. Separating the influence of resource 'availability' from resource 'imbalance' on productivity-diversity relationships. Ecology Letters 12:475-487.

Dieckmann, U., and R. Law. 1996. The dynamical theory of coevolution: A derivation from stochastic ecological processes. Journal of Mathematical Biology 34:579-612.

Dodson, S. I., S. E. Arnott, and K. L. Cottingham. 2000. The relationship in lake communities between primary productivity and species richness. Ecology 81:2662-2679.

Doebeli, M., and U. Dieckmann. 2000. Evolutionary branching and sympatric speciation caused by different types of ecological interactions. American Naturalist 156:S77-S101.

Finkel, Z. V. 2007. Does Phytoplankton Cell Size Matter? The Evolution of Modern Marine Food Webs. Pages 334-351 in P. G. Falkowski and A. H. Knoll, editors. Evolution of primary producers in the sea. Academic Press, San Diego.

Geritz, S. A. H., E. Kisdi, G. Meszena, and J. A. J. Metz. 1998. Evolutionarily singular strategies and the adaptive growth and branching of the evolutionary tree. Evolutionary Ecology 12:35-57.

Gillman, L., and S. Wright. 2006. The influence of productivity on the species richness of plants: A critical assessment. Ecology 87:1234-1243.

Gurevitch, J., and K. Mengersen. 2010. A statistical view of synthesizing patterns of species richness along productivity gradients: devils, forests, and trees. Ecology 91:2553-2560.

Hansen, B., P. K. Bjornsen, and P. J. Hansen. 1994. The Size Ratio between Planktonic Predators and Their Prey. Limnology and Oceanography 39:395-403.

Havlicek, T. D., and S. R. Carpenter. 2001. Pelagic species size distributions in lakes: Are they discontinuous? Limnology and Oceanography 46:1021-1033.

Hillebrand, H., and B. J. Cardinale. 2010. A critique for meta-analyses and the productivity-diversity relationship. Ecology 91:2545-2549.

Hochberg, M. E., and M. van Baalen. 1998. Antagonistic coevolution over productivity gradients. American Naturalist 152:620-634.

Huisman, J., J. Sharples, J. M. Stroom, P. M. Visser, W. E. A. Kardinaal, J. M. H. Verspagen, and B. Sommeijer. 2004. Changes in turbulent mixing shift competition for light between phytoplankton species. Ecology 85:2960-2970.

Irigoien, X., J. Huisman, and R. P. Harris. 2004. Global biodiversity patterns of marine phytoplankton and zooplankton. Nature 429:863-867.

Ito, H. C., and T. Ikegami. 2006. Food-web formation with recursive evolutionary branching. Journal of Theoretical Biology 238:1-10.

Jansen, V. A. A., and G. Mulder. 1999. Evolving biodiversity. Ecology Letters 2:379-386.

Jiang, L., O. M. E. Schofield, and P. G. Falkowski. 2005. Adaptive evolution of phytoplankton cell size. American Naturalist 166:496-505.

Korhonen, J. J., J. J. Wang, and J. Soininen. 2011. Productivity-Diversity Relationships in Lake Plankton Communities. Plos One 6.

Leibold, M. A. 1996. A graphical model of keystone predators in food webs: Trophic regulation of abundance, incidence, and diversity patterns in communities. American Naturalist 147:784-812.

Leibold, M. A. 1998. Similarity and local co-existence of species in regional biotas. Evolutionary Ecology 12:95-110.

Loeuille, N., and M. Loreau. 2005. Evolutionary emergence of size-structured food webs. Proceedings of the National Academy of Sciences of the United States of America 102:5761-5766.

Maranon, E., P. Cermeno, D. C. Lopez-Sandoval, T. Rodriguez-Ramos, C. Sobrino, M. Huete-Ortega, J. M. Blanco, and J. Rodriguez. 2013. Unimodal size scaling of phytoplankton growth and the size dependence of nutrient uptake and use. Ecology Letters 16:371-379.

Mittelbach, G. G., C. F. Steiner, S. M. Scheiner, K. L. Gross, H. L. Reynolds, R. B. Waide, M. R. Willig, S. I. Dodson, and L. Gough. 2001. What is the observed relationship between species richness and productivity? Ecology 82:2381-2396.

Moczydlowska, M. 2002. Early Cambrian phytoplankton diversification and appearance of trilobites in the Swedish Caledonides with implications for coupled evolutionary events between primary producers and consumers. Lethaia 35:191-214.

Nielsen, S. L. 2006. Size-dependent growth rates in eukaryotic and prokaryotic algae exemplified by green algae and cyanobacteria: comparisons between unicells and colonial growth forms. Journal of Plankton Research 28:489-498.

Oksanen, J., F. G. Blanchet, R. Kindt, P. Legendre, P. R. Minchin, R. B. O'Hara, G. L. Simpson, P. Solymos, M. H. H. Stevens, and H. Wagner. 2013. vegan: Community Ecology Package. R package version 2.0-10.

Partel, M., L. Laanisto, and M. Zobel. 2007. Contrasting plant productivity-diversity relationships across latitude: The role of evolutionary history. Ecology 88:1091-1097.

Pärtel, M., K. Zobel, L. Laanisto, R. Szava-Kovats, and M. Zobel. 2010. The productivity-diversity relationship: varying aims and approaches. Ecology 91:2565-2567.

Ptacnik, R., L. Lepisto, E. Willen, P. Brettum, T. Andersen, S. Rekolainen, A. L. Solheim, and L. Carvalho. 2008. Quantitative responses of lake phytoplankton to eutrophication in Northern Europe. Aquatic Ecology 42:227-236.

Raven, J. A. 1994. Why Are There No Picoplanktonic O(2) Evolvers with Volumes Less-Than 10(-19) M(3). Journal of Plankton Research 16:565-580.

Rosenzweig, M. L., and Z. Abramsky. 1993. How are diversity and productivity related? Pages 52-65 in R. E. Ricklefs and D. Schluter, editors. Diversity in Ecological Communities. University of Chicago Press.

Servais, T., O. Lehnert, J. Li, G. L. Mullins, A. Munnecke, A. Nutzel, and M. Vecoli. 2008. The Ordovician Biodiversification: revolution in the oceanic trophic chain. Lethaia 41:99-109.

Servais, T., A. W. Owen, D. A. T. Harper, B. Kroger, and A. Munnecke. 2010. The Great Ordovician Biodiversification Event (GOBE): The palaeoecological dimension. Palaeogeography Palaeoclimatology Palaeoecology 294:99-119.

Stomp, M., J. Huisman, G. G. Mittelbach, E. Litchman, and C. A. Klausmeier. 2011. Large-scale biodiversity patterns in freshwater phytoplankton. Ecology 92:2096-2107.

Tappan, H., and A. R. Loeblich. 1973. Evolution of Oceanic Plankton. Earth-Science Reviews 9:207-240.

Tilman, D. 1982. Resource competition and community structure. Princeton University Press, Princeton, N.J.

Tilman, D., and S. W. Pacala. 1993. The maintenance of species richness in plant communities. Pages 13-25 in R. E. Rickleffs and D. Schluter, editors. Species Diversity in Ecological Communities. University of Chicago Press.

Vecoli, M., and A. Le Herisse. 2004. Biostratigraphy, taxonomic diversity and patterns of morphological evolution of Ordovician acritarchs (organic-walled microphytoplankton) from the northern Gondwana margin in relation to palaeoclimatic and palaeogeographic changes. Earth-Science Reviews 67:267-311.

Verdy, A., M. Follows, and G. Flierl. 2009. Optimal phytoplankton cell size in an allometric model. Marine Ecology-Progress Series 379:1-12.

Vergnon, R., N. K. Dulvy, and R. P. Freckleton. 2009. Niches versus neutrality: uncovering the drivers of diversity in a species-rich community. Ecology Letters 12:1079-1090.

Waide, R. B., M. R. Willig, C. F. Steiner, G. Mittelbach, L. Gough, S. I. Dodson, G. P. Juday, and R. Parmenter. 1999. The relationship between productivity and species richness. Annual Review of Ecology and Systematics 30:257-300.

Wirtz, K. W. 2011. Non-uniform scaling in phytoplankton growth rate due to intracellular light and CO2 decline. Journal of Plankton Research 33:1325-1341.

Wright, D. H. 1983. Species-energy theory: an extension of species-area theory. Oikos:496-506.

Zobel, M., and M. Partel. 2008. What determines the relationship between plant diversity and habitat productivity? Global Ecology and Biogeography 17:679-684.

APPENDIX A

SUPPLEMENT TO CHAPTER 1

Measuring protist species intrinsic growth rate *r* and carrying capacity *K*

We measured the intrinsic growth rates and carrying capacities of the five protist species (*B. americanum, C. kleini, G. scintillans, P. aurelia,* and *P. bursaria*) that persisted in our experiment in a supplemental experiment that established monocultures of each species. The intrinsic growth rate and carrying capacity of each species were measured under the same experimental conditions as the main experiment. We set up five monocultures for each species, each starting with ~100 individuals. The populations were sampled daily (every 12hr for *G. scintillans*) until they no longer followed exponential growth. Using population densities during the exponential growth phase, we performed linear regressions on the natural-log transformed population densities against time; the slopes of the linear regressions gave rise to species intrinsic growth rates. Using the estimated intrinsic growth rate, we then fitted monoculture population dynamics to the logistic growth model to estimate the carrying capacity of each species.

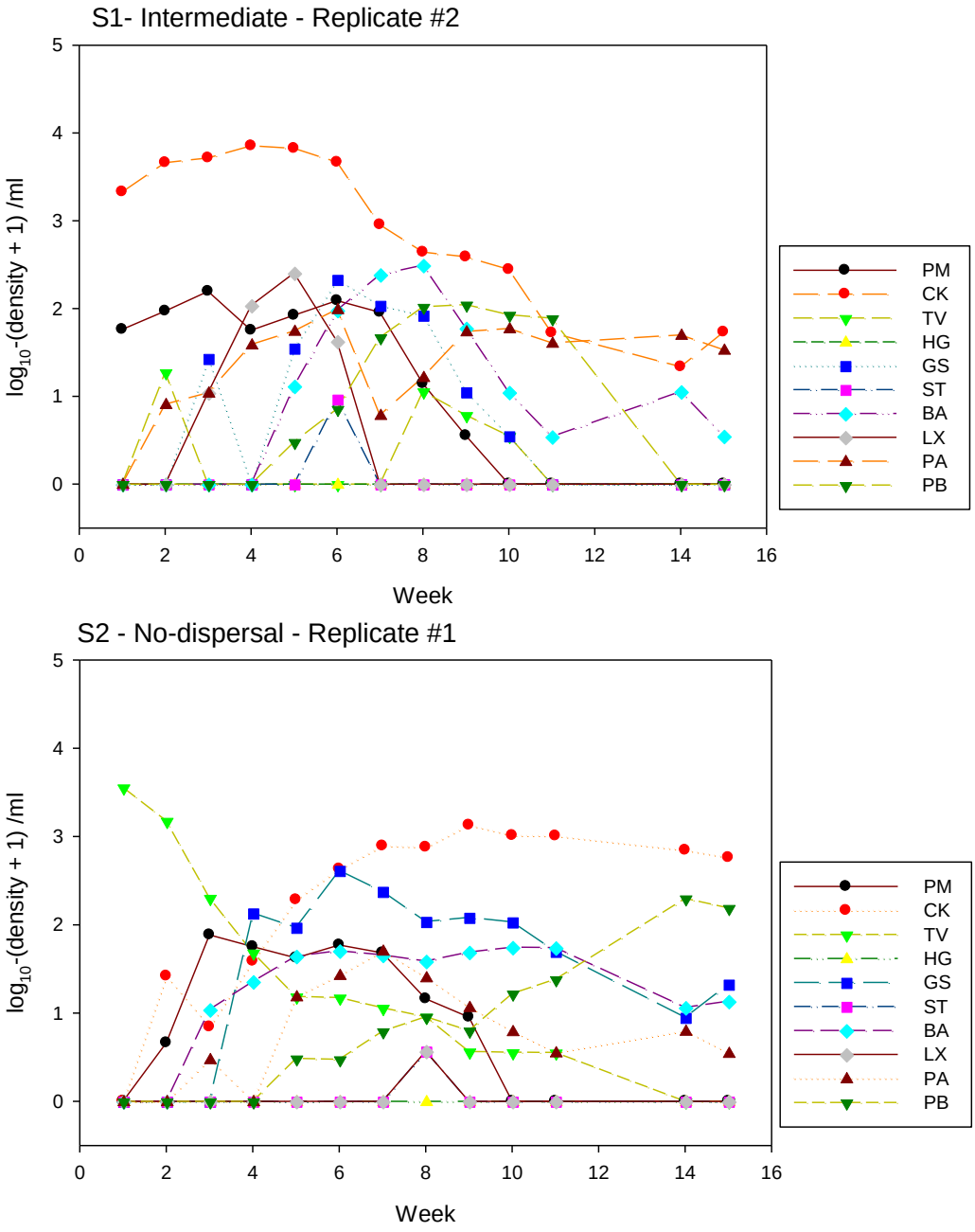

Fig. A1. Protist community dynamics in different assembly history treatments. One representative community was randomly selected from each history treatment (S1-S5), irrespective of dispersal rates among local communities. See Table 1 for species names and assembly sequences.

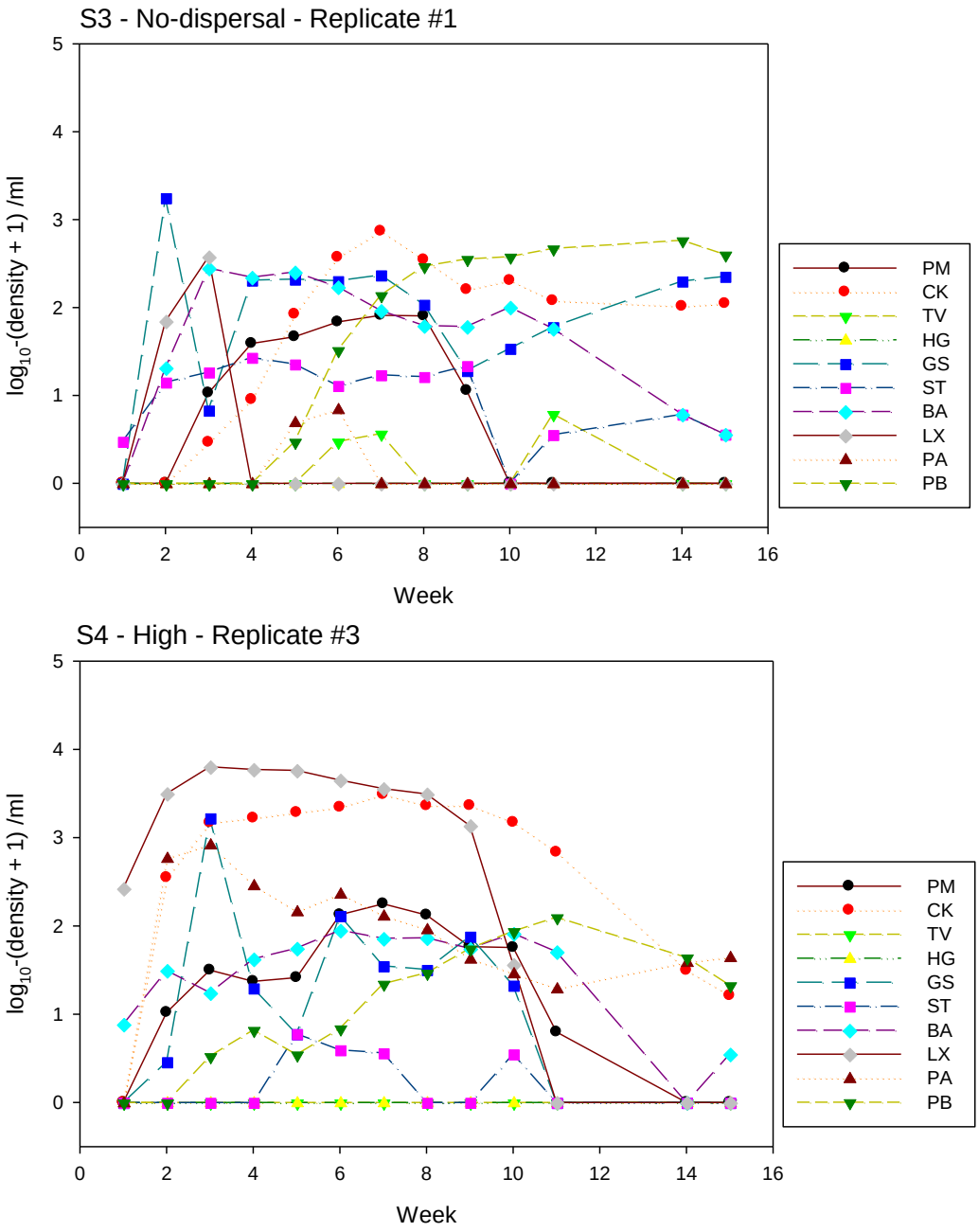

Fig. A1. (continued).

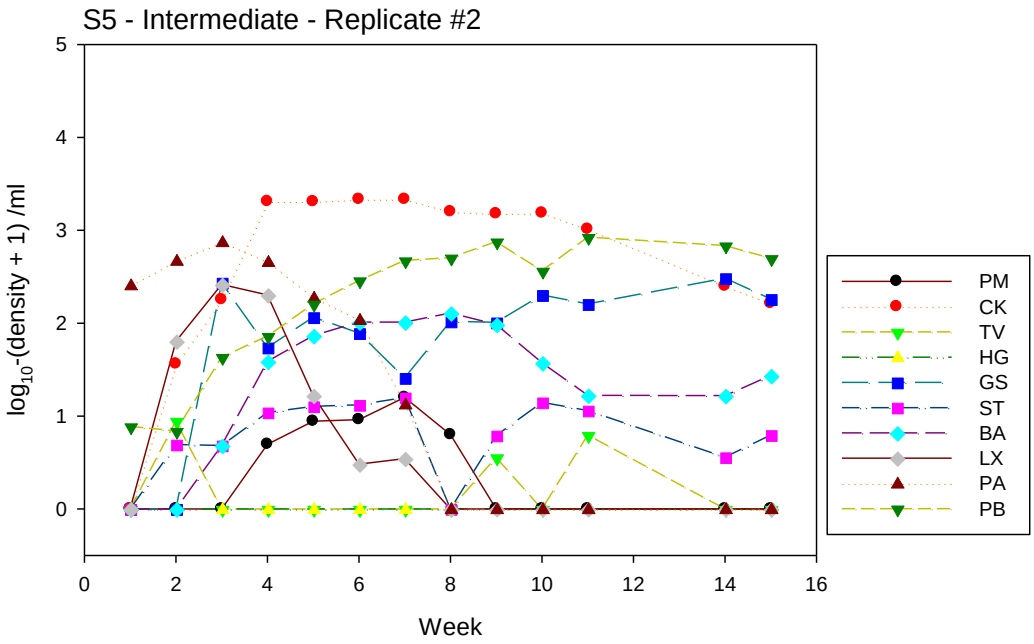

Fig. A1. (continued).

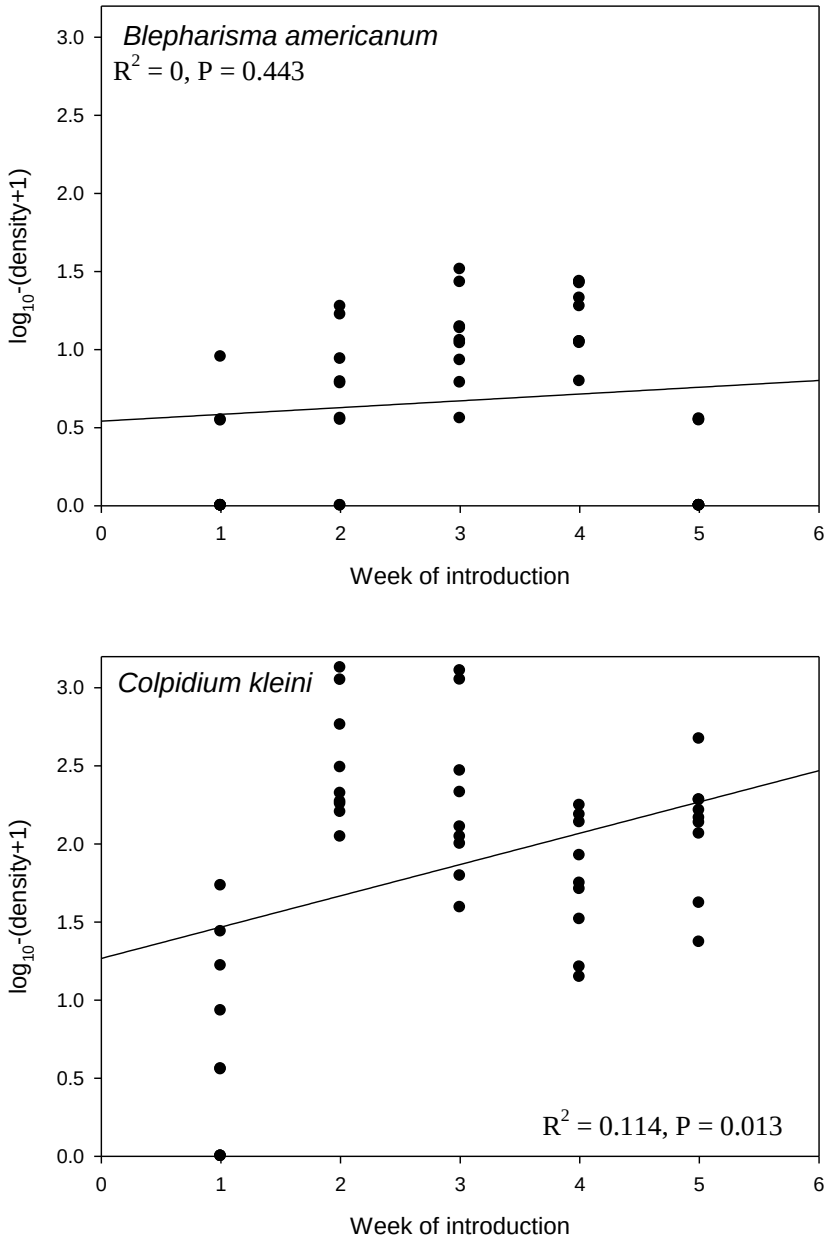

Fig. A2. The relationship between species abundance at the end of the experiment and its colonization order. The solid line, with adjusted R^2 and P values, in each plot represents the fitted line in a simple linear regression. Dispersal did not affect the fitted relationship, except for *S. teres* (ANCOVA: dispersal, $F_{2,39} = 4.350$, P = 0.020) for which separate regression was performed at each dispersal level. Analyses for *H. grandinella*, *Loxocephalus sp.*, and *P. multimicronucleatum* were not done because of their regional extinction in all metacommunities.

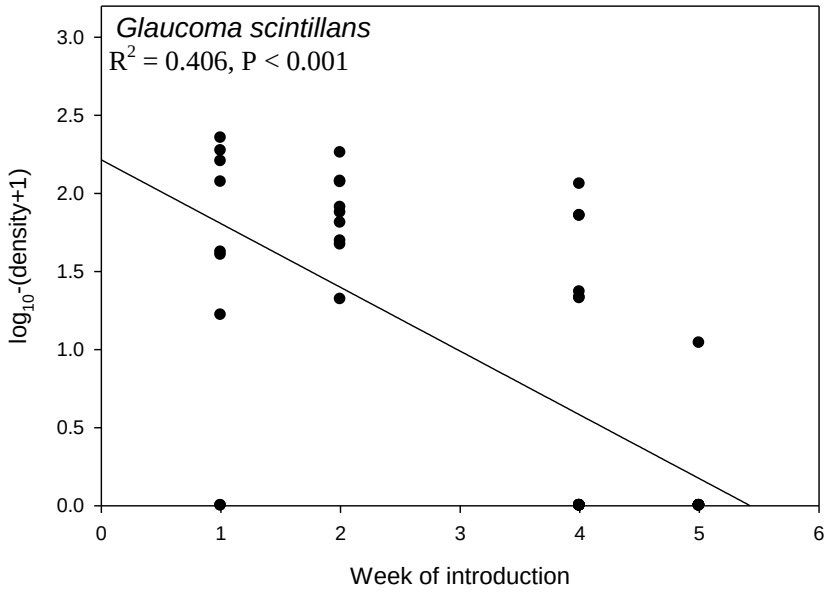

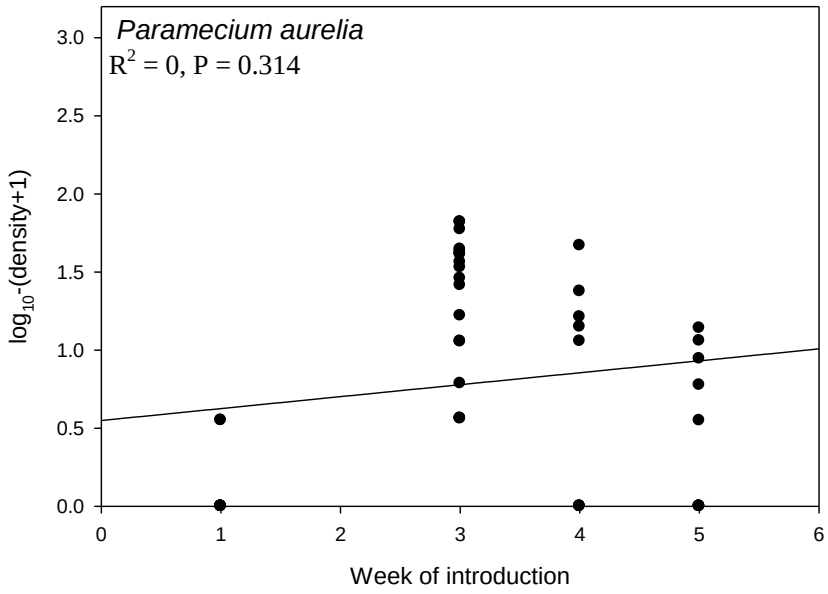

Fig. A2. (continued).

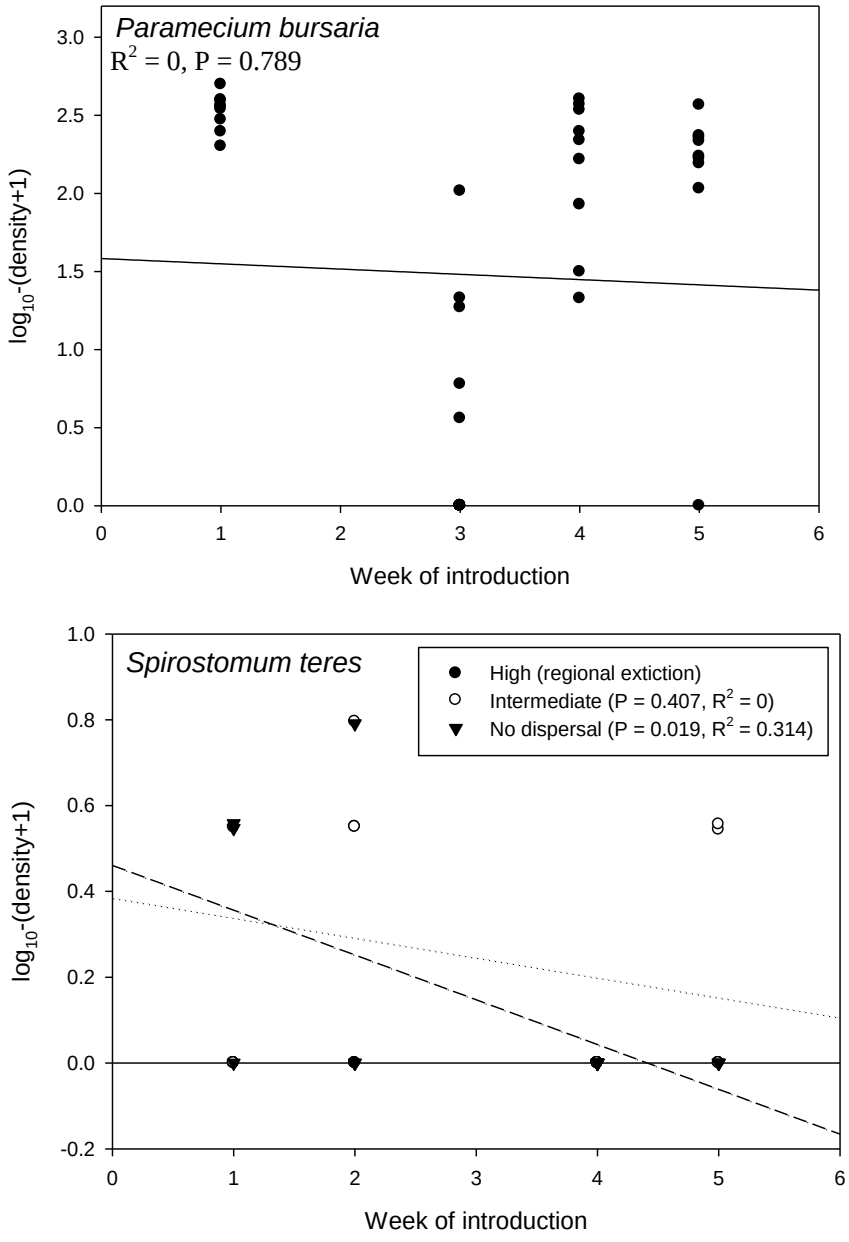

Fig. A2. (continued).

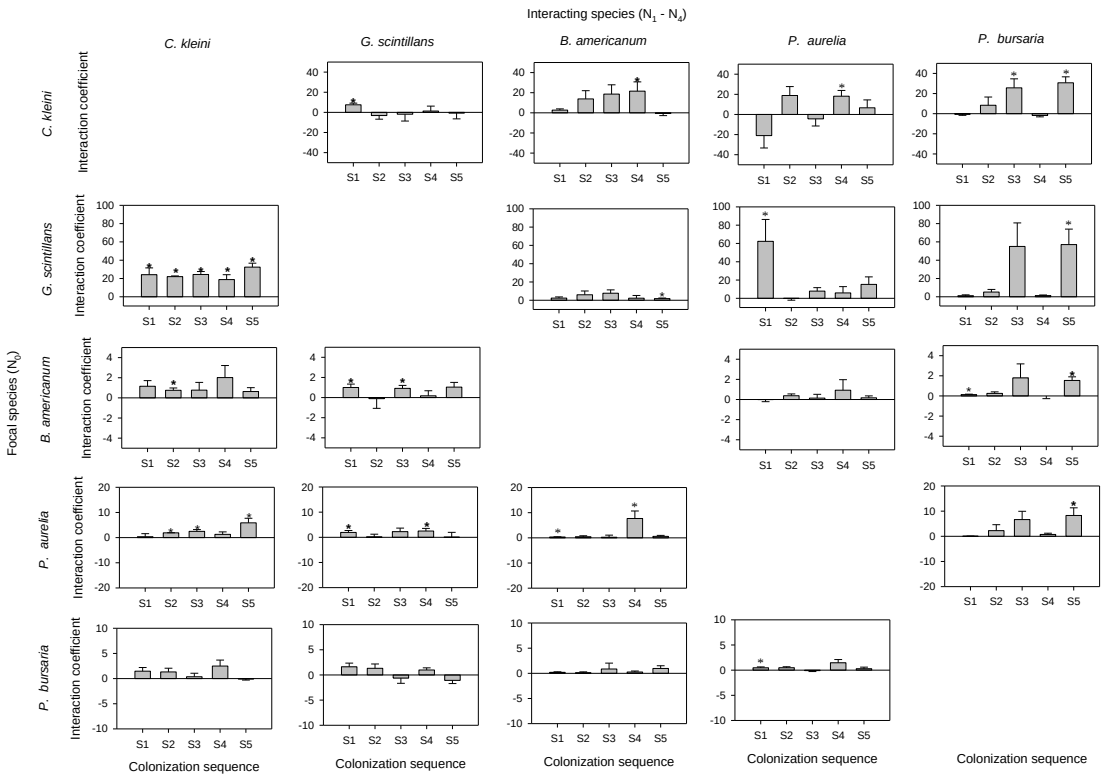

Fig A3. Interaction coefficients between the five common protist species estimated from Lotka-Volterra models (Equation 1 in the main manuscript). Plots in each row represent the interactions between a focal species (N_0) and the other four interacting species ($N_1 - N_4$), whereas plots in each column represent the interactions of one interacting species with different focal species. The interaction coefficients are categorized by colonization sequences (S1 – S5, Table 1). Asterisks indicate that the interaction coefficients significantly differed from 0 (T test, $P < 0.05$).

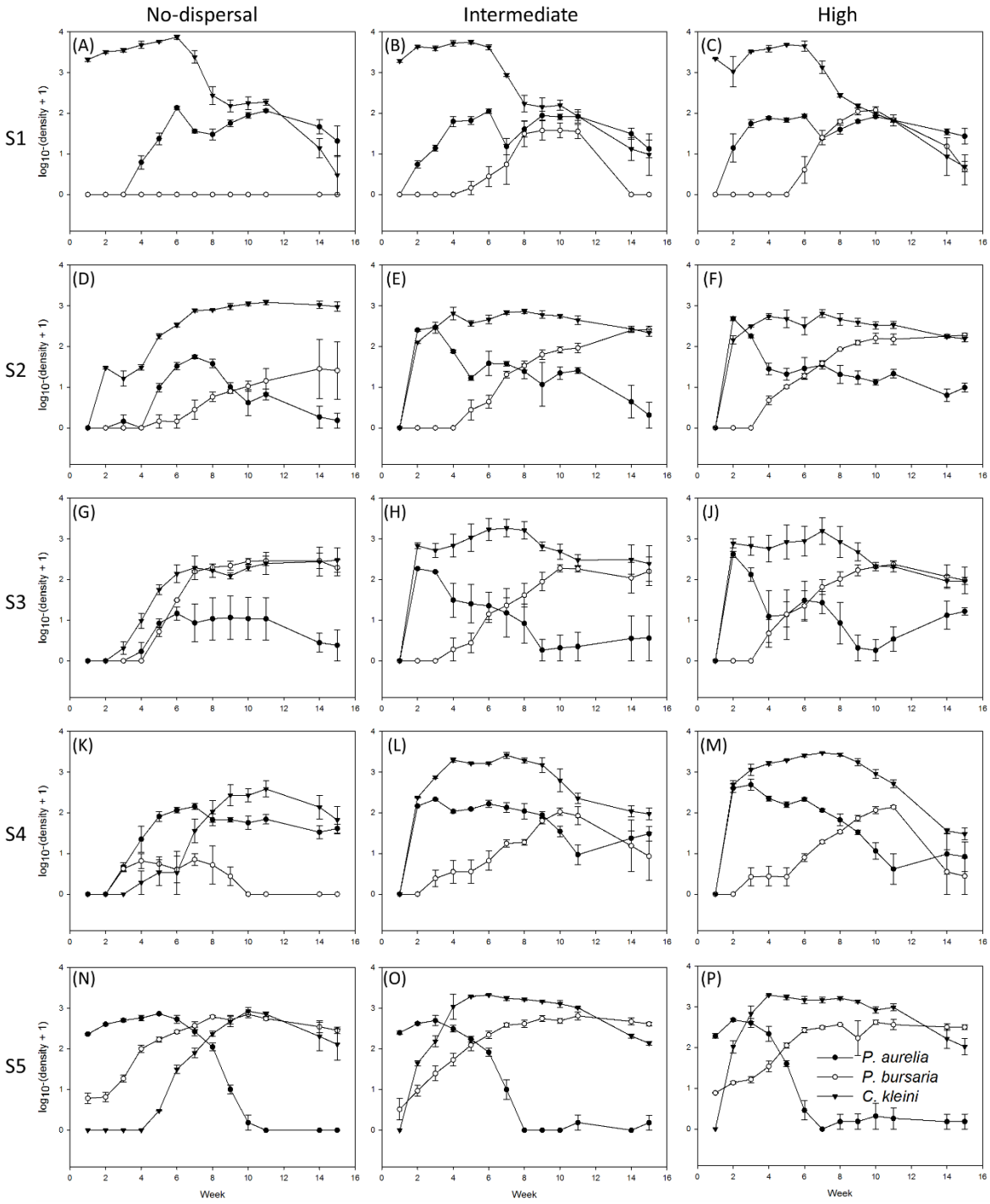

Fig. A4. Population dynamics of *P. aurelia*, *P. busaria*, and *C. kleini* in each treatment. Filled triangles: *C. kleini*; filled circles: *P. aurelia*; open circles: *P. bursaria*. Population density data are log-transformed [$\log_{10}$ (number of individuals/ml+1)]. Values are means ± SE.

APPENDIX B

SUPPLEMENT TO CHAPTER 2

B.1 Measuring functional traits

To measure intrinsic growth rates and carrying capacities, we inoculated ~100 individuals of each species into a microcosm and monitored population growth in the monocultures every 12 or 24hr (12hr for *Colpoda sp., Glaucoma scintillans*, and *Tetrahymena pyriformis*, and 24hr for the other species), until the populations reached their carrying capacities. Each monoculture had three replicates, totaling 45 microcosms. The intrinsic growth rate of each species was determined by regressing natural logarithm of population densities against time during exponential population growth.

To estimate cell volumes and mouth sizes, we randomly selected 20 cells of each species from 15-day old stock cultures and measured cell length, width and the size of oral cavity under a compound microscope. Cell volumes were calculated based on equations that approximate cell shapes (Likens & Wetzel 1991).

To estimate swimming speed, we recorded the movement of five cells of each species randomly selected from 15-day old stock cultures by using a camera (Olympus DP71) attached to a dissecting microscope. For each cell, we recorded its movement for at least three seconds (six seconds for *Halteria grandinella*). The time length was sufficiently to estimate the average swimming speed of each species. We measured the total length of the path that the cell moved and calculated swimming speed as the average length a cell moved per second.

B.2 Phylogeny construction

The aligned SSU rRNA sequences of the 15 species and one outgroup species, *Sarcocystis lacerate*, were obtained from the SILVA rRNA database (Pruesse *et al.* 2007). For *Colpoda sp.* and *Loxocephalus sp.*, which we were unable to identify to the species level, we used the sequences of their cogeners instead. Omitting these species or using other cogeners' sequences led to no qualitative change in the phylogeny. We removed the poorly aligned and highly divergent regions in the sequences by checking the alignment manually and in Gblocks (Castresana 2000). We built a maximum likelihood (ML) phylogenetic tree in PhyML (Guindon *et al.* 2010) with a BIONJ starting tree and a TrN substitution model with a proportion of invariable sites and a gamma-distributed variation of rates (TrN+I+G, I = 0.509, G = 0.668) as suggested by jModeltest2 (Darriba *et al.* 2012). The ML tree was then transformed to an ultrametric tree (Fig. B1) by using the nonparametric rate smoothing method implemented in r8s (Sanderson 2003). A phylogeny constructed with the Bayesian method is qualitatively similar to the ML tree.

References

Castresana, J. (2000). Selection of conserved blocks from multiple alignments for their use in phylogenetic analysis. Mol Biol Evol, 17, 540-552.

Darriba, D., Taboada, G.L., Doallo, R. & Posada, D. (2012). jModelTest 2: more models, new heuristics and parallel computing. Nat Methods, 9, 772-772.

Guindon, S., Dufayard, J.-F., Lefort, V., Anisimova, M., Hordijk, W. & Gascuel, O. (2010). New algorithms and methods to estimate maximum-likelihood phylogenies: assessing the performance of PhyML 3.0. Systematic biology, 59, 307-321.

Likens, G. & Wetzel, R. (1991). Limnological analyses. Springer-Verlag, New York.

Pruesse, E., Quast, C., Knittel, K., Fuchs, B.M., Ludwig, W.G., Peplies, J. et al. (2007). SILVA: a comprehensive online resource for quality checked and aligned ribosomal RNA sequence data compatible with ARB. Nucleic Acids Res, 35, 7188-7196.

Sanderson, M.J. (2003). r8s: inferring absolute rates of molecular evolution and divergence times in the absence of a molecular clock. Bioinformatics, 19, 301-302.

Table B1. The relationships between each individual trait and niche difference, between individual trait and relative fitness; and the phylogenetic signals of individual traits. Mantel's test with 9,999 permutations was used to assess the relationship between Euclidean distance based on the standardized values of each individual trait and niche difference estimated from the bacteria experiment. Liner regression was used to assess the relationship between the value of each individual trait and it relative fitness measured by the bacterial R*. The Blomberg's K tests with 9,999 permutations were used to estimate phylogenetic signals. Asterisks in the table indicate $P < 0.05$.

Trait	Niche difference (Mantel's *r*)	Relative fitness (R^2)	Phylogenetic signal (Blomberg's K)
Cell volume	0.260*	0.038	0.617*
Mouth size	0.053	0.001	0.315*
Filtration mode	0.384*	0.163	2.778*
Intrinsic growth rate	0.207	0.013	0.222
Carrying capacity	-0.091	0.005	0.029
Swimming speed	0.268	0.200	0.154

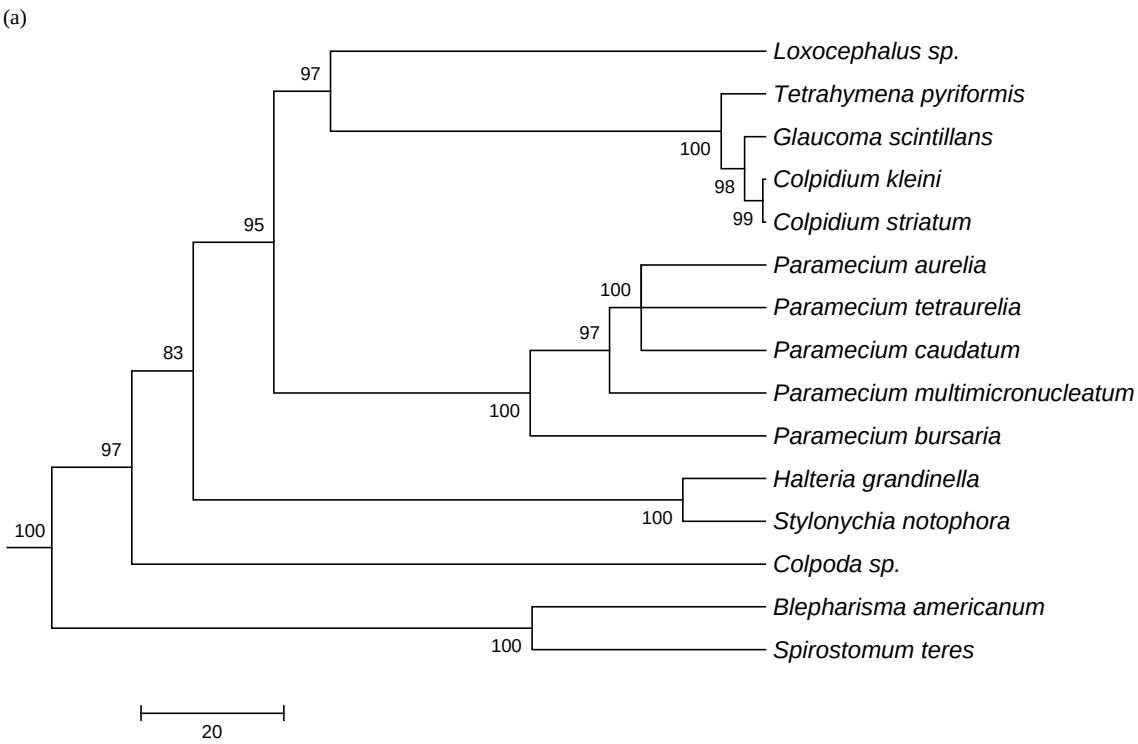

Fig. B1. The phylogeny (a) and functional dendrogram (b) of the relations between the fifteen species used in the experiment. The functional dendrogram is based on the group average (UPGMA) clustering. The interval branch length between each pair of species represents the dissimilarity between the species, calculated from the trait values. The phylogeny was reconstructed using the ML method based on the SSU rRNA sequences of each species. Values on the nodes represent scores of approximate likelihood ratio test as measures of support for the divergences.

(b)

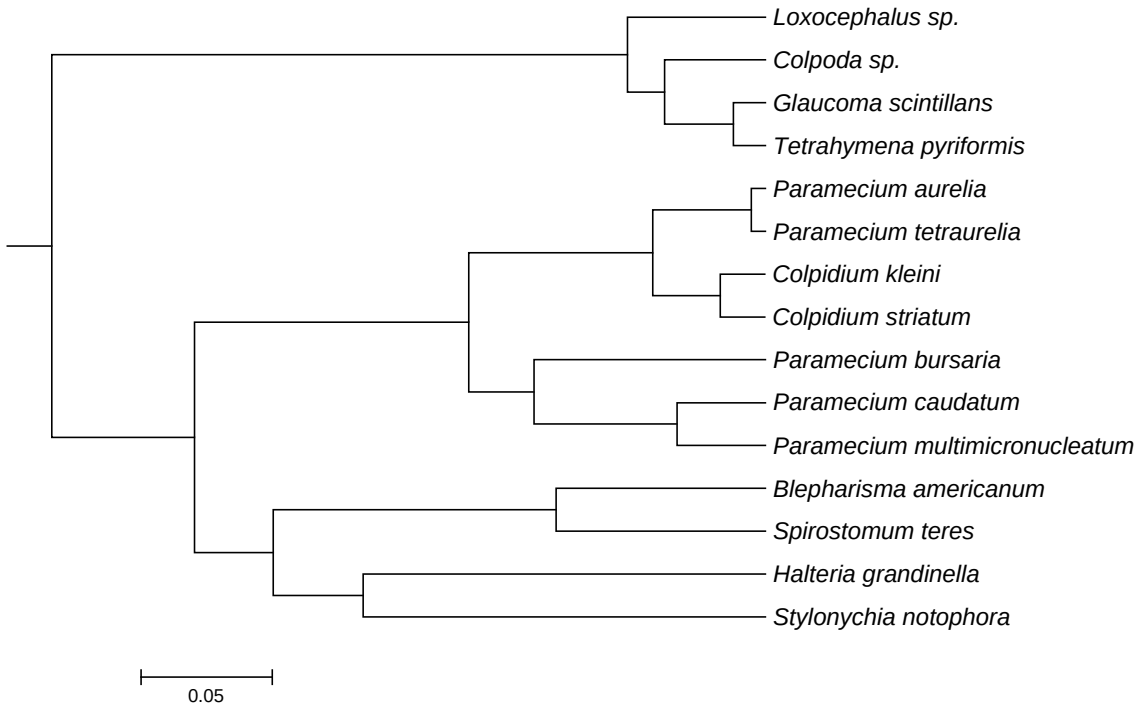

Fig. B1. (Continued).

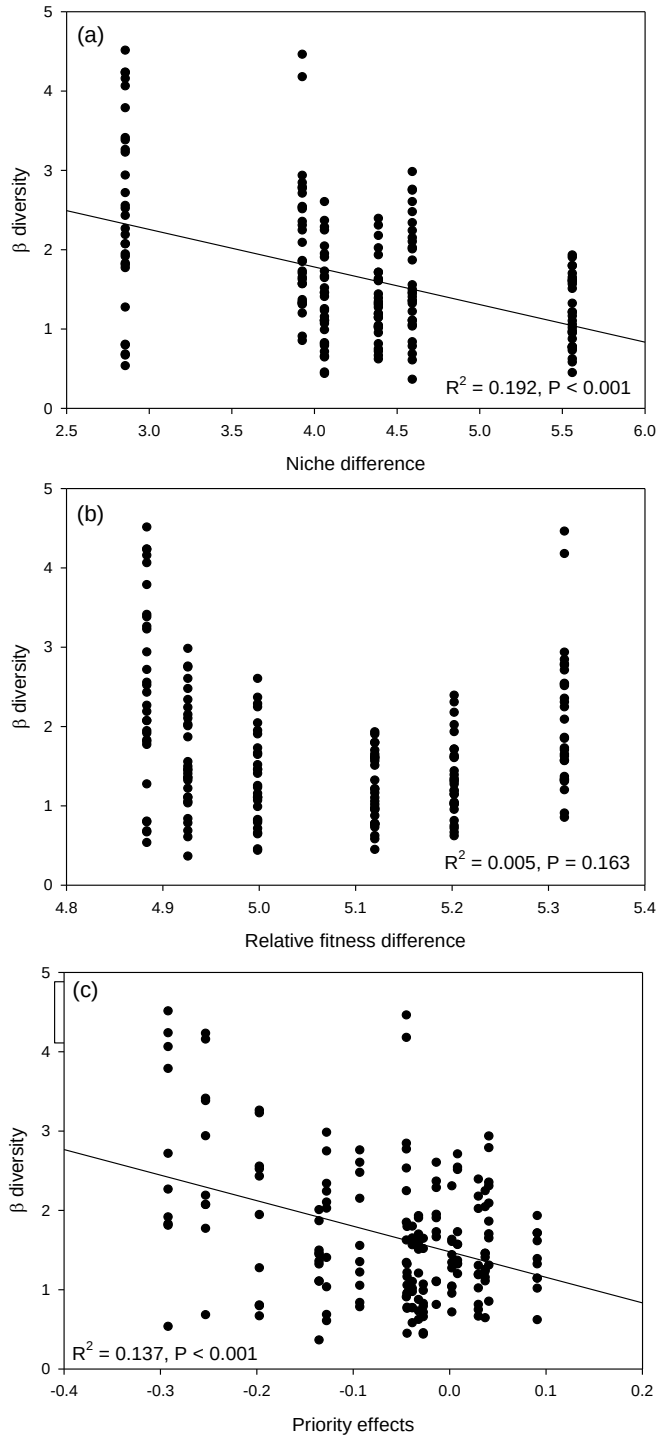

Fig. B2. The relationships between β diversity across the communities characterized by the same species pool and (a) niche difference, (b) relative fitness difference, (c) overall priority effects of each species pool.

APPENDIX C

SUPPLEMENT TO CHAPTER 4

C.1 Analysis of Model without Nutrient Recycling

To simplify the analytical analysis of the model, we focus on the special case where there is no nutrient recycling in the system, i.e., $\gamma = 0$. To simplify the notation, we combine the mortality terms $\bar{s}(x) = s(x) + m$ and then rename $\bar{s}(x)$ by $s(x)$. Similarly, we combine the terms $\bar{q}(y) = q(y)/\phi$ and rename $\bar{q}(y)$ by $q(y)$. Thus, in the following we focus on the following model.

$$\frac{dN}{dt} = I - dN - \mu(x)g(N)PQ(x)$$

$$\frac{dP}{dt} = P[\mu(x)g(N) - s(x) - C(x,t)Z] \qquad \text{(Equation C1)}$$

$$\frac{dZ}{dt} = Z[C(x,y)\frac{Q(x)}{q(y)}P - \delta(y)]$$

Throughout we will use subscripts to denote the differentiation with respect to a particular variable when a function has multiple dependent variables, e.g., $C_x = \partial C/\partial x$. When a function has a single dependent, we will use primes to denote differentiation with respect to the dependent variable, e.g., $\mu' = d\mu/dx$. We assume $\mu(x)$ is a unimodal function of x, $g'(N) > 0, s'(x) > 0, Q'(x) > 0, q'(y) > 0$, and $\delta'(y) > 0$. We assume that $C(x,y)$ is a unimodal function of x and y and that $\text{sign}(C_x) = -\text{sign}(C_y)$. All of the functions used in our simulations satisfy these assumptions.

C.1.1 Ecological Equilibrium

Let (N^*, P^*, Z^*) denotes the coexistence equilibrium of system (Equation C1) for fixed trait values x and y. The equilibrium values are defined by the equations

$$P^* = \frac{\delta q}{QC}$$

$$0 = I - dN^* - \mu(x)g(N^*)P^*Q(x) \qquad \text{(Equation C2)}$$

$$Z^* = \frac{\mu(x)g(N^*)}{C(x,y)} - \frac{s(x)}{C(x,y)}$$

The Jacobian evaluated at the coexistence equilibrium is

$$J = \begin{pmatrix} -1 - g'(N)Q\mu P & -\mu g(N)Q & 0 \\ P\mu g'(N) & 0 & -CP \\ 0 & CZQ/q & 0 \end{pmatrix}\Bigg|_{N^*,P^*,Z^*} \qquad \text{(Equation C3)}$$

The characteristic polynomial for the Jacobian is

$$p(\rho) = \rho^3 + (1 + g'\mu QP^*)\rho^2 + \frac{QP^*}{q}(C^2Z^* + \mu^2 g' gq)\rho + \frac{C^2Z^*QP^*}{q}(1 + g'\mu P^*).$$

(Equation C4)

Via the Routh-Hurwitz criteria, all roots of the characteristic polynomial have negative real part if (i) all coefficients are positive and (ii) the product of the linear and

quadratic coefficients minus the constant term is positive. Since $g'(N^*) > 0$, all of the coefficients are positive. The second ondition simplifies to

$$(1 + g' \ \mu P^* Q) Q P^* \mu^2 g' \ g > 0, \qquad \text{(Equation C5)}$$

which is always true. Thus, all roots of the characteristic polynomial have negative real part and the coexistence equilibrium is stable whenever it exists.

C.1.2 No Phytoplankton Evolutionary Branching In the Absence of Zooplankton

We first show that evolutionary branching cannot occur in the phytoplankton in the absence of zooplankton. In the absence of zooplankton, the ecological dynamics are

$$\begin{aligned} \frac{dN}{dt} &= I - N - \mu(x) g(N) P Q(x) \\ \frac{dP}{dt} &= P[\mu(x) g(N) - s(x)] \end{aligned} \qquad \text{(Equation C6)}$$

The ecological equilibrium of this system satisfies

$$P^* = \frac{I - N^*}{\mu(x) g(N^*) Q(x)} \quad \text{and} \quad g(N^*) = \frac{s(x)}{\mu(x)} \qquad \text{(Equation C7)}$$

The evolutionary dynamics of the phytoplankton are given by

$$\frac{dx}{dt} = M_1 P^* \frac{\partial}{\partial x_1}\Big|_{x_1=x} = M_1 P^* (\mu'(x) g(N^*) - s'(x) \qquad \text{(Equation C8)}$$

where x is the trait value for the resident and x_1 is the trait value for a mutant. Evolutionary equilibria occur at trait values satisfying $dx/dt = 0$. The evolutionary equilibrium is dynamically stable (i.e., a stable equilibrium point) if

$$0 > \frac{\partial}{\partial x}\frac{dx}{dt} = \mu''(x) g(N^*) + \mu'(x) g'(N^*) \frac{\partial N^*}{\partial x} - s''(x) = \mu''(x) g(N^*) - s''(x).$$

(Equation C9)

The last equality in the previous equation follows from

$$\frac{\partial N^*}{\partial x} = -\frac{\mu' g - s'}{\mu g'} = 0, \qquad \text{(Equation C10)}$$

which can be derived by differentiating the second equality in Equation C8 with respect to x, solving for $\frac{\partial N^*}{\partial x}$, and recalling that $dx/dt = 0$ at the evolutionary equilibrium. Evolutionary branching occurs at an evolutionary equilibrium when $''(x) g(N^*) - s''(x) > 0$. Since this equality is the opposite of Equation C9, an evolutionary equilibrium cannot be both dynamically stable and an evolutionary branching point. Thus, in our model, phytoplankton evolutionary branching cannot occur in the absence of zooplankton.

C.1.3 Conditions for Evolutionary Branching in System (Equation C1)

The fitness of an invading phytoplankton with trait x_1 and the fitness of an invading zooplankton with trait y_1 is denoted by equations 7a and 7b in the main text. Evolutionary equilibria arise at points x_1 and y_1 satisfying

$$\left.\frac{\partial F(x,x_1)}{\partial x_1}\right|_{x_1=x} = \mu' g(N^*) - s' - C_x Z^* = 0 \qquad \text{(Equation C11)}$$

$$\left.\frac{\partial G(y,y_1)}{\partial y_1}\right|_{y_1=y} = P^* Q\left(\frac{C_y q - q' C}{q^2}\right) - \delta' = 0. \qquad \text{(Equation C12)}$$

Note that because $\delta' > 0$ and $q' > 0$, equation (A12) is only satisfied for values of y such that $C_y > 0$. Since we assume $\text{sign}(C_x) = -\text{sign}(C_y)$, we have that $C_y > 0$ and $C_x < 0$ at an evolutionary equilibrium point.

The Jacobian evaluated at the evolutionary equilibrium points x and y is

$$J_{Ev} = \begin{bmatrix} M_1 \dfrac{\partial}{\partial x}\left(\left.\dfrac{\partial F}{\partial x_1}\right|_{x_1=x}\right) & M_1 \dfrac{\partial}{\partial y}\left(\left.\dfrac{\partial F}{\partial x_1}\right|_{x_1=x}\right) \\ M_2 \dfrac{\partial}{\partial x}\left(\left.\dfrac{\partial G}{\partial y_1}\right|_{y_1=y}\right) & M_2 \dfrac{\partial}{\partial y}\left(\left.\dfrac{\partial G}{\partial y_1}\right|_{y_1=y}\right) \end{bmatrix}$$

$$= \left.\begin{bmatrix} M_1 \dfrac{\partial^2 F}{\partial x_1^2} + M_1 \dfrac{\partial^2 F}{\partial x\, \partial x_1} & M_1 \dfrac{\partial^2 F}{\partial y\, \partial x_1} \\ M_2 \dfrac{\partial^2 G}{\partial x\, \partial y_1} & M_2 \dfrac{\partial^2 G}{\partial y_1^2} + M_2 \dfrac{\partial^2 G}{\partial y\, \partial y_1} \end{bmatrix}\right|_{x_1=x, y_1=y} \qquad \text{(Equation C13)}$$

where M_1 and M_2 are the mutation rates of the phytoplankton and the zooplankton at the evolutionary equilibrium, respectively. An evolutionary equilibrium point is an evolutionary attractor if all of the eigenvalues of the Jacobian have negative real part. If one or more of the eigenvalues have positive real part, then the equilibrium point is a evolutionary repellor. In this appendix we will focus on evolutionary equilibria where the determinant of the Jacobian is positive and the trace of the Jacobian is negative, i.e., both eigenvalues of the Jacobian have negative real parts. It is important to note that coevolutionary cycles can arise when the trace and the determinant of the Jacobian are positive, i.e., the eigenvalues have positive real parts (Dieckmann et al., 1995; Doebeli and Dieckmann, 2000; Mougi and Iwasa, 2011). The analysis of the dynamics that arise in this case is beyond the scope of this study.

The entries of the Jacobian J_{Ev} are computed by implicitly differentiating equations (C2). We use subscripts to denote the partial derivatives of the equilibrium density values with respect to the traits, e.g, $N_x = \partial N^* / \partial x$. Implicit differentiation with respect to x yields

$$N_x = \frac{\partial N^*}{\partial x} = \frac{-\mu g P_x Q - \mu' g P Q - \mu g P Q'}{1 + \mu g' P Q} \qquad \text{(Equation C14)}$$

$$P_x = \frac{\partial P^*}{\partial x} = -\delta q \frac{Q'C + QC_x}{Q^2 C^2} \qquad \text{(Equation C15)}$$

$$Z_x = \frac{\partial Z^*}{\partial x} = -\frac{N_x}{\delta q} - \frac{s'C - C_x s}{C^2} \qquad \text{(Equation C16)}$$

Implicit differentiation with respect to y yields

$$P_y = \frac{\partial P^*}{\partial y} = \frac{1}{Q}\frac{\partial}{\partial y}\left(\frac{\delta q}{C}\right) = \frac{q}{CQ}\left[\delta' - \frac{\delta q}{C}\left(\frac{C_y q - q' C}{q^2}\right)\right] = 0 \quad \text{(Equation C17)}$$

$$N_y = \frac{\partial N^*}{\partial y} = \frac{-\mu g P_y Q}{1 + \mu g' P Q} = 0 \quad \text{(Equation C18)}$$

$$Z_y = \frac{\partial Z^*}{\partial y} = \frac{1}{C}\left(\mu g'^{N_y} - C_y Z\right) = \frac{C_y Z}{C} \quad \text{(Equation C19)}$$

Using the above, the terms of the Jacobian J_{Ev} in equation (A13) are

$$\left.\frac{\partial^2 F}{\partial x_1^2}\right|_{x_1 = x} = M_1(\mu'' g - s'' - C_{xx} Z^*)$$

$$\left.\frac{\partial^2 F}{\partial x\, \partial x_1}\right|_{x_1 = x} = M_1(\mu' g'^{N_x} - C_x Z_x) = M_1 g'^{N_x} C \frac{\partial}{\partial \mu}\left[\frac{\mu}{C}\right]$$

$$\left.\frac{\partial^2 F}{\partial x_1\, \partial y}\right|_{x_1 = x} = M_1\left(\mu' g'^{N_y} - C_{xy} Z - C_x Z_y\right) = M_1 Z C \frac{\partial}{\partial y}\left[\frac{C}{C_x}\right]$$

$$\left.\frac{\partial^2 G}{\partial y_1^2}\right|_{y_1 = y} = M_2\left[P^* Q \frac{\partial^2}{\partial y^2}\left(\frac{C}{q}\right) - \delta'\right]$$

$$\left.\frac{\partial^2 G}{\partial y_1\, \partial y}\right|_{y_1 = y} = M_2 P_y Q\left(\frac{C_y q - q' C}{q^2}\right) = 0$$

and

$$\left.\frac{\partial^2 G}{\partial y_1\,\partial x}\right|_{y_1=y} = (Q'P + P_x Q)\left(\frac{C_y q - q' C}{q^2}\right) + QP\left(\frac{C_{xy} q - q' C_x}{q^2}\right)$$

$$= (Q'P + P_x Q)\left(\frac{C_y q - q' C}{q^2}\right) + QP\left[\frac{C_{xy} q}{q^2} - \frac{C_x}{q^2}\left(\frac{-\delta' q^2}{PQC} + \frac{C_y q}{C}\right)\right]$$

$$= \frac{QP}{q}\left(C_{xy} - \frac{C_x C_y}{C}\right) + P\left(\frac{C_y q - q' C}{q^2}\right)\left[Q' - \frac{Q}{QC}(Q'C + C_x Q) + Q\frac{C_x}{C}\right]$$

$$= \delta\frac{\partial}{\partial y}\left(\frac{C_x}{C}\right).$$

The trace and determinant of J_{Ev} are

$$\begin{aligned}\mathrm{tr}(J_{Ev}) \quad &= M_1(\mu'' g - s'' - C_{xx} Z^*) + M_1 g' N_x C\frac{\partial}{\partial \mu}\left(\frac{\mu}{C}\right) \\ &\quad + M_2\left[P^* Q\frac{\partial^2}{\partial y^2}\left(\frac{C}{q}\right) - \delta''\right]\end{aligned} \qquad \text{(Equation C20)}$$

$$\begin{aligned}\det(J_{Ev}) \quad &= M_1 M_2\left[(\mu'' g - s'' - C_{xx} Z^*) + g'^{N_x} C\frac{\partial}{\partial \mu}\left(\frac{\mu}{C}\right)\right]\left[P^* Q\frac{\partial^2}{\partial y^2}\left(\frac{C}{q}\right) - \delta''\right] \\ &\quad - M_1 M_2 Z C\frac{\partial}{\partial y}\left[\frac{C}{C_x}\right]\delta\frac{\partial}{\partial y}\left(\frac{C_x}{C}\right).\end{aligned}$$

(Equation C21)

Evolutionary branching can occur at an evolutionary when either

$$\left.\frac{\partial^2 F}{\partial x_1^2}\right|_{x_1=x} = \mu'' g(N^*) - s'' - C_{xx} Z^* > 0 \qquad \text{(Equation C22)}$$

or

$$\left.\frac{\partial^2 G}{\partial y_1^2}\right|_{y_1=y} P^* Q \frac{\partial^2}{\partial y^2}\left(\frac{C}{q}\right) - \delta'' > 0 \qquad \text{(Equation C23)}$$

First consider the condition for evolutionary branching initially driven by the phytoplankton when Equation C22 is satisfied. When do we expect condition (C22) to be satisfied? The third term in equation (C22) is positive when $C_{xx} < 0$. Biologically, this occurs when there is a nearly optimal match between the zooplankton and the phytoplankton trait values, i.e., the attack rate of the zooplankton is nearly maximal. Thus, nearly optimal matches between the zooplankton and phytoplankton traits promote evolutionary branching. Note that we expect $C_{xx} < 0$ to arise in most cases since the opposite condition, $C_{xx} > 0$, implies that there is a large mismatch between the zooplankton and phytoplankton traits.

Our derivation of $s(x)$ is based on Stoke's Law and predicts that $s'' > 0$. Thus, the second term in condition (C22) is negative, implying that mortality due to sinking inhibits evolutionary branching. Consequently, evolutionary branching is more likely to occur when s'' is small, i.e., the acceleration in the mortality rate due to an increase in cell size is small. The first term in condition (C22) is positive when $\mu'' > 0$. For the unimodal functions considered in this study, $\mu'' > 0$ when the phytoplankton trait is very large. Thus, evolutionary branching is promoted when selection favors large phytoplankton ESDs. Evolutionary branching can also occur if μ'' is small in magnitude relative to the third term in condition (C22). When the maximum growth rate of the phytoplankton is relatively linear (i.e., μ does not have much curvature), then μ'' will be

small in magnitude. Previous work on the shapes of $\mu(x)$ (Bec et al., 2008; Nielsen, 2006) suggest that $\mu(x)$ is linear for small phytoplankton ESDs. Hence, evolutionary branching may also be promoted when selection favors small phytoplankton ESDs. Note that for our functional forms of $\mu(x)$ and $s(x)$, evolutionary branching cannot occur in the phytoplankton in the absence of zooplankton. Indeed, evolutionary equilibria satisfy $\mu' g(N^*) - s' = 0$. Since $s' > 0$ for all x, $\mu' > 0$ at the equilibrium. For the functional forms of $\mu(x)$ considered in this study, $\mu' > 0$ only when $\mu'' < 0$. Hence, $\partial^2 G / \partial x_1^2$ is negative at all evolutionary equilibria in the absence of zooplankton, implying that the evolutionary branching cannot occur.

In total, in our model, evolutionary branching in the phytoplankton is promoted when there is a nearly optimal match between the zooplankton and phytoplankton trait values, when the acceleration in phytoplankton sinking rate is small, and when selection favors large or small phytoplankton ESDs. In addition, evolutionary branching can only occur in our model in the presence of zooplankton.

Now consider the condition for evolutionary branching initially driven by the zooplankton when (C23) is satisfied. In this case, evolutionary branching occurs initially in the zooplankton species. Note that because $G_{y_1 y} = 0$, if the zooplankton were the only evolving species and $G_{y_1 y_1} > 0$, then the evolutionary equilibrium would be an evolutionary repeller. This mean that evolutionary branching in the zooplankton cannot occur in the absence of evolution in the phytoplankton. This also means that evolutionary branching in the zooplankton can only occur if phytoplankton-zooplankton coevolution drives the system to a state where the zooplankton are trapped at fitness minimum.

The second term of condition (C23) is positive when $\delta'' < 0$. That is, evolutionary branching is promoted when the death rate of the zooplankton is a decelerating function of the zooplankton trait. Evolutionary branching will be inhibited when the death rate is an accelerating function of the zooplankton trait. The first term in condition (C23) is positive when $\frac{\partial^2}{\partial y_1^2}\left(\frac{C}{q}\right) > 0$, or equivalently

$$C_{xx}q^2 - 2C_x q_x q + 2C q_x^2 - C q'' q > 0. \qquad \text{(Equation C24)}$$

The second and third terms of the left hand side of condition (C24) are always positive. Since we expect a nearly optimal match between the zooplankton and the phytoplankton, i.e., $C_{xx} < 0$, the first term is expected to be negative. Our functional form for $q(y)$ satisfies $q'' > 0$, thus the third term on the left hand side of equation (C24) is negative. Condition (C24) is likely to be satisfied when the curvatures of C_{xx} and q'' are small, e.g., the attack rates and nutrient quotas are nearly linear.

In total, evolutionary branching is expected in the zooplankton when the death rate of the zooplankton is a decelerating function of the zooplankton trait and when the attack rate and zooplankton nutrient quota have little curvature. In addition, evolutionary branching driven by selection in the zooplankton can only arise if the coevolutionary dynamics of the system are driven to state where the zooplankton are trapped a fitness minimum.

C.2 Parameter Estimates and Derivations

Parameters ranges were derived from empirical estimates published in the literature. Because we are interested in PDRs across different communities, we use data from a wide range of phytoplankton and zooplankton species. The estimates for all parameters are summarized in Table C2. Our derivations for each estimate follow.

Cell Sizes

The Estimated Spherical Diameters (ESDs) of phytoplankton range from less than 2μm to greater than 2000μm (Sieburth and Smetacek, 1978; Beardall et al., 2009). Phytoplankton are typically characterized as picoplakton ($< 2\mu$m), nanoplankton (2-20μm), microplankton (20-200μm), or macroplankton (200-2000μm). The ESDs of zooplankton (in particular, ciliates, rotifers, and copepods) range from 25μm to 900μm (Hansen et al., 1994). We will primarily concern ourselves with phytoplankton between 0 and 200 μm in size.

Zooplankton Selectivity (θ, λ)

We use the optimal prey size data in Hansen et al. (1994) to estimate the values of θ and λ; see Table C3 below. We estimate θ by dividing the optimal prey body size (column 2 in Table C3) by the body size of the zooplankton (column 1 in Table C3). The estimated values of θ lie between 0.025 and 0.2. For example, $\hat{\theta}$ for the ciliate *Strombidium reticulatum* is 0.19 and $\hat{\theta}$ for the copepod *Temora longicornis* is 0.027. Two estimates for λ were computed. Let $x_{50\%min}$ denote the phytoplankton body size that is smaller than the optimal body size and at which the consumption rate is half of the

maximum value. Similarly, let $x_{50\%max}$ denote the phytoplankton body size that is greater than the optimal body size and at which the consumption rate is half of the maximum value. To estimate λ, we solve the equation $C_m = 0.5C_m \exp[-(x_{50\%} - \frac{\theta y)^2}{\lambda}]$ where $x_{50\%} = x_{50\%min}$ or $x_{50\%} = x_{50\%max}$, θ is the value estimated above, and y is the reported ESD of the phytoplankton. This approach yields two estimates, λ_{min} and λ_{max} respectively, for λ. The estimates for λ range over four orders of magnitude, particularly the values of λ_{max}. In our model, for very large values of λ, the zooplankton can eat phytoplankton of all sizes. Since this tends to inhibit evolutionary diversification, restricted the λ to the range $(0.2,50)$. This range contains 18 out of 22 of the λ_{min} values and 8 out of 19 of the λ_{max} values.

Sinking Rates $s(x)$

Estimates for phytoplankton sinking rates $s(x) = \alpha x^2$ are based on the study by Walsby and Holland (2006).. In that study, the sinking rate of *Planktothrix rubescens*, a rod like phytoplankton with an ESD of about 8.7, was measured in freshwater. Stokes formula predicts that phytoplankton sink at a rate give by νr^2 where r is the radius of the phytoplankton and ν is a constant that is determined by the density of the zooplankton, the density and viscosity of the liquid, and other fluid dynamic constants. The authors computed the sinking rates of the rod shaped phytoplankton for different orientations (in particular, horizontal and vertical positioning of the rod). We use an average of the sinking rates to get an estimate for ν. The estimate for ν is then used to compute α for the function $s(x)$; see Table C4.

The coefficient α_L in Table C4 describes the rate at which individuals of a particular size sink out of the system, i.e., it is a size dependent per capita mortality rate for the phytoplankton when the habitable region is L meters deep. To compute α_L, we first computed the volume of the cylindrical cells (using the width and height values). Then we computed the ESD from the volume using the equation $\text{ESD} = 2(3V_{cell}/4\pi)^{1/3}$. We then solved for v by solving the velocity equation of a sinking sphere, $v_{avg} = v(\text{ESD}/2)^2$. This gives a parameterization for the equation describing the velocity at which phytoplankton with an ESD of x sink, $v = v(x/2)^2$. The average amount of time for a phytoplankton of size x to sink L meters is given by $L/v(x)$. Thus, the average rate at which phytoplankton die due to sinking is $v(x)/L = \alpha_L$. After converting units, one obtains the values in the α_1 and α_{10} columns of the table.

Note the following simplifications we make when modeling the phytoplankton sinking rates. First, our model implicitly assumes that phytoplankton cell densities are constant across ESDs. Second, the above measurements were done in freshwater. We expect smaller sinking rates in salt water due to the increased density and viscosity of salt water. Third, our estimates do not take into account the effects of cell shape on sinking rates; sinking rates can vary greatly depending on the orientation and the shape of the organism. Fourth, our model does not account for the fact that many species can change their sinking rate by changing their buoyancy.

Estimates for the sinking rate of phytoplankton were also reported in Raven (1998). In that study, the sinking velocity of phytoplankton cells in a medium with density 50 kg m $^{-}3$ is predicted by the equation $v_{cell} = 0.0104r$ where r is the radius of the cell. Here, v_{cell} has units m·day $^{-1}$, the coefficient has units m/μm ^{2}day $^{-1}$, and the

cell radius is in μm. If the depth of the habitable layer is L meters, then these sinking rates result in the sinking mortality term $s(x) = 0.0026x^2/L$ where x is the ESD of the cells (i.e. twice the radius). The coefficient in $s(x)$ sits within the range of values in Table C4.

Zooplankton Mortality Rate δ

Our estimate of δ is based on rotifers. We expect rotifers to survive for a length of time between fifteen days and 3 months. Thus, we expect $\delta \in (0.0167, 0.067)$. Note that the mortality rate reported in Jones and Ellner (2007) for the rotifer species *Brachionus calyciflorus* was 0.055 day $^{-1}$, which falls within this range.

Nutrient Quota for Phytoplankton $Q(x)$

We estimate the minimum nutrient quota using the nutrient quota data reported in Litchman et al. (2007). The minimum nutrient quota reported in Litchman et al. (2007) for nitrate is $1.36\times10^{-9}V_{cell}^{0.77}$ where V_{cell} is the volume of the cell. The volume of the cell can be converted to the ESD (x) via the equation $\text{ESD} = 2(3V_{cell}/4\pi)^{1/3}$. Hence, our estimate for the nutrient quota is $Q(x) = 8.26\times 10^{-10}x^{2.31}$.

Half Saturation Constant K

Estimates for K in Litchman et al. (2007) lie in the range $(1.8,4)$ μmol N L $^{-1}$. The estimate of K in Jones and Ellner (2007) for *Chlorella vulgaris* in a chemostat is $K = 4.3\mu$mol N L $^{-1}$.

Phytoplankton Growth Rates $\mu(x)$

Our estimates of phytoplankton growth rate are based on two studies that recorded phytoplankton growth rates as a function of body size (Nielsen, 2006; Bec et al., 2008). The ranges of growth rates are given in Table C5. Table C5 suggests that the peak in growth rates occurs for body sizes between 1 and 2.5 μm. The maximum growth rate is between 3.3 day $^{-1}$ and 10 day $^{-1}$ (depending on the amount of nutrients). Thus, we want to choose parameter values for $\mu(x) = x/(c_1x^2 + c_2x + c_3)$ such that $\mu(x)$ is increasing for small body sizes (less than 5 μm) and decreasing for large body sizes (greater than 5 μm). We also want the function $\mu(x)$ to fall within the ranges given in the above table.

These conditions result in the following constraints on the parameters c_1, c_2, and c_3:

c_1, c_2, and c_3 are positive

$\sqrt{c_3/c_1} \in (1,5)$, where $\sqrt{c_3/c_1}$ is where the maximum of $\mu(x)$ occurs

$\mu(100) \in (0.1,1)$

$\mu(\sqrt{c_3/c_1}) \in (3,10)$

Choosing values for $\sqrt{c_3/c_1}$, $\mu(\sqrt{c_3/c_1})$, and $\mu(100)$ that satisfy the above conditions yields a system of equations that can be solved for values of c_1, c_2, and c_3. In simulations we use different sets of values for c_1, c_2, and c_3 that satisfy these constraints.

Clearance Rates C_m

The clearance rate reported in Jones and Ellner (2007) for the rotifer *Brachionus calyciflorus* is $5 \cdot 10^{-5}$ L·day $^{-1}$ per rotifer. The clearance rates reported in Bogdan and Gilbert (1984) for various zooplankton range from 0.1 μL/hr per individual to 400 μL/hr per individual, or equivalently $2.4 \cdot 10^{-6}$ to $9.6 \cdot 10^{-3}$ L·day $^{-1}$ per individual.

Nutrient Inflow (I) and Outflow (d) Rates

First consider the influx rates of nitrogen. The nitrogen fixation rates in Montoya et al. (2007) vary between 10 and 800 μmol N m $^{-2}$ d $^{-1}$. Assuming a well mixed upper layer of depth L (i.e. the influx rate does not depend on the depth), this results in nitrogen fixation rates that range between $0.01L$ and $0.8L$ μmol/L/day. This range could be used to approximate I. It is unclear how to approximate d in this setting. In our simulations we set $d = 0.01$.

Now consider the influx rates of phosphorus. The standing concentrations of phosphate were reported to be between 0.01 and 2 μM in Conkright et al. (2000). Note that these values depend on the ecological community. The study by Froelich et al. (1982) estimated the influx of P to be 10^{-8} moles/cm ^{2}/yr. Assuming the upper layer is L meters and well mixed, this corresponds to an influx rate of $10^2 L$ moles/m ^{3}/yr, which is equivalent to $0.00027L\mu$mol/L/day. In combination, the data from Conkright et al. (2000) and Froelich et al. (1982) suggest that the value of d is between $0.027L$ and $0.00014L$ μmol/L/day. This value is very small and suggests that the estimate for I from Froelich et al. (1982) is too small.

Zooplankton Conversion Efficiency ϕ

The conversion efficiency reported in Jones and Ellner (2007) for the rotifer *B. calyciflorus* is 54,000 rotifers per 10^9 algal cells, or $5.4 \cdot 10^{-5}$ indv./cells. We use the range 10^{-4} to 10^{-4} indv./cells around this value for the conversion efficiency because it depends on the nutrient quotas of the zooplankton and phytoplankton.

Zooplankton Nutrient Quota $q(y)$

Based on the stoichiometry of cladocera, Grover et al. (2012) estimated that the nutrient quota per unit zooplankton volume for those cladocera to be $0.061 \cdot 10^{-9}$ μmol/μm^3 for phosphorous and $1.2 \cdot 10^{-9}$ μmol/μm^3 for nitrogen. Converting volume to ESD yields the nutrient quota $q(y) = 0.12y^3 \cdot 10^{-9}$ μmol/μm^3 for phosphorous and the nutrient quota $q(y) = 2.5y^3 \cdot 10^{-9}$ μmol/μm^3 for nitrogen. Note that in the Grover et al. (2012) study the nutrient quotas for the cladocera and cyanobacteria were comparable (ratio of approximately 1:1). In contrast, the nutrient quotas for the cladocera and *Prymnesium parvum* differed by multiple orders of magnitude (ratio of zooplankton quota to phytoplankton quota was approximately 100:1). Because of this variability, our range for ρ is $(10^{-10}, 10^{-8})$. The exponent b_2 is always set to 3.

C.3 Relation to a mechanistic model (Verdy et al. 2009)

We now show the relation between system (C1) and the chemostat model in Verdy et al. (2009), hereafter referred to as the Verdy model. After changing notation, the Verdy model is

$$\frac{dP}{dt} = \mu_\infty \left(\frac{Q - Q_{min}}{Q}\right) P - sP$$

$$\frac{dQ}{dt} = V_{max} \left(\frac{Q_{max} - Q}{Q_{max} - Q_{min}}\right) g(N) - \mu_\infty (Q - Q_{min}) \qquad \text{(Equation C25)}$$

$$\frac{dN}{dt} = I - dN - V_{max} \left(\frac{Q_{max} - Q}{Q_{max} - Q_{min}}\right) g(N) P$$

where Q (μmol/cell) is the cell quota, μ_∞ (1/day) is the maximum phytoplankton growth rate, Q_{min} (μmol/cell) is the minimum nutrient quota for growth, Q_{max} (μmol/cell) is the maximum nutrient quota, i.e., the maximum amount of nutrient a cell can have, V_{max} (μmol/cell/day) is the maximum nutrient uptake rate, and $g(N) = N/(N + K)$. The first term in the dQ/dt equation describes the uptake rate of the cells, which depends on cell quota. All other terms are interpreted as in system (C1).

System (C1) and the Verdy model (C25) are related in the following way. System (C1) can be thought of as a special case of the Verdy model, where the nutrient quota dynamics are at a quasi steady state, i.e., the nutrient quota dynamics go to steady state much faster than the nutrient or phytoplankton dynamics. To see this, assume that the dynamics of the dQ/dt equation are much faster than the dynamics of the nutrient and the

phytoplankton densities. Hence, the nutrient quota dynamics satisfy $dQ/dt = 0$, or equivalently

$$0 = V_{max}\left(\frac{Q_{max} - Q}{Q_{max} - Q_{min}}\right) g(N) - \mu_{\infty}(Q - Q_{min}). \qquad \text{(Equation C26)}$$

Solving equation (C26) for Q yields the nutrient quota for a given nutrient concentration,

$$Q = \frac{\mu_{\infty} Q_{min}(Q_{max} - Q_{min}) + V_{max} Q_{max} g(N)}{\mu_{\infty}(Q_{max} - Q_{min}) + V_{max} g(N)}. \qquad \text{(Equation C27)}$$

Substituting (C26) into system (C25) and simplifying yields

$$\frac{dP}{dt} = \frac{V_{max}}{Q^*} R g(N) P - sP$$

$$\frac{dN}{dt} = I - dN - V_{max} R g(N) P \qquad \text{(Equation C28)}$$

where $R = (Q_{max} - Q)/(Q_{max} - Q_{min})$.

Let $\mu = V_{max} R/Q$, which can also be written as

$$\mu = \frac{V_{max}\mu_{\infty}(Q_{max} - Q_{min})}{\mu_{\infty} Q_{min}(Q_{max} - Q_{min}) + V_{max} Q_{max} g(N)}. \qquad \text{(Equation C29)}$$

Then under our quasi-steady state approximation the Verdy model (C25) becomes

$$\frac{dP}{dt} = \mu g(N) P - sP$$

$$\frac{dN}{dt} = I - dN - \mu Q g(N) P \qquad \text{(Equation C30)}$$

$$Q = \frac{\mu_\infty Q_{min}(Q_{max} - Q_{min}) + V_{max} Q_{max} g(N)}{\mu_\infty (Q_{max} - Q_{min}) + V_{max} g(N)}.$$

System (C6) is system (C1) for particular phytoplankton and zooplankton ESDs provided that μ and Q are roughly constant values. μ and Q are roughly constant when (i) K is small, which implies $g(N)$ is roughly constant, (ii) μ_∞ is large, and (iii) V_{max} is large. Thus, system (C1) can be thought of as an approximation of the Verdy model (C25) under the conditions that the phytoplankton have (i) low half saturation constants, (ii) high maximum growth rates, and (iii) high maximum nutrient uptake rates.

Table C1. The shape of PDRs in (a) phytoplankton and (b) zooplankton summarized at different evolutionary time in the simulations. $\mu_1 - \mu_5$ represent the different forms of phytoplankton size scaling relationship of growth that resulted in the diversification of phytoplankton and zooplankton. μ_6 led to no diversification and thus is not reported here. The symbol "U" indicates that the PDR is significantly unimodal with the highest species richness occurred between the range of environmental productivity in our simulation. The symbol "+" indicates that the PDR is significant positive and the symbol "NS" indicates non-significant trend of PDRs.

(a) Phytoplankton

Evolutionary time (k days)	The form of phytoplankton growth rate $\mu(x)$				
	μ_1	μ_2	μ_3	μ_4	μ_5
0.5	NS	NS	NS	+	NS
1.0	NS	NS	NS	+	NS
1.5	NS	NS	NS	NS	NS
2.0	NS	NS	NS	NS	NS
2.5	NS	NS	NS	NS	NS
3.0	NS	NS	NS	NS	NS
3.5	NS	NS	NS	NS	NS
4.0	NS	NS	NS	NS	NS
4.5	NS	NS	NS	NS	NS
5.0	NS	NS	NS	NS	NS
5.5	NS	+	NS	NS	NS
6.0	NS	+	U	NS	NS
6.5	NS	NS	U	NS	NS
7.0	NS	NS	U	NS	+
7.5	NS	NS	+	NS	+
8.0	NS	+	+	U	+
8.5	+	+	+	+	+
9.0	+	+	U	+	+
9.5	+	+	U	+	+
10.0	U	+	+	+	U
10.5	U	+	+	+	+
11.0	+	+	U	+	+
11.5	+	+	U	+	+
12.0	U	+	U	+	+
12.5	+	+	U	+	U
13.0	+	+	U	+	U
13.5	+	+	+	+	+
14.0	+	+	+	+	+
14.5	+	+	U	+	+
15.0	+	+	+	+	+
15.5	+	U	+	+	+
16.0	U	+	+	+	+
16.5	U	+	+	+	+
17.0	+	+	+	U	+
17.5	U	+	+	+	+
18.0	+	+	+	+	+
18.5	+	+	+	+	+
19.0	+	+	+	+	+
19.5	+	+	+	+	+
20.0	+	+	+	+	+

(b) Zooplankton

Evolutionary time (k days)	The form of phytoplankton growth rate $\mu(x)$				
	μ_1	μ_2	μ_3	μ_4	μ_5
0.5	NS	NS	NS	NS	NS
1.0	NS	NS	NS	NS	NS
1.5	NS	NS	NS	NS	NS
2.0	NS	NS	NS	NS	NS
2.5	NS	NS	NS	NS	NS
3.0	NS	NS	NS	+	NS
3.5	NS	+	NS	NS	NS
4.0	+	U	NS	NS	NS
4.5	U	U	NS	NS	+
5.0	U	U	NS	U	U
5.5	U	U	+	NS	U
6.0	U	U	+	NS	U
6.5	U	NS	U	NS	U
7.0	NS	NS	U	NS	U
7.5	+	NS	+	+	U
8.0	NS	+	+	+	+
8.5	NS	+	+	+	U
9.0	NS	+	+	+	NS
9.5	NS	+	U	+	NS
10.0	NS	+	U	+	NS
10.5	NS	+	U	+	NS
11.0	+	+	+	+	+
11.5	+	+	+	+	NS
12.0	+	+	U	+	+
12.5	+	+	U	+	+
13.0	+	+	U	+	+
13.5	+	+	U	+	+
14.0	+	+	+	+	+
14.5	U	+	+	+	+
15.0	+	+	+	+	+
15.5	+	+	+	U	+
16.0	U	+	+	+	+
16.5	+	+	+	+	+
17.0	+	+	+	+	+
17.5	+	+	+	+	+
18.0	+	+	+	+	+
18.5	+	+	+	+	+
19.0	+	+	+	+	+
19.5	U	+	+	+	+
20.0	U	+	+	+	+

Table C2. The estimates of parameters in the model (Equations 1a-c). See details of parameter estimations in Appendix C.2.

Parameter/Function	Range (min, max)	Reference
N	var.	
P	var.	
Z	var.	
x	var.	(1, 10)
y	var.	(5)
I	var.	(8)
d	0.01	set
$\mu(x) = x/(c_1x^2 + c_2x + c_3)$	(0, 10)	
(c_1, c_2, c_3)	*	(2, 9)
$g(N) = N/(N + K)$	(0, 1)	(2, 9)
K	(1.8, 4.5)	(6, 7)
β	(10^{-10}, 10^{-9})	(7)
b_1	2.31	(7)
γ	[0, 0.25]	set
m	(1/7, 1/21)	set
$s(x) = \alpha x^2$	var.	(12)
α	(10^{-4}, 10^{-2})	(10, 12)
C_m	(2.4×10^{-6}, 9.6×10^{-3})	(3, 6)
λ	(0.2, 50)	(5)
θ	(0.025, 0.2)	(5)
ϕ	(10^{-5}, 10^{-4})	(6)
ρ	(10^{-10}, 10^{-8})	(4)
b_2	3	(4)
δ	(0.0167,0.067)	(6)

References are (1) Beardall et al. (2009), (2) Bec et al. (2008), (3) Bogdan and Gilbert (1984), (4) Grover et al. (2012), (5) Hansen et al. (1994), (6) Jones and Ellner (2007), (7) Litchman et al. (2007), (8) Montoya et al. (2007), (9) Nielsen (2006), (10) Raven (1998), (11) Sieburth and Smetacek (1978), and (12) Walsby and Holland (2006).
*See section on μ(x) in Appendix C.2.

Table C3. Zooplankton selectivity parameters based on Hansen et al. (1994).

Phytoplankton Species	ESD	Prey ESD *	$x_{50\%min}$	$x_{50\%max}$	$\hat{\theta}$	λ_{min}	λ_{max}
	µm	µm	µm	µm	unitless	µm^2	µm^2
Lohmaniella spiralis	66	9.7	5.4	15.2	0.15	27	44
Strombidium reticulatum	42	7.9	3.3	8.6	0.19	31	0.7
Strombidium vestitum	26	2.1	1.6	2.9	0.08	0.36	0.9
Brachionus angularis	66	3.5	1	5.7	0.05	9	6.9
Brachionus "strain F"	83	6.1	2.7	12.6	0.07	17	61
Brachionus "strain B"	126	6	2.1	16.7	0.048	22	165
Brachionus calyciflorus	139	8.8	6.2	NA	0.063	10	NA
Acartia tonsa N2-N3	97	6.8	5.4	7.9	0.07	2.8	1.7
Acartia tonsa N2-N3	100	7.2	6.1	14.7	0.072	1.7	81
Acartia tonsa N2-N3	112	7	4.5	12.4	0.062	9	42
Acartia tonsa N4-N5	135	4	3.6	17.5	0.03	0.23	263
Calanus pacificus N5	237	28.7	19	29.6	0.12	136	1.2
Diaptomus sicilis	398	14.1	8.9	22	0.035	40	90
Acartia tonsa C3-C4	279	14.5	8.8	NA	0.052	47	NA
C. pacificus C1	289	28.7	12.3	NA	0.099	388	NA
Acartia tonsa males	453	14.5	11.2	91	0.032	16	8400
Acartia tonsa females	499	14.8	11.1	77	0.029	20	5600
Pseudocalanus minutus	414	14.4	6	28	0.034	102	270
Temora longicornis	558	15	6.5	33	0.027	104	470
Eurytemora herdmani	381	16	8	33	0.042	92	420
Calanus finmarchicus	855	80	27	137	0.094	4000	4700
Diaptomus graciloides	325	31	27	35	0.095	23	23

*ESD of prey for which the zooplankton species had the highest feeding rate.

Table C4. Phytoplankton sinking rates from the Walsby and Holland (2006) study. v_{avg} is the average sinking rate from Walsby and Holland (2006); V_{cell} is the volume of the phytoplankton; ν is the coefficient for the sinking rate defined by $v_{avg} = \nu r^2$ where r is the radius of a sphere; α_L (L = 1 or 10) is coefficient for $s(x)$ assuming the habitable layer for zooplankton is L meters deep.

Width µm	Length µm	v_{avg} µm/s	V_{cell} µm^3	ESD µm	ν µm^{-1}/s	α_1 µm^{-2}/s	α_{10} µm^{-2}/s
4.5	174	5.9	2767	8.71	0.078	0.0067	0.00067
4.5	164	5.42	2608	8.54	0.074	0.0064	0.00064
4.5	173	5.18	2751	8.7	0.068	0.0059	0.00059

Table C5. Approximate ranges of phytoplankton growth rates from Nielsen (2006) and Bec
et al. (2008).

Cell Size	1 µm	2.5 µm	5 µm	10 µm	30 µm	100 µm
Growth Rate (day^{-1})	0.025–10	0.1–3.5	0.5–3	0.1–3	0.1–2	0.1–1

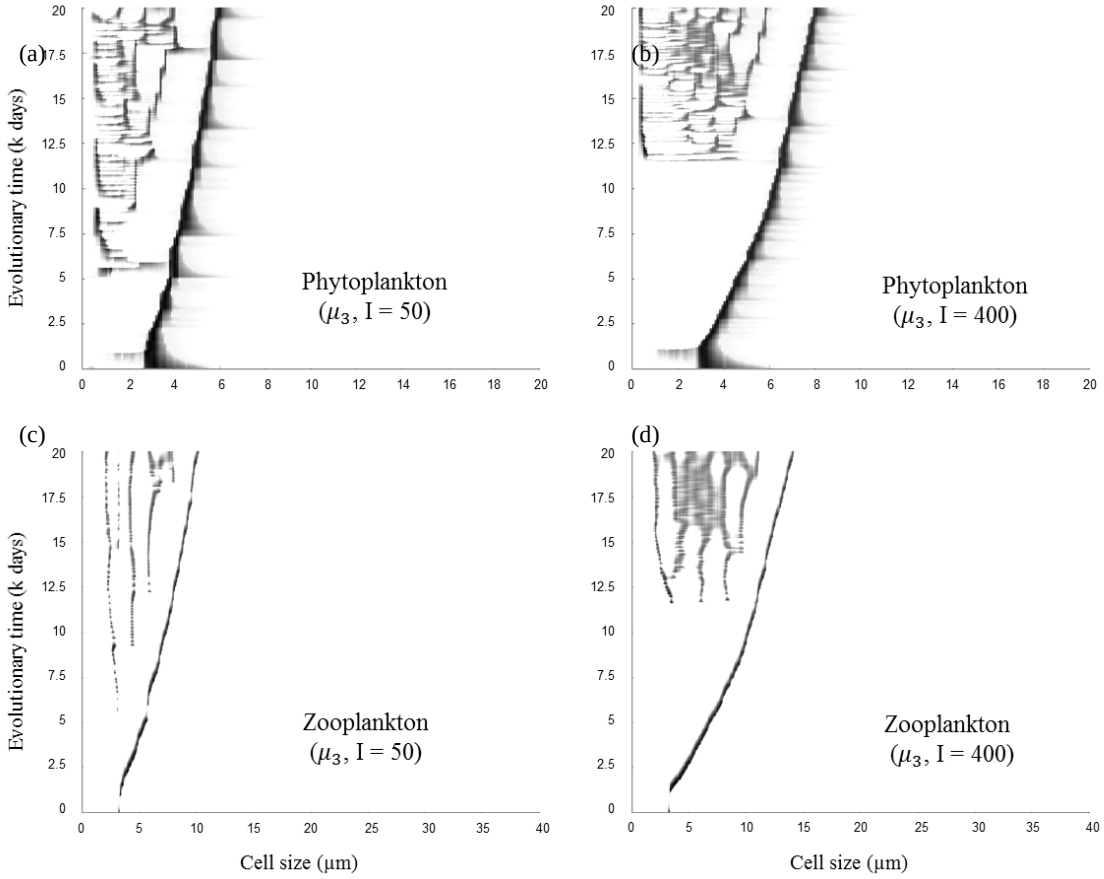

Fig. C1. Examples of the population abundance (a,b) of phytoplankton and (c,d) zooplankton with different cell size during the simulated evolution. The darkness in the plots represents the weights in the log-transformed population abundance.

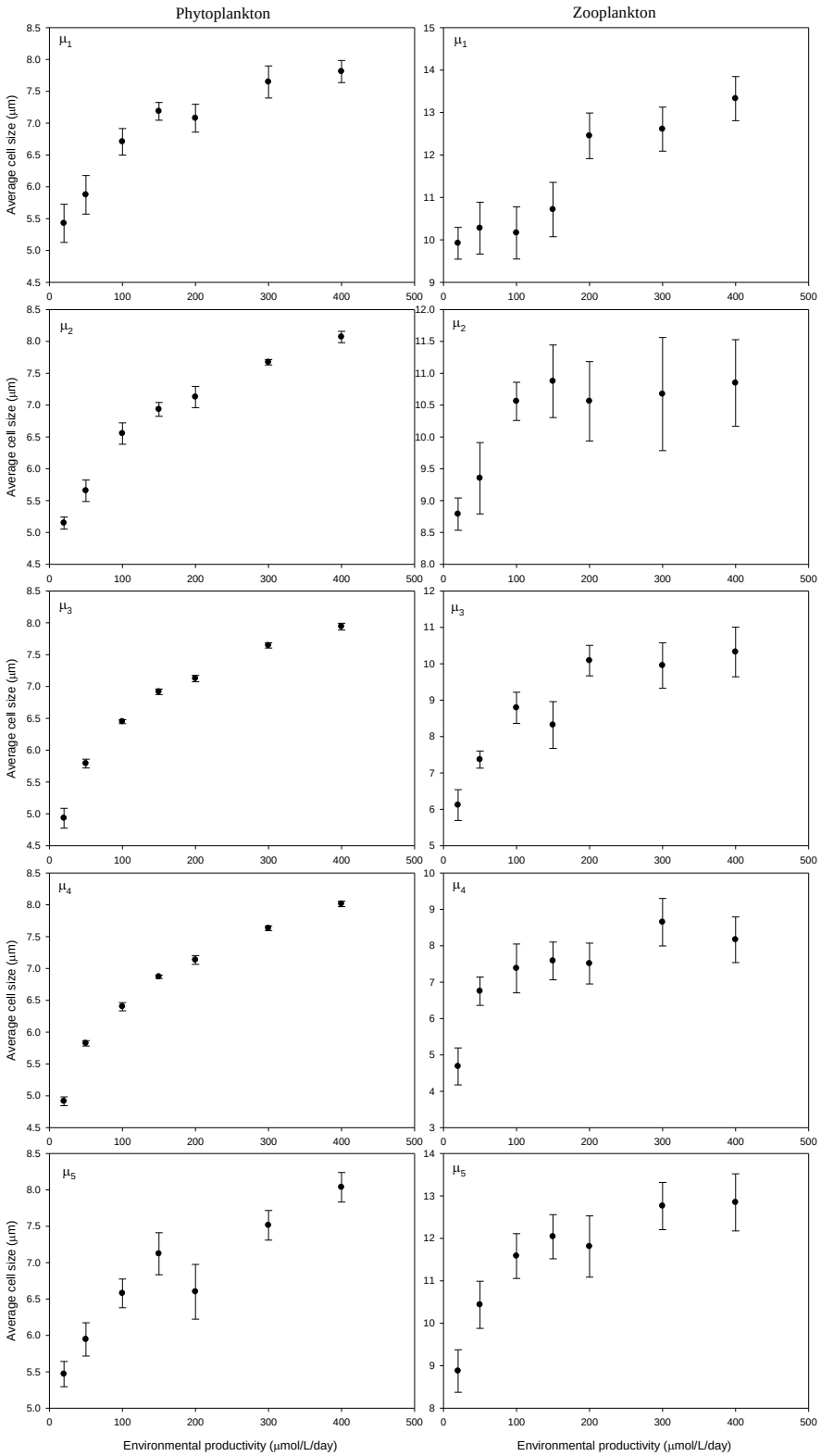

Fig. C2. The average size of phytoplankton and zooplankton weighed by population abundance along the environmental productivity gradient at the end of numerical simulations. $\mu_1 - \mu_5$ represent the different forms of size scaling relationship of growth.

References

Beardall, J., D. Allen, J. Bragg, Z. V. Finkel, K. J. Flynn, A. Quigg, T. A. V. Rees, A. Richardson, and J. A. Raven. 2009. Allometry and stoichiometry of unicellular, colonial and multicellular phytoplankton. New Phytologist 181:295-309.

Bec, B., Y. Collos, A. Vaquer, D. Mouillot, and P. Souchu. 2008. Growth rate peaks at intermediate cell size in marine photosynthetic picoeukaryotes. Limnology and Oceanography 53:863-867.

Bogdan, K. G., and J. J. Gilbert. 1984. Body Size and Food Size in Fresh-Water Zooplankton. Proceedings of the National Academy of Sciences of the United States of America-Biological Sciences 81:6427-6431.

Conkright, M. E., W. W. Gregg, and S. Levitus. 2000. Seasonal cycle of phosphate in the open ocean. Deep-Sea Research Part I-Oceanographic Research Papers 47:159-175.

Dieckmann, U., and R. Law. 1996. The dynamical theory of coevolution: A derivation from stochastic ecological processes. Journal of Mathematical Biology 34:579-612.

Dieckmann, U., P. Marrow, and R. Law. 1995. Evolutionary Cycling in Predator-Prey Interactions - Population-Dynamics and the Red Queen. Journal of Theoretical Biology 176:91-102.

Doebeli, M., and U. Dieckmann. 2000. Evolutionary branching and sympatric speciation caused by different types of ecological interactions. American Naturalist 156:S77-S101.

Froelich, P. N., M. L. Bender, N. A. Luedtke, G. R. Heath, and T. Devries. 1982. The Marine Phosphorus Cycle. American Journal of Science 282:474-511.

Geritz, S. A. H., E. Kisdi, G. Meszena, and J. A. J. Metz. 1998. Evolutionarily singular strategies and the adaptive growth and branching of the evolutionary tree. Evolutionary Ecology 12:35-57.

Grover, J. P., D. L. Roelke, and B. W. Brooks. 2012. Modeling of plankton community dynamics characterized by algal toxicity and allelopathy: A focus on historical

Prymnesium parvum blooms in a Texas reservoir. Ecological Modelling 227:147-161.

Hansen, B., P. K. Bjornsen, and P. J. Hansen. 1994. The Size Ratio between Planktonic Predators and Their Prey. Limnology and Oceanography 39:395-403.

Jones, L. E., and S. P. Ellner. 2007. Effects of rapid prey evolution on predator-prey cycles. Journal of Mathematical Biology 55:541-573.

Litchman, E., C. A. Klausmeier, O. M. Schofield, and P. G. Falkowski. 2007. The role of functional traits and trade-offs in structuring phytoplankton communities: scaling from cellular to ecosystem level. Ecology Letters 10:1170-1181.

Montoya, J. P., M. Voss, and D. G. Capone. 2007. Spatial variation in N-2-fixation rate and diazotroph activity in the Tropical Atlantic. Biogeosciences 4:369-376.

Mougi, A., and Y. Iwasa. 2011. Unique coevolutionary dynamics in a predator-prey system. Journal of Theoretical Biology 277:83-89.

Nielsen, S. L. 2006. Size-dependent growth rates in eukaryotic and prokaryotic algae exemplified by green algae and cyanobacteria: comparisons between unicells and colonial growth forms. Journal of Plankton Research 28:489-498.

Raven, J. A. 1994. Why Are There No Picoplanktonic O(2) Evolvers with Volumes Less-Than 10(-19) M(3). Journal of Plankton Research 16:565-580.

Sieburth, J. M., V. Smetacek, and J. Lenz. 1978. Pelagic Ecosystem Structure - Heterotrophic Compartments of Plankton and Their Relationship to Plankton Size Fractions - Comment. Limnology and Oceanography 23:1256-1263.

Verdy, A., M. Follows, and G. Flierl. 2009. Optimal phytoplankton cell size in an allometric model. Marine Ecology Progress Series 379:1-12.

Walsby, A. E., and D. P. Holland. 2006. Sinking velocities of phytoplankton measured on a stable density gradient by laser scanning. Journal of the Royal Society Interface 3:429-439.

VITA

ZHICHAO PU

PU was born in Shanghai, China. He attened Gezhi High School and received a B.S. in Life Sciences from Fudan University, Shanghai, China in 2006 before coming to Georgia Institute of Technology to pursue a doctorate in Biology. PU enjoyed hiking in Georgia State Parks and travelling when he is not working on his research..